ABSTRACT

RUDOLF, STACY MICHELLE. Durable, Self-extinguishing and Halogen-free Flame Retardants for Nonwovens. (Under the direction of Ahmed El-Shafei and Peter Hauser).

The purpose of this study is to develop new paradigm of novel halogen-free flame retardant finishes that are durable, sustainable, self-extinguish with no dripping and no smoking during testing and are covalently linked to nonwoven polypropylene and polyethylene terephthalate via UV treatment. Novel halogen-free flame retardant monomers were developed and characterized with FTIR and NMR analysis, and different char-forming agents and crosslinkers were assessed for flame retardant ability. Pentaerythritol triacrylate was determined to be the most effective char forming crosslinker. Both the monomer and crosslinker were needed to promote FR behavior in the nonwoven substrates, and different

ratios of monomer and crosslinker were tested for each monomer were each tested, with the best results at an 80:20 monomer:crosslinker ratio for all but one of the monomers developed, which performed best at a 50:50 ratio. The monomer and crosslinker were graft polymerized to the nonwoven substrates via UV irradiation in the presence of a photoinitiator, and polymerization yields were determined based on weight after soxhlet extraction. UV exposure time and photoinitiator concentration were varied to optimize coating yield, and over 90% polymerization yield was obtained for most samples tested. SEM images and analysis confirmed that a coating was present and contained phosphorus as expected. The FR performance was evaluated with a vertical flame test and TGA. All monomers tested were able to form a char over the surface and retard the flame propagation.

Durable, Self-extinguishing and Halogen-free Flame Retardants for Nonwovens

by
Stacy Michelle Rudolf

A thesis submitted to the Graduate Faculty of
North Carolina State University
in partial fulfillment of the
requirements for the degree of
Master of Science

Textile Chemistry

Raleigh, North Carolina

2015

APPROVED BY:

____

Ahmed El-Shafei
Committee Chair

____

Peter Hauser

____

Gavin Williams

DEDICATION

Dedicated to the North Carolina natives who made my lab feel like home.

BIOGRAPHY

Stacy Michelle Rudolf was raised in Somers, CT. She attended Worcester Polytechnic Institute and graduated with a Bachelor of Science Degree in Chemical Engineering. While at WPI, she was a three sport athlete competing in soccer, indoor track and field where she specialized in pentathlon and outdoor track and field where she competed in the heptathlon. Following graduation, she pursued a career with the Escanaba Paper Company in Escanaba, MI working first as a process engineer and then as a shift foreman. While in Escanaba, she began to compete in endurance sports after deciding to run a marathon for a friend. She started completing triathlons, and in 2012 successfully completed Ironman Wisconsin alive and still walking. Looking for new direction in life, she pursued an opportunity to work towards her Master of Science degree in textile chemistry. Following graduation, she will begin a career with Freudenberg Performance Fabrics.

ACKNOWLEDGMENTS

I could not have completed this degree without the help and guidance of many people around me. The many wonderful people of the College of Textiles who guided and coached me were invaluable in my success, especially Dr. Peter Hauser and Dr. Ahmed El-Shafei who gave advice and suggestions throughout the whole of my research project. I also want to recognize Gavin Williams for his critical role serving on my advisory committee and help understanding the physical methods of organic chemistry. Birgit Anderson, Judy Elson, Jennifer Sun, and Chuck Mooney offered help and guidance to complete all necessary tasks. Without them, the project would not have happened. The Nonwovens Institute and Industrial Advisory Board also offered funding, support, and advice throughout the process. The students in the college of textiles have been of immeasurable importance, offering advice, laughter, and sanity in times that insanity seemed immeasurable, and the friends that I have shared an office with have become lifelong friends. Finally, the support of my family in a time when I decided to leave a good job to come back to school was amazing. Thank you to everyone who helped me along my journey.

TABLE OF CONTENTS

LIST OF TABLES

LIST OF FIGURES

1 INTRODUCTION

The need for flame retardancy has been recognized since ancient times; as early as 360 B.C. timber was coated with vinegar to try to prevent fires. [1] Though flame retardant science has improved, fires still devastate. In 2013, there was $11.5 billion in property damage due to fires and 3,240 civilian deaths. 15% of the total fires were caused by highway vehicles, resulting in 300 deaths. [3] Between 2005 and 2009, an average of 7,040 home fires per year began with upholstered furniture, and an addition of 10,260 fires per year began with bedding resulting in annual averages of 841 deaths and $824 million in damages. [4]

Polypropylene and polyester are two commonly used polymers for applications within the home. Polypropylene is commonly used for textiles and is also a common component of car parts such as the dashboard and bumper, while polyethylene terephthalate (PET), a common form of polyester, is primarily used in clothing apparel and food packaging. About 65% of the annual production of PET is in the form of fibers. [8] Due to the high production of both polypropylene and PET, the need to make these polymers flame retardant is apparent.

Traditionally, effective flame retardants for both polypropylene and polyester have included halogenated compounds. However, in recent years legislation has been passed to limit or ban the use of many of these compounds. [7] Halogenated compounds are further an environmental detriment. They are persistant, bioaccumulative and endocrine disruptive. [43] Halogen-free flame retardant coatings are a technology that could be effective for the global competitiveness of the US textile industry.

While some halogen-free flame retardants have been extruded into polypropylene, none have been applied as durable coatings to the best of our knowledge. However, novel halogen-free flame retardant monomers have been developed in Dr. El-Shafei's lab for durable coatings on cotton substrates. [46] UV irradiation is an emerging coating technology with advantages over the traditional pad, dry, thermal cure method in that it requires much less energy and results in a graft polymerized coating on the substrate. [48]

For this work, novel halogen-free monomers utilizing the FR effect of phosphorus/nitrogen synergy were synthesized and applied via UV irradiation with a char forming crosslinking agent to nonwoven polypropylene and polyester fibers. Optimum stoichiometry, UV exposure time, and percent add-on of the monomer/crosslinker were assessed, and the structure-property relationships were determined. The purpose of the research is to develop safe and more efficient techniques to impart flame retardant properties to polypropylene and polyester.

2 LITERATURE REVIEW

The purpose of this section is to give a review of different aspects of flame retardancy. Fire and polymer degradation must be understood as well as the mechanism of different types of flame retardants. Further, the past and current history of flame retardants, laws and regulations regarding flame retardants, and different evaluation methods will be discussed.

2.1 History of Flame Retardants

The discovery of fire was a crucial milestone for the survival of mankind. However, humans were unable to control this natural force. Fire destruction in ancient times led to the investigation of flame retardants. As early as 360 B.C., timber was painted with vinegar to try to prevent home fires and especially the spread of fires. In 83 B.C., the Piraeus townspeople coated their siege towers with alum to prevent the Romans from setting them alight during battle. Addressing a problem with the flammability of canvas in theater presentations, Nicolas Sabbatini coated the fabrics with gypsum and clay as a flame retardant in 1638. It wasn't until 1735 that the first patent regarding flame retardancy was established by Obadiah Wyld in England using alum, borax and vitriol. Responding to the volume of fire damage in the late 18th century, Gay-Lussac was asked to investigate potential flame retardants. In 1820, he presented an FR system of ammonium phosphate, ammonium chloride, and borax. Finally, in the 19th century, William Henry Perkin began to try to understand flame retardant mechanisms and behavior. The current research today is based off his work. [1]

From 1950 to 1980, there was a great deal of research into flame retardants as laws governing flammability of different materials were introduced. From this period, tris(2,3-dibromopropyl) phosphate, or "tris" was developed. In 1977, an Ames test determined that tris was carcinogenic, and research into flame retardant additives all but stopped. In its place, scientists searched for inherently FR materials such as polyamides, and especially aramid fibers. Recently, more research has gone back to FR additives that do not have adverse environmental effects. [2]

2.2 Legislation and FR Need

Textiles are widely used throughout many industries including apparel, upholstery, filters, and mattresses. However, these polymeric substances are flammable. Fires are a major cause of property damage and death. In 2013, there was $11.5 billion in property damage due to fires. In 1,240,000 fires, there were 3,240 civilian deaths and 15,925 civilian injuries. 15% of the total fires were caused by highway vehicles, resulting in 300 deaths. [3] Between 2005 and 2009, an average of 7,040 home fires per year began with upholstered furniture, and an addition 10,260 fires per year began with bedding resulting in annual averages of 841 deaths and $824 million in damages. [4]

To better prevent fires, flame retardants (FR) are commonly used which impede the burning process. Ideally, the flame retardant system should not easily ignite and have a low flame propagation. Further, the system should have a low rate of combustion and generate little smoke which should not contain toxic or combustible gases. The FR properties of the textile should not be affected during use, and the FR additive shouldn't negatively impact the properties of the textile. Finally, the addition of the FR shouldn't have a significant economic impact. Thus, the FR should be inexpensive and able to be applied via systems already in place. [5]

Fire protection and environmental impact must be balanced, and thus flame retardancy is highly regulated. State laws dictate that certain textiles must pass specific flame tests and ban the use of some FR additives. Lawmakers in California as well as the Federal Consumer Product Safety Commission have increased the caliber of the FR required for many furniture applications. [6] Some of the mandatory FR tests are discussed in the Evaluation section of this literature review. In 2011, the EPA began to investigate five different halogenated FR chemicals that are believed to be toxic and persistent. Though it can take years to conduct the studies required to ban chemicals, some companies have already begun phasing them out.

The five chemicals being reviewed are: polybrominated diphenyl ethers (PDBEs), hexabromocyclododecane (HBCD), 2-ethylhexyl-2,3,4,5-tetrabromobenzoate (TBB), bis(2-ethylhexyl)-3,4,5,6-tetrabromophthalate (TBPH), and tris(2-chloroethyl)phosphate (TCEP). An example of each of these chemicals can be seen in Figure 1. Penta, octa, and deca PDBEs were banned in California in 2008, and the EU also banned certain PDBEs in 2004. [6] On November 24, 2014, the Stockholm Convention took global action against HBCD, banning it from all use but that in polystyrene foams. However, the chemical must be phased out of all remaining applications by 2019. [7] With increasing demands for FR materials, an environmentally friendly solution is required.

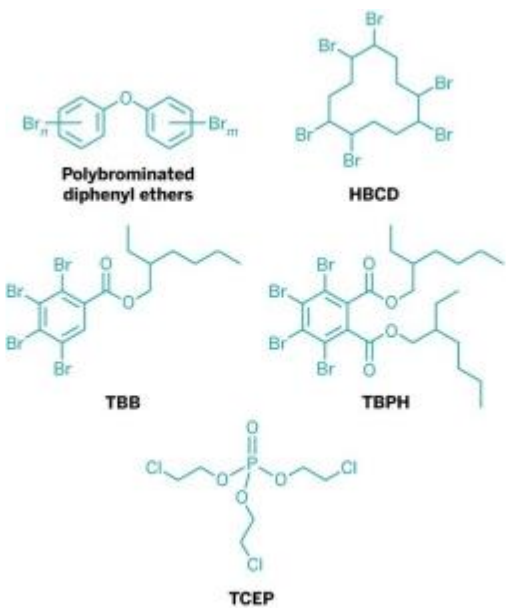

Figure 1: Chemicals investigated by EPA for toxicity concerns [6]

2.3 Polypropylene and Polyester

Both polypropylene (PP) and polyester are thermoplastic polymers commonly used in industrial and everyday settings. PP has many advantageous properties including: low density, high stiffness, heat resistance, chemical inertness, modulus and some transparency. It is further relatively easy to recycle. The chemical structure of PP can be seen in Figure 2. About 52.2

million tonnes per year of PP are produced worldwide, going into such applications as textiles, rigid packaging (crates), films, toys, and technical parts like car bumpers or dashboards. In many of these applications, there are flame retardant requirements.

The most common form of polyester is polyethylene terephthalate (PET). The chemical structure of PET can be seen in Figure 2. It is used as a primary component of clothing fabric, as food packaging, and for plastic water and carbonated beverage containers among other uses. 53.3 million tonnes are produced globally each year, with 65% being converted to fibers and 30% being used for packaging. The remaining 5% is used for PET films. In PET fibers, the polymer is mostly oriented in one direction. The polymer has good heat insulation and resistance to wear, and also is used in many applications that maintain flame retardant standards. [8]

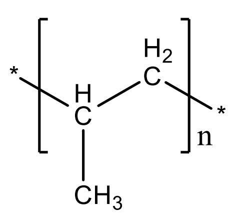

Repeating unit of PP

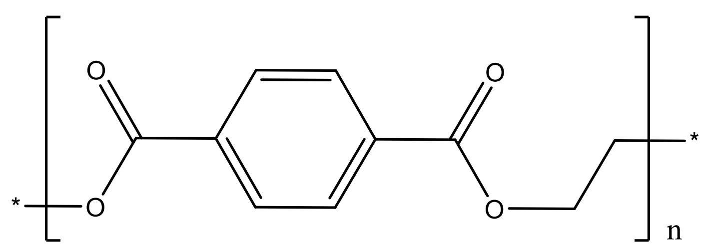

Repeating unit of PET

Figure 2: Chemical Structures of PP and PET [8]

2.4 The Burning Process

As flame retardancy is essentially an interruption of the burning process, it is important to understand combustion. Plastics combust via two different mechanisms. Some degrade the main chain completely and melt, while others form a char. Often volatiles are given off as a result of the process, and there are some polymers that undergo a combination of both processes. [1] Textiles are typically polymeric substances and can undergo combustion. Flammability is dependent upon different factors including fiber, textile composition, pore size, and other chemicals in or around the substrate. As a polymer is heated, it can undergo changes. First, a polymer is heated to its melting temperature where it becomes liquid, and then to the decomposition temperature defined as the temperature range at which the polymer begins to degrade in the presence of oxygen. Higher still is the ignition temperature, at which the polymer will ignite in the presence of oxygen. Some common values of Tm, Td, and Ti can be seen in Table 1. [5]

2.4.1 Polymer Degradation

In general, as a polymer is heated it begins to undergo degradation primarily in the form of chain scission. However, in the presence of oxygen, this process occurs at a lower temperature and is more exothermic. This study primarily focuses on polypropylene and polyester.

2.4.1.1 Polypropylene Degradation

The degradation of polypropylene results in many volatile byproducts including: 2,4-dimethyl-1-heptene, 2-pentene, propylene, 2-methyl-1-pentene and even some isobutene. [1] Some of the mechanisms of PP degradation can be seen in Figure 3. Though it has a high self ignition temperature of 570^{o}C, its aliphatic structure results in a rapid decomposition compared to cellulosic materials. The heat of combustion for polypropylene has been reported as 40 kJ/g, which is higher than many other polymeric substances further enhancing the flammability of polypropylene. However, because the carbon chain is wholly aliphatic there is little smoke generation. [9]

At ambient temperatures, the formation of free radicals is relatively low. However, as temperatures increase, hydroperoxyl group formation and thus the concentration of free radicals also increases. A hydroperoxyl group combines with a carbon based polymer according to the reaction seen in Figure 3. Depending on the chemical surrounding of the reacting carbon, the rate of formation varies. Because polypropylene has a tertiary carbon, it reacts much faster than polyethylene. Often, chain transfer agents such as halogens, amines and phenols are used as thermo-oxidative stabilizers. [5]

As the temperature increases, the degradative effect is compounded. At temperatures between 180 and 250^{o}C, the formation of free radicals drastically increases along the main chain. This chain reaction is exothermic and contributes to an increased temperature resulting in the production of volatile and flammable products. At these temperatures, polypropylene begins to melt which results in increased surface area with which oxygen can react. [5] Water, formaldehyde, acetaldehyde, acetone, methanol, hydrogen, hydrogen peroxide, carbon monoxide and carbon dioxide have all been identified during the oxidation of polypropylene. During cool flame burning at 350^{o}C toxic gasses, most likely carbon monoxide, were released at high enough concentrations to kill mice. In oxygen rich environments, there are very low soot emissions for polypropylene. However, with limited oxygen, the soot emission rate drastically increased as the oxygen content decreased producing a very fine soot (70-97% of the mass was 2μm or smaller). [5]

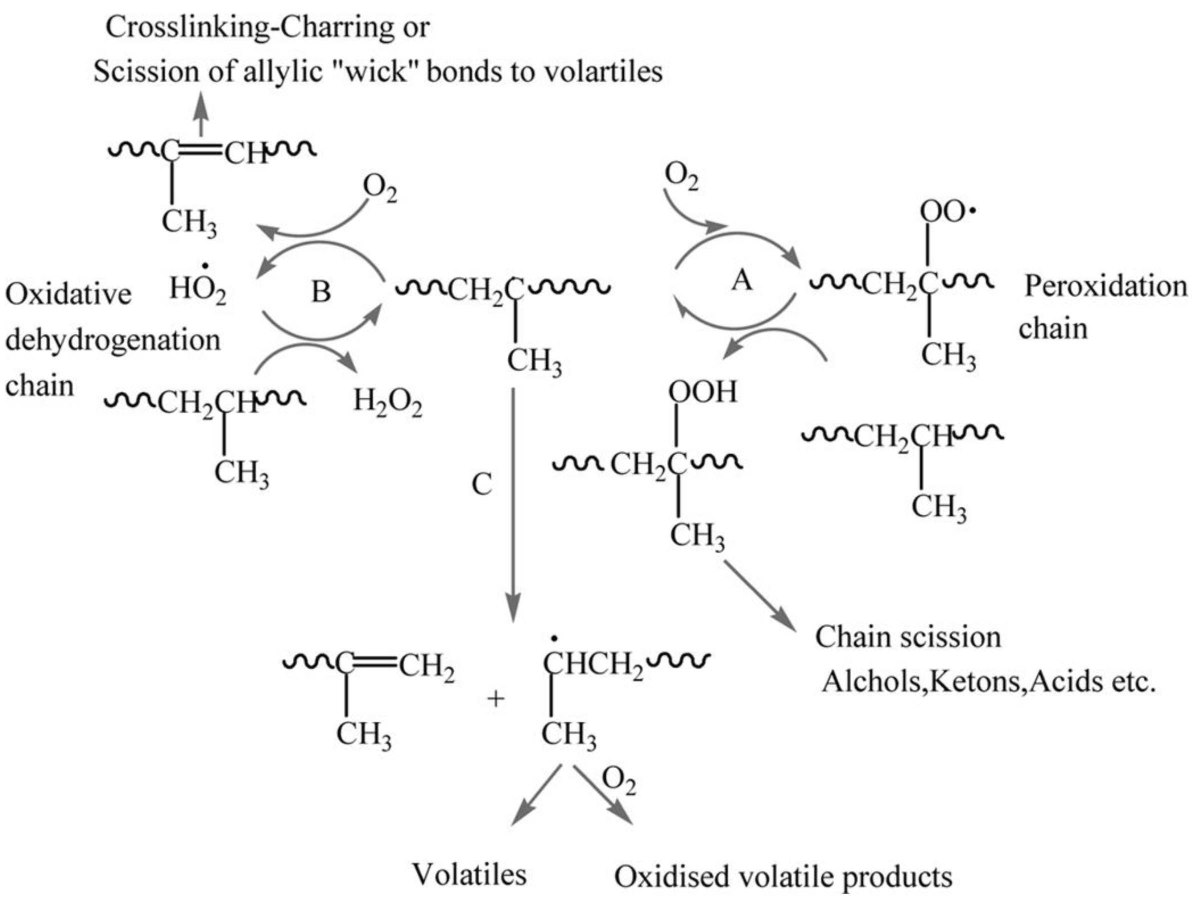

Figure 3: Thermal oxidation and degradation of PP [10]

2.4.1.2 Polyester Degradation

Polyester is typically processed around 265-290°C, but it begins to degrade at 280°C. [5] In the first step of degradation, it is believed that an ester degradation takes place as shown in Figure 4. The products from the initial degradation lead to the volatile products observed during degradation. Carbon dioxide, methane, carbon monoxide, alkanes, alkenes, alkynes and some alcohols are formed. These products can be seen below in Figure 5. [1] A table including some of the important degradation values for PP and PET are listed below in Table 1.

Table 1: Various Reported Temperature Benchmarks for PP and PET [5]

	PP (°C)	PET (°C)
Glass Transition Temperature	-22	80
Melting Temperature	175	260
Decomposition Temperature	320-400	280-320
Self-ignition Temperature	550	480
Flash Ignition Temperature	520	440

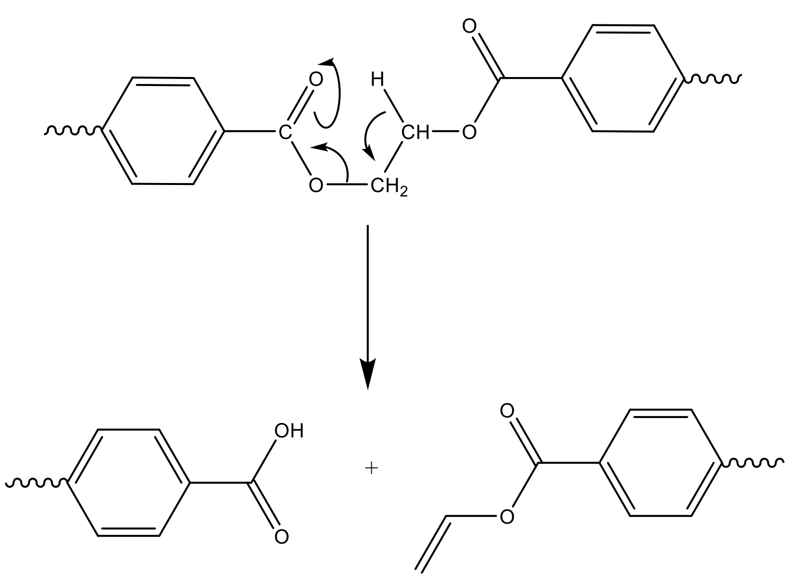

Figure 4: Degradation of PET to a carboxylic acid and a vinyl ester [1]

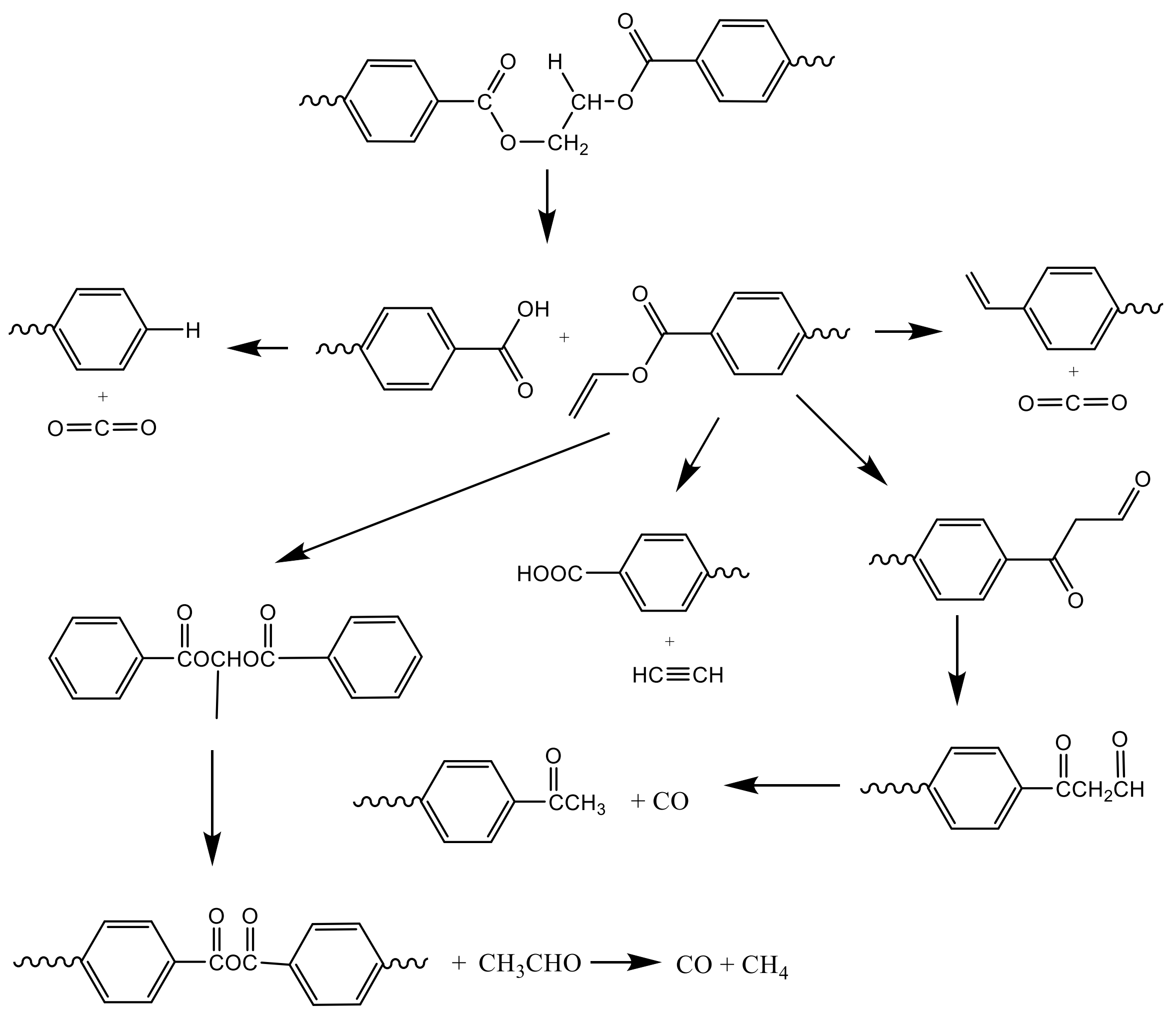

Figure 5: Decomposition pathway of PET that leads to volatile products [1]

2.4.2 Combustion

For a fire to occur, three components are required: fuel (the fiber), heat, and oxygen. At elevated temperatures, polymers first undergo pyrolysis at the pyrolysis temperature. This signifies when the substrate as reached a temperature where it begins to have irreversible chemical changes including char formation and the evolution of flammable and nonflammable gases. As the temperature continues to rise, eventually the combustion temperature is reached. At this stage, the flammable gaseous byproducts combine with oxygen to create a rapid free radical combustion reaction. A schematic of this process can be seen in Figure 6.

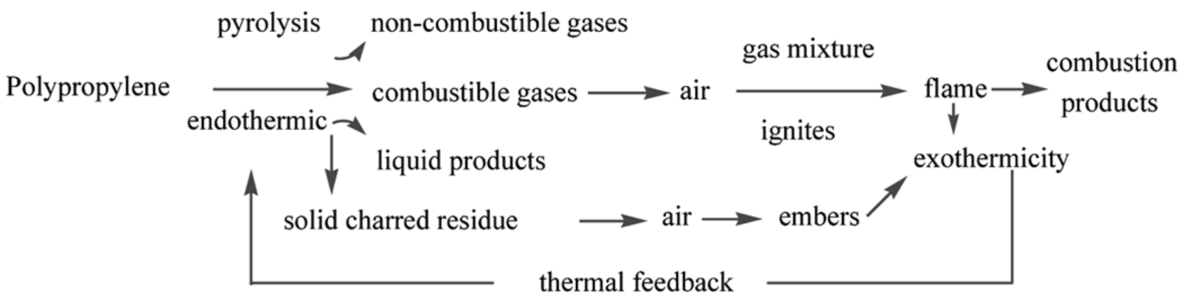

Figure 6: Schematic of PP combustion process [10]

These reactions occur very quickly and result in light and further reactions. The flammability is thus more affected by the rate of heat release rather than the overall heat generation. The most exothermic of the reactions generated in combustion is the free radical reaction of oxygen as seen below in equations 1-3. [11]

$$H^{\bullet} + O_2 \rightleftharpoons HO^{\bullet} + O^{\bullet} \quad (1)$$

$$O^{\bullet} + H_2 \rightleftharpoons HO^{\bullet} + H^{\bullet} \quad (2)$$

$$HO^{\bullet} + CO \rightleftharpoons CO_2^{\bullet} + H^{\bullet} \quad (3)$$

2.4.3 Smoke

The leading cause of fire-related death is not related to heat or burning, but rather to smoke inhalation. Toxic smoke can pervade the area more quickly than the flame itself. ASTM defines smoke as “airborne solid and liquid particulates and gases evolved when a material undergoes pyrolysis or combustion.” Thus, all materials have some form of smoke generation upon combustion. Soot particles are typically the primary component of smoke. Though smoke is the leading cause of death in fire-related fatalities, it can be beneficial as it serves as an early indication of smoldering or a small fire. [1]

Smoke can occur from both the thermooxidative process of ignition and also from the free radical reactions of combustion. Gaseous smoke contains many compounds. Pyrolysis generates many different gaseous contributions to the smoke cloud including: hydrogen-halides, hydrogen cyanide, carbon monoxide (CO), carbon dioxide (CO_2), ammonia, and hydrocarbons. The gaseous contribution of the thermooxidative process include: carbon oxides, water, NO_x, sulfur dioxide alcohols, aldehydes, and ketones. [1] The hydrogen halides are only released from halogen containing polymers. Studies have shown that CO combined with hydrogen halides is more deadly than CO alone. Further, the hydrogen halides are toxic by themselves. [12] There are additives that can aid in smoke suppression, such as magnesium hydroxide. [13]

Both polypropylene and polyester release gases upon combustion. Polypropylene releases toxic acrolein, while polyester combustion generates aldehydes and terephthalic acid. Terephthalic acid is the primary component of the visible smoke generated. One method used to measure the toxicity of gases is by measuring the LC_{50} of different compounds. To do so, subjects, typically rats or rodents, are subjected to the toxic gas. The LC_{50} value is the concentration of the gas in ppm where 50% of the rats die from exposure after 30 minutes. LC_{50} values of common smoke components can be seen below in Table 2. Polymers give off 10-

20% of their weight in CO. [12] One study estimated that 80% of deaths caused by fire gas are due to CO. [14] Thus, though a greater concentration of CO is needed to be lethal, the toxicity of the CO overshadows the toxicity of other gases.

Table 2: LC_{50} Values of Gases [12]

Gas	**LC50 Value (ppm)**
CO	4000-5100
HCN	150-200
HCl	3700
HBr	3000
HF	2500-2900
Acrolein	90-200

2.4.4 Rate of Heat Release

The rate of heat release can be defined as the product of the heat of combustion and the burning rate. Another expression of heat release is the ratio of the net flux of heat reaching the condensed phase to the heat of vaporization. However, this is difficult to calculate and must be verified experimentally. Incomplete combustion must be taken into account and soot emission can be affected by the physical and chemical environment surrounding the flame (oxygen content, temperature, pyrolysis rate, and entrapment of air). Though there are some analytical equations to determine rate of heat release, the turbulent nature of the plume of air over a flame limits the practical applicability of the equations. Nonetheless, they can be used for correlations to burning rate. [1] A schematic of flame spread can be seen in Figure 7.

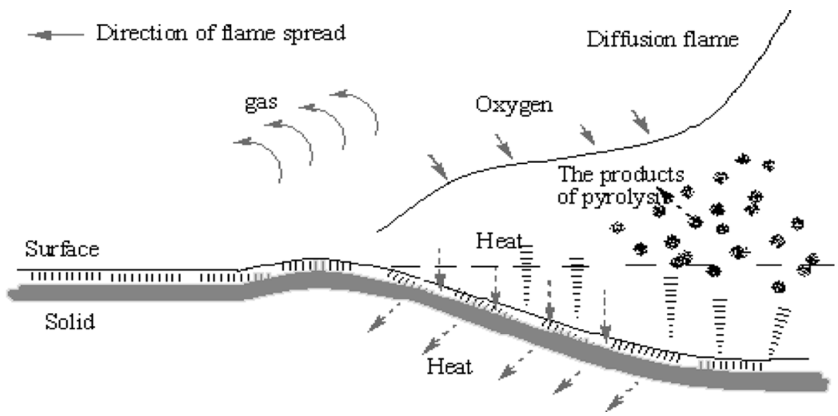

Figure 7: Schematic of Flame Spread [10]

2.4.5 Effect of Fabric Structure on Flammability

Many factors affect flammability including: the type of ignition, the amount of time the fabric is exposed to the ignition source, the fabric orientation, the point of ignition (fabric edge or face), temperature, air flow, relative humidity and finally fabric structure. Lower density fabrics are more susceptible to flames because they have an open structure which allows for greater air flow. They perform significantly worse in flame tests compared to heavier or multilayered fabrics. A loose logarithmic correlation was found between the increasing air permeability of fabrics and decreasing LOI. Some studies have also suggested that assuming the overall fabric density remains constant, coarser yarns are more resistant to flame than smooth yarn. [1]

2.5 Flame Retardant Requirements in Polypropylene

There are unique requirements for PP FR based on its processing parameters and chemical structure. The structure must be thermally stable to the normal processing temperatures of PP, 260^{o}C while being compatible with PP without leaching or migrating. The

FR must retain its FR characteristics when combined with PP and ideally reduce the toxicity of the gas and smoke of PP combustion. Further, it should be effective at relatively low add-on to reduce cost and preserve the properties of the PP. [9]

2.6 Approaches to Flame Retardancy

To achieve flame retardancy, the combustion cycle shown above must be impeded. Several approaches have been attempted and will be discussed below. Typically, flame retardants can be a coating to prevent the heat from reaching the substrate, can act as a heat sink to prevent rapid heat release, work to react with the free radicals to impede the combustion reactions, form a char over the substrate, or release agents to impede the fire propagation such as water upon combustion. [9, 11]

2.6.1 Vapor Phase Mechanism

FR utilizing the vapor phase mechanism typically impede chemical combustion reactions in the air. Halogen based FR operate via this mechanism. The halogen compounds replace the highly combustible hydroxyl and hydrogen radicals in the air with less reactive halogen radicals as seen in equations 4-6. [11] In this figure, RX is representative of the flame retardant while PH is the polymer. These halide radicals further act to dilute the flammable gasses in the air surrounding the flame. Flame inhibition studies show that effectiveness of halogens decreases in the following order: HI > HBr > HCl > HF. However, HI is not stable at normal processing temperatures and the efficacy of HF is not practical. Thus, chlorine and bromine are most commonly used for vapor phase reactions. The optimal halogen choice is the one that decomposes around the same temperature as the polymer so that the halide and fuel are working the gas phase at the same time. [1, 11]

$$RX + PH \longrightarrow HX + RP \tag{4}$$
$$HX + H^{\bullet} \longrightarrow H_2 + X^{\bullet} \tag{5}$$
$$HX + HO^{\bullet} \longrightarrow H_2O + X^{\bullet} \tag{6}$$

2.6.2 Condensed Phase Mechanism

In the condensed phase, a barrier is formed over the fiber in the form of a char to prevent the fire from reaching the fuel of the fiber, essentially preventing heat and mass transfer. Phosphorus based flame retardants are effective via this mechanism. [15] The condensed phase mechanism differs from the vapor phase mechanism in several crucial aspects. A larger ratio of FR to substrate is often needed for condensed phase FR. Also, where the vapor phase mechanism involves the FR decomposing at roughly the same temperature as the substrate, in the condensed phase the FR should decompose at a temperature lower than the fiber. There are two primary modes of condensed phase flame retardancy: dehydration and cross-linking. [1]

2.6.2.1 Dehydration

The dehydration reaction proposed works with primarily cellulosic materials using acids and acid-forming agents of phosphorus and sulfur derivatives resulting in char formation. It can be achieved two ways: the esterification then pyrolytic ester decomposition or carbonium ion catalysis seen in equations 7 and 8 respectively.

$$R_2CH\text{-}CH_2OH + ROH \rightarrow R_2CH\text{-}CH_2OR + H_2O \rightarrow R_2C{=}CH_2 + HOR \tag{7}$$

$$R_2CH\text{-}CH_2OH + H^+ \rightarrow R_2CH\text{-}CH_2OH_2^+ \rightarrow R_2CH\text{-}CH_2^+ + H_2O \rightarrow R_2C{=}CH_2 + H^+ \tag{8}$$

Phosphorous compounds are effective with cellulosic materials, primarily through the first mechanism shown above. Less crystalline regions pyrolyze at lower temperature than the more crystalline regions, resulting in some of the substrate pyrolyzing before the full ester decomposition resulting in higher percentages of phosphorus needed for flame retardant efficacy. Sulfated celluloses primarily act through the second equation and dehydrated by carbonium ions with strong acid activity to rapidly decrystallize and hydrolyze the crystalline regions. [1]

2.6.2.2 Crosslinking

Crosslinking enhances the char formation of the condensed phase, particularly in phosphorus-nitrogen based systems. Studies have shown that both the number of crosslinks and strength of the crosslinked bonds has an effect on flame retardancy. Likely this phenomenon is a function of the energy required to cleave the bonds of the crosslinked structures. As crosslinks are covalent bonds, they are stronger than hydrogen bonds and add a step to the pyrolysis process. [1]

Phosphorus based flame retardants form crosslinks with cellulosic substrates according to the mechanism seen in Figure 8. The phosphorus compounds yield phosphoric acid upon decomposition which reacts with the cellulose to prevent the cellulose chain from scission reactions that produce levoglucosan, the precursor to the flammable volatiles of cotton. The result is char over the surface of the cotton which further helps prevent the spread of the flame and the formation of flammable volatiles. [11]

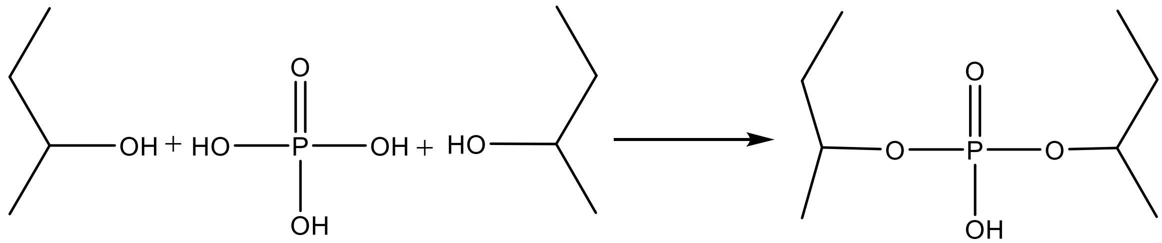

Figure 8: Phosphorous Crosslinks in Cellulosic Substrates

2.6.2.3 Char Formation

Char formed through condensed phase FR is useful as it protects the substrate from acting as fuel for flame propagation by forming a physical barrier over the fiber. A carbaceous char can increase the limiting oxygen index (LOI) to greater than 50. This indicates that the oxygen content of air must be greater than 50% to propagate the flame. [16] For maximum efficiency, the char layer should be continuous and coherent. Cracks or holes in the char can result in the fire reaching the substrate and render the FR ineffective. “Turbostratic” char composed of amorphous phase carbon black and randomly distributed spots of graphitized carbon form the most protective char layer. In the amorphous phase, the char is able to melt at high temperatures creating a fluid layer than mold as the shape of the fiber changes lowering the incidence of holes and cracks in the layer. The graphite layer enhances the FR to reinforce the layer and prevent oxidation. Because it is not able to form a continuous layer, powered carbon or chars are ineffective with the exception of expandable (acid-treated) graphite. This type of graphite can expand to one hundred times its volume forming an excellent barrier to the fiber, but is coarse, black, and electrically conductive rendering it impractical for many applications. [15]

In a study on char formation, researchers found that a better and more homogenous char is formed at lower heat fluxes. A lower heat flux leads to a lower expansion rate resulting in a uniform char with small holes. At larger heat fluxes, larger holes and cracks were found in the char. After 10 seconds of burning, a char sample from PP sample treated with Ammonium Polyphosphonate (APP) and Pentarythritol was tested. The char was fine, and found to contain phosphate ester, acid, ester, and crosslinked char as well as some PP and decomposition gasses such as ammonia in the char. A suggested structure of the char can be seen in Figure 9. [17] The char formation of APP/PER substrates can be enhanced using hyperbranched char forming agents (HCFA) from triazine derivatives. These agents foam and create a greater char barrier to the fiber upon combustion when used in a 3/1 ration with APP. [18] Char formation and efficiency can also be increased using synergistic char forming agents such as silicone additives, the catalytic charring of metals or the synergistic effects of nanocomposites. [19]

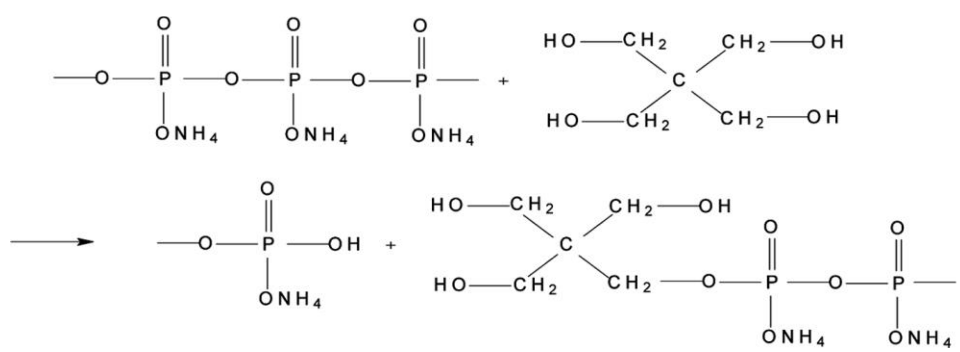

Figure 9: Suggested Structure of Char Formation on PP [17]

2.6.2.4 Intumescent Systems

Intumescent flame retardant (IFR) mechanisms involve an expanded foam char which forms a protective barrier and also helps to reduce the toxic gasses and smoke emitted upon combustion. [10,11] These systems interrupt the combustion cycle prior to pyrolysis at the stage where the polymer is just beginning to form a self-sustaining combustion cycle. Three elements are required to for effective intumescence: an acid source, a carbonific compound, and a spumific or blowing agent. First, at about 280^{o}C, the acid and carbonific compound decompose to form the char. As the temperature continues to rise, the spumific agent decomposes and releases gasses which cause the initial char to swell. At about 430^{o}C the material further decomposes and loses its foamed nature. The remaining carbonaceous substance acts to trap gasses from decomposition. [1] A typical IFR system is comprised of a polyphosphate, amine, and polyol. The char formed in these types of systems has been shown to be resistant to oxidation up to 1200^{o}C. [16]

Recent research into intumescent PP FR systems has been to uncover catalysts to reduce the amount of FR needed for PP. Polyoxometalates (POMs) which are early transition metal oxygen clusters, known to act as an FR synergist, and ionic liquids (IL) were combined as a catalyst for the APP/PER intumescent FR. Using this system, the amount of FR needed on polypropylene, typically about 25% was able to be reduced to 14.5% with similar results. [20] In a different study, silicone dioxide was used as an effective catalyst in the APP/PER/PP IFR system, increasing the flame retardancy of the PP while holding the percent add-on constant. [21,22] Both the intumescent system and POM/IL catalysts are regarded as green alternatives to traditional FR systems as they aren't harmful to the environment and help to capture toxic gases emitted by combustion. [1,20]

2.6.3 Physical Approach to FR

The final FR mechanism is using a heat sink. The FR is a compound with decomposes endothermically, preventing the substrate from reaching its pyrolysis temperature. These compounds sometimes release flame inhibiting substances, such as water or carbon dioxide, upon combustion further increasing the FR efficacy. Alumina trihydrate (ATH) and calcium carbonate are examples of FR chemicals that perform this way as seen in equations 9 and 10. [10,11] This mechanism acts in several ways: the reaction is endothermic to absorb heat, the water acts to help put out the fire and also dilute the combustible gases to increase the flame retardancy. ATH begins to release water at 200 ^{o}C, far below the pyrolysis temperature of both PP and Polyester. [15] Unfortunately, this also falls below the typical processing temperatures for PP and polyester, and typically 50-65% add-on is required for effective flame retardancy rendering ATH an impractical solution for FR on these thermoplastics. [1]

$$Al_2O_3 \cdot 3H_2O \xrightarrow[\triangle]{} Al_2O_3 + 3H_2O \tag{9}$$

$$CaCO_3 \xrightarrow[\triangle]{} CaO + CO_2 \tag{10}$$

Additives are also used as heat sinks and can include clays, talc, silica, or magnesia. If an additive has a high specific heat, it can also raise the amount of thermal energy needed to reach the pyrolysis temperature. They can further enhance char formation. However, these substances must be added in bulk, and typically only elastomers can support enough of the additives to achieve flame retardancy without a loss of properties. [1,15]

Foamed glass is another example of a physical approach to FR. These compounds decompose to form a glassy barrier prevent the flame from reaching the polymer substrate.

2.7 Classes of FR

Different classes of FR use the mechanisms above to achieve flame retardancy. In this section, different types of FR will be discussed based on their chemical mode of action.

2.7.1 Phosphorus-Based FR

Phosphorus based flame retardants typically work in the condensed phase. Phosphorus crosslinks with hydroxyl groups to form the char as seen in Figure 8 above. [10,11] However, because PP does not contain hydroxyl groups, the system must be modified. The phosphorus compound combines with a char forming agent as well as a blowing agent in phosphorus based IFR systems for polypropylene. While only 2% phosphorus is needed in most cellulosic systems, 5-15% phosphorus is often needed for effective FR activity in polyolefin systems. [1] There are many different types of phosphorus-containing FR with different oxidation states including: Phosphines, phosphine oxides, phosphonium compounds, phosphonates, elemental red phosphorus, phosphites and phosphate. However, not all of these are effective FR for polyolefins. [9]

Phosphorus based FR are being studied widely as an alternative to halogen based FR. There are several advantages to the use of phosphorus FR: lower density, no need for antimony oxide synergist, more likely to be environmentally responsible, char formation, photostability, and less smoke and less acid gas upon combustion. However, because it is difficult to form molecules with a high percentage of phosphorus, these FR tend to be less efficient and more expensive. Further, they are more likely to be hydrophilic resulting in moisture uptake and may hydrolyze. Thermal stability can be a concern with phosphorus FR as well. [9,23] Various types of phosphorus based-FR that have been used with PP will be discussed below.

2.7.1.1 Ammonium Polyphosphate Systems

The most common phosphorus based FR used in PP systems is ammonium polyphosphate (APP). While APP is relatively water insoluble, it can be chemically modified to become water resistant. Because the phosphorus acts by reacting with hydroxyl groups, a char forming agent must be added. Pentaerythritol (PER) is a common choice. [15] The APP/PER/PP systems work as an IFR with less dripping than traditional halogen based FR, but require higher add-ons to be effective. [24]

Much of the recent research into FR for PP revolves around finding synergists to enhance the efficacy of the APP/PER/PP systems. One option is to synergize the mixture with organic montmorillonite, which has been shown to be effective at as low as 1% add-on. Using the same ration of APP/PER/PP with the 1% addition, one study showed the UL-94 rating to improve from a V-0 to V-1 and the limiting oxygen index (LOI) to increase from 30.8 to 33. [25]

Other research has investigated silicone derivatives as synergists for the system. One research group found that a silicone elastomer synergized the APP/PP system to improve flame retardancy. [26] Borosiloxane was a synergist to an APP/PER/PP system at only 1.5% add-on. A proposed mechanism for the silicone synergy is to reduce the peak heat release to form a ceramic protective layer over the substrate. However, the mixture was unable to pass achieve an V-0 rating until the add-on was greater than 9% due to dripping. [9]

Heavy metal salts such as those from zinc or manganese are another synergist explored for use to enhance flame retardancy. These additives need to be applied at an optimum percent, about 1.5%; too much or too little of the salt decreases flame retardance. It is believed that the metal ions help accelerate the phosphorylation of PER and hydroxyl groups that had formed on the PP while potentially helping to crosslink and stabilize the structure. [9] PA6, Zinc borate, and zeolite were all tested with APP/PP to better understand the char formation, and found that lower heat fluxes improved the char structure with these additives. [17]

2.7.1.2 Melamine Phosphates

Melamine phosphates are used to as a blowing agent in IFR systems containing phosphorus to expand the char. The expansion depends on the ratio of the rates of gas/volatile evolution, the viscosity of the liquefied pyrolysis products, and the transformation of these products to the char. [9] These compounds are typically added as a coating because they are not thermally stable at thermoplastic processing temperatures, [27] but give the PP mixture better water resistance and thus less mold deposition. [15]

The efficacy of melamine compounds is enhanced in the presence of PER as a char forming agent. [27] However, other charring agents have been explored. Bis(2,6,7-trioxa-1-phosphabicylclo[2.2.2]octane-1-oxo-4-hydroxymethyl)phenylphosphate was found to be an acceptable PER substitute in one study. [28] Other additives prove beneficial to the phosphorus/melamine system as well. Using a phosphorus compound, melamine, and hydroxyethylmethacrylate extruded with an elastomer, Li et al were able improve the flame retardant behavior of PP systems. This combination increased the char expansion in the IFR system as an improved FR. [29]

2.7.1.3 Red Phosphorus

In the elemental form, red phosphorus can be an effective flame retardant. Ironically, it is extremely flammable as a powder and thus poses difficulties for processing and must be added either as an emulsion or in a masterbatch. [15] Red phosphorus is stable to 320^{o}C and able to be processed with PP. Because red phosphorus highly concentrated, it is effective at much lower addition rates. It can be effective in polymers that contain nitrogen or oxygen or used with char formers or metal hydroxides. Using nitrogen containing synergists, a V-0 rating can be achieved at 20-25% loading. [30] However, this compound has a reddish brown color which can lead to aesthetic problems when applied to textiles. [9]

2.7.1.4 Ethylene Diamine Phosphate

Ethylene diamine phosphates are self-intumescent, and attractive as no char forming agent is required. They are typically synergized with nitrogen containing compounds such as melamine or melamine pyrophosphate. The melting point of ethylene diamine phosphate is 250^{o}C, so it is a liquid at the typical processing temperatures of PP. [9,15]

2.7.1.5 Nitrogen Synergism in Phosphorus FR

Nitrogen is known to have a synergistic effect with phosphorous FR. Several mechanisms may be responsible for the synergy. The P/N compounds may convert to phosphoric acid amides upon combustion and catalyze the dehydration and carbonation in cellulosic substrates. Also for cellulosic substrates, the nitrogen component is believed to control the pH of the system for optimum flame retardant ability due to its ability to become protonated and reduce the available acid. At a low pH, the cellulose may undergo acid hydrolysis. At an elevated pH (alkaline), acid catalysis occurs preventing the phosphorous from crosslinking. [11] The alkaline hydrolytic stability of the P-N bond is not great, and if hydrolytic resistance is required, electron donating groups can be connected through a P-C bond to enhance the stability. [5] Though this effect is described specifically for cotton, one can imagine these same reactions taking place with the hydroxyl group on the crosslinking agent in FR polypropylene systems based on P/N chemistry.

2.7.1.6 Metallic Hydride Synergists

Another interesting approach to enhancing the IFR ability of APP/PER/MA(melamine) in PP systems is through the use of metallic hydrides as a synergist. One group used polyoxometalates (POMs) as a synergist in conjunction with ionic liquids (IL) as a catalyst. The POMs were effective in enhancing the FR ability, but were not alone able to significantly reduce the weight percent needed to achieve acceptable flame retardance (UL 94 V0). Thus, an IL, shown to have a catalytic effect on polycarbonate treated with a siloxane based FR, was added to the system. Using 12-phosphomolbdic acid with 1-butyl-3-methylimidazolium as a POM/IL hybrid, the weight percent needed to achieve acceptable flame retardant behavior was reduced from 25 wt% to 15 wt%, with 14.5 wt% attributed to the POM and 0.5 wt% attributed to the IL. [20] However, there is an optimized value for the amount of POM added. A research group working with $LaMnO_3$ perovskite composite metal oxide found that too large a fraction of the metal oxides results in an agglomerated char which is more brittle and prone to cracking. Above 3 wt%, it was found that metal oxides have a detrimental effect on the FR properties of the PP composites. [31]

Another research group investigated which metal chelates provided the most effective enhancement to flame retardancy. Testing NiO_3, ZnO, and BiO_3, researchers were able to determine that transition metals (NiO_3 and ZnO) performed best due to increased complexation through the d orbitals. Though these metals did not impact FR performance below 400°C, above this temperature the dehydration and NH_3 elimination rates were decreased allowing a more dense char to form, which enhanced the FR properties of the composite material. [32] Another group corroborated this research, first developing a novel phosphorus-nitrogen based IFR (poly(4,4-diamino diphenyl methane-*O*-bicyclicpentaerythritol phosphate-phosphate)) and then using metal chelates to enhance FR properties. These compounds were dried into a powder and mixed with PP. Again, it was found that transition metals provided the greatest enhancement of FR properties by forming a denser crosslinked char layer through salt bridges formed by the metal chelate. [33]

2.7.2 Halogen Containing FR

Halogen containing FR are a very effective class of FR. These compounds operate in the gas phase, and bind with combustible hydroxyl and hydrogen free radicals in the air to prevent further combustion. The effectiveness of these compounds depends heavily on the reactivity of the halogen. If the halogen forms a strong bond with the carbon, it is not an effective leaving group and not as easily released when burned. In general, aliphatic or alicyclic halogen compounds are more effective than aromatic halogen compounds due to lower bond energies. A high ratio of halogens to carbons is also desired, as there are more halogens free to inhibit combustion. Because bromine is less electronegative than chlorine, the bond energy with carbon is lower, and brominated compounds tend to have better FR properties than chlorinated compounds. [9]

2.7.2.1 Synergy in Halogen-Antimony Systems

Halogen FR systems in PP are needed at about 30-40% to achieve UL94 V-0 ratings. It is important to make sure that these compounds do not adversely affect the polymer properties, and the high percentage of flame retardant needed in this system fiber properties and UV stability may be negatively impacted. Thus, synergists are typically used to make the system more efficient. The most commonly used synergist is antimony III oxide, though phosphorous, nitrogen, zinc, and tin containing compounds are all considered halogen synergists. Antimony acts to trap the halogen gases in the SbX_3 form (where X is the halogen) so that they cannot escape the flame zone, resulting in a higher percentage of halogen gas in the flame zone. [9] The exact mechanism can be seen in equations 11-18. [11] In one antimony-bromine system, the weight percent was reduced from 20% in the halogenated system without the synergist to 5-10% in the system with a synergist with similar FR performance. While halogenated systems are effective in FR performance, there are increasing environmental concerns which will be discussed below. Overall, halogenated systems are being substituted with non-halogenated systems. [9]

$$Sb_2O_3 + 6HX \longrightarrow 2SbX_3\uparrow + 3H_2O \tag{11}$$
$$SbX_3 + 3H^{\bullet} \longrightarrow Sb + 3HX \tag{12}$$
$$Sb + OH^{\bullet} \longrightarrow SbOH \tag{13}$$
$$SbOH + H^{\bullet} \longrightarrow SbO + H_2 \tag{14}$$
$$SbO + H^{\bullet} \longrightarrow SbOH \tag{15}$$
$$SbX_3 \longleftrightarrow SbX_2^{\bullet} + X^{\bullet} \tag{16}$$
$$RH + X^{\bullet} \longleftrightarrow R^{\bullet} + HX \tag{17}$$
$$R^{\bullet} + X^{\bullet} \longrightarrow RX \tag{18}$$

2.7.3 Metal Hydrides

Metal hydrides operate via the physical approach to FR, typically acting as a heat sink. ATH is the most commonly used metal hydride in FR applications. It can be combined with magnesium hydroxide to improve the flame retardant behavior, but typically high ratios of the FR composite to PP are needed for adequate flame retardation. The fraction of FR needed can be decreased by increasing the interfacial adhesion and surface area using surface modification of the filler or a polymeric coupling agent such as silane without compromising the flame retardant behavior. [10] However, because these compounds tend to degrade at temperatures lower than those used in the processing of PP, they are not a common FR for PP. [1]

2.7.4 Nanocomposites

In general terms, nanocomposites are two materials combined to achieve greater properties than either of the two individual components could provide. Typical nanocomposites have three components: two materials joined with a resin. However, in the context of polymer nanocomposites, there are only two components: the polymer nanoparticles and binding agent. When creating polymer nanocomposites, compatibility of the nanoparticle with the polymer matrix and any additives are important considerations. Typically, these composites are more flammable than their virgin counterparts. Several theories have been proposed, but there is not currently an agreed upon reason for this behavior. Polymer nanoparticles can be one dimensional (layered), two dimensional (tubes/rods), or three dimensional (spheres/colloids). All three of these types of composites have the same FR mechanism. After the polymer nanocomposite is made using a polymer that is inherently flame retardant, most flame retardant polymer nanocomposites reduce the rate at which the polymer is pyrolyzed which effectively reduces the rate of mass loss and heat release rate. [23] Polymethylmethacrylate and polyhedral oligomeric silsesquioxane (POSS) are two polymers often used in nanocomposites. In the case of POSS, there is a one dimensional layered structure in the nanocomposite. In order to achieve good FR behavior, much of the silicates must be near the surface. [10] Nanocomposites can also be combined with other flame retardants such as halogen based, phosphorus and mineral based FR to increase the FR behavior. [23]

Another study increased the flame resistance of PP by creating a composite of PP and inherently flame resistant polyamide 6 with maleic anhydride as a compatibilizer to increase thermal stability. This FR composite worked in the condensed phase, forming a char upon burning to prevent further thermooxidative degradation. The further found that by adding 5 wt% sepiolite natural nanoparticles, the stability of the char and FR behavior were increased. [34]

2.7.5 Other Char Forming Agents

Carbon nanotubes (CNT), polyamides, and silicones have all been explored as potential char forming agents in PP. CNTs are primarily used to enhance the mechanical properties of polymers due to their high stiffness, electrical conductivity and thermal conductivity. CNTs work in the condensed phase, forming a char over the surface of the polymeric substrate and lowering the heat release rate. They can begin to be effective at as low as 5 wt%. Often, CNTs are used as a synergistic to other FR, including phosphorus based IFR. [35,36] Graphene was also introduced into the polymer matrix. The researchers created a composite of 80wt% PP, 18wt% IFR, 1wt% CNT and 1wt% graphene and were able to achieve a V-0 rating after performing the UL 94 test and increase the LOI to 31.4%. [36] Research into this area of FR continues.

Polyamides have also shown promising results as char forming agents in IFR systems. However, polyamide 6 (PA6) and polyamide 6,6 (PA66) tend to be less effective because of their low melting point, melting before a uniform char is formed over the PP surface. However, aromatic polyamide systems are too thermally stable and do not degrade with the polymer matrix, rendering these types of polyamides ineffective as well. In one study, researchers synthesized a hybrid aromatic-aliphatic polyamide: poly(p-ethylene terephthalamide) (PETA). Using APP as the acid with a ratio of 3:1 APP:PETA at 30wt% of the PP/IFR mixture, excellent flame retardancy was achieved. The LOI was increased to 35%, and a V-0 rating was found with the UL 94 test. The research into this type of charring agent continues as well. [37]

2.7.6 Silicone as a Synergist

An optimized amount of silicone containing additives can enhance the flame retardant behavior of IFR. The exact mechanism of the synergy is not known, but a more uniform char layer is clearly present in IFR systems containing an optimum amount of silicone. In one study, Silicone dioxide (SiO_2) was added to an APP/PER IFR system. At 30 wt% APP/PER in PP, the char layer formed is loose with some cracking resulting in greater heat and mass transfer through the protective char layer, in turn decreasing the flame resistance. After adding 3.5% of SiO_2, the char layer was stronger as demonstrated with mechanical testing and visually contained fewer cracks. UL-94 testing revealed greater flame resistance than the APP/PER system alone. However, at 9 wt% SiO_2 addition, the char layer is less compatible, and cracks again form in the char layer and the flame retardancy is reduced. The researchers tested the system with TGA thermograms to determine that no chemical reaction took place between the SiO_2 and APP and SiO_2 and PER. Thus, it was determined that the silicone's mode of action was through a physical mechanism, strengthening the char layer up to a certain point where the additive was no longer compatible with the existing char layer. [22]

Another study investigated the effect of silicone combined with an n-alkoxy hindered amine (NOR) as a synergist in an IFR system. Similar to the previous study, it was found that there was an optimized amount of the silicone containing additive at 1 wt% addition. Above this value, the flame retardant behavior of the composite was negatively impacted. Because the silicone in this instance was directly bonded to the NOR, a two different mechanisms are proposed and can be seen in Figure 10. As the compound degrades via thermolysis, regenerable free radical scavengers are formed. These radicals may work in the vapor phase, combining with combustion gases in the air. Another proposed mechanism is that the radicals help to crosslink the char to form a more stable protective char layer over the substrate. Both studies demonstrate that silicone containing additives can be useful for FR synergism in small amounts. [38]

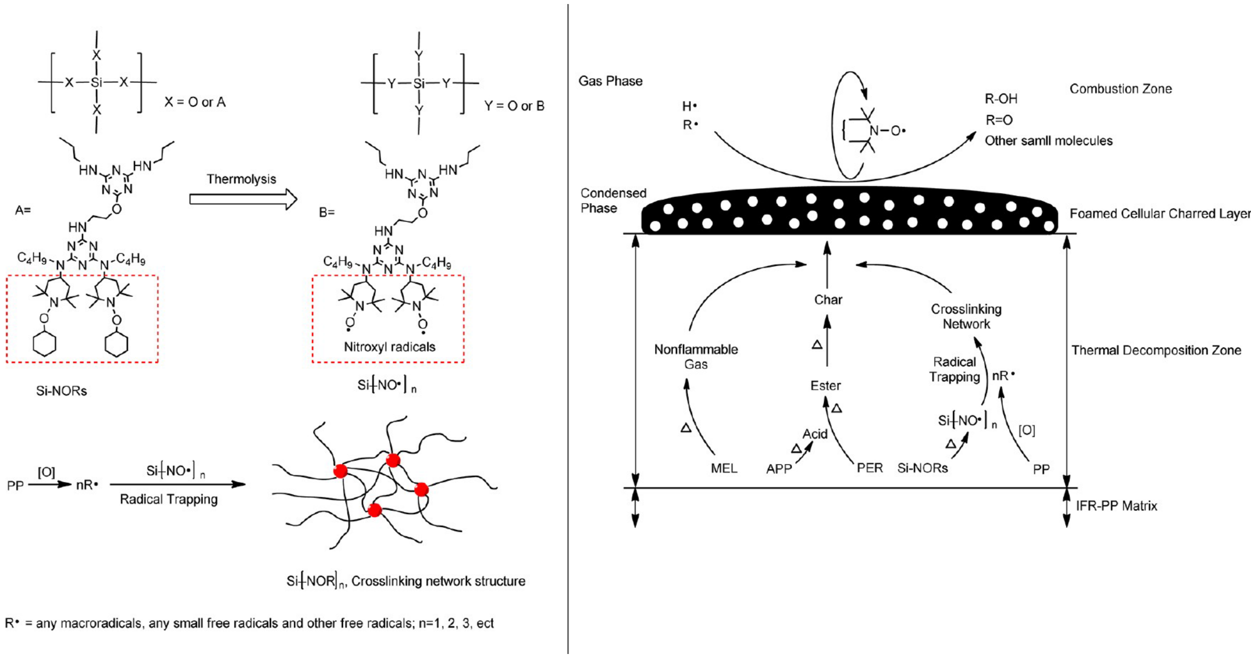

Figure 10: Two proposed FR mechanisms for silicone synergism [38]

2.7.7 Other Additives

There is sometimes a need for other additives in FR PP. Specifically, in halogen containing FR, an acid is often formed that causes rapid UV degradation. Thus, UV stabilizers can be used. [39,40,41] In one study, UVA blockers were successfully used to help stabilize brominated FR PP to UV light. It appeared that these compounds helped prevent the UV light from reaching the compound, thus preventing the formation of bromine acids and degradation. [39] A review of additives in PP was completed by Jha et al. [42]

2.8 Environmental Impact and Health Concerns

While FR can be useful to prevent fire death, there are concerns for the toxicity and environmental impact.

2.8.1 Halogenated FR

Halogenated FR are being recognized more for their adverse impact on the environment. They are known to be persistent and bioaccumulative. Studies also find associations between halogenated flame retardants and certain conditions in humans, but have not been able to provide causal evidence. Brominated flame retardants (BFR) are believed to interfere with thyroid hormone homeostasis and neurodevelopment. This type of FR is also associated with diabetes, developmental disorders, and adverse reproductive health effects. Digestive cancers and lymphoma are also evident in conjunction with BFR. [43]

Typically, FR can be introduced to the human system from dietary sources (from FR stored in animal fats), inhalation of dust, ingestion of dust, and through occupational exposures. [43] FR are introduced into the air from sofa, mattress, or chair foams, and the concentration can vary from 1 ng/m^3 to 250 ng/m^3 depending on the furniture present in the room, temperature, ventilation, and the types of building and electric equipment present. [14] Despite regulations, BFR have become increasingly more prevalent in humans and the environment. Disturbingly, a study in Australia examining polybrominated diphenyl ether (PBDE) revealed that children have 5-6 times higher concentration of FR in their system as compared to adults. Several factors may contribute. Infants breastfeeding may be exposed to the toxin from the mother's breastmilk. Further, children tend to be closer to the ground and thus to dust in the room, which may facilitate increased exposure. It is further speculated that children have less metabolic capacity to detoxify the bloodstream from these toxins. [43] Though these types of chemicals are no longer used as FR, older furniture and carpets may still contain halogenated FR.

Studies of the environmental impact of these chemicals shed light as to how chemicals that have been banned for many years can still be accumulating in the environment and in human bodies. One study looked specifically at Firemaster BP-6 produced by Michigan Chemical from 1970-1974 using hexabromobyphenyl (hexaBB). The study focused on the great lake region as it was most exposed to the chemical waste from the production of hexaBB. The researchers found that for each million kg of production, 0.07 kg of polybrominated biphenyls (PBBs) were released to the air, 1,000 kg were present in water, and 50,000 kg were present in the soil. Because the PBBs were non-volatile and resistant to bacterial degradation, they persisted in the environment. The PBBs in the soil eventually leached to the water, where the smaller fish would consume them. Because the PBBs are lipophilic, they remained within the fatty tissue of the small fish. These smaller fish were then eaten by the predatory fish, resulting in about a 4 year lag between peak PBB production and peak concentration of flame retardants in fish. As humans consume the fish, their exposure increases. [44]

2.8.2 Phosphorus Based FR

Phosphorus based FR have been found to have some toxic qualities and adverse environmental effects. This mostly applies to halogenated PFR which are carcinogenic. Non-halogenated PFR are believed to have very little adverse impact on human health, though they may contribute to the decomposition of red blood cells. Regardless, non-halogenated PFR are considered a less toxic more environmentally responsible alternative to halogenated PFR. [14]

2.9 Future Trends

Most of the trends in flame retardant research are a result of trying to improve the sustainability, environmental impact, performance, cost and toxicity of the treatments. Dr

Horrocks, an expert in the flame retardant field for over thirty years, has outlined the future trends of flame retardants in several reviews. Many FR treatments for cotton involve chemistry that releases formaldehyde, and thus research in that area is focused on avoiding formaldehyde release. In synthetic fibers, the research is focused on developing char forming abilities and reducing the use of halogens. [2,45]

2.9.1 Formaldehyde-free Cotton FR Additives

Two common FR additives to cotton were tetrakis(hydroxymethyl) phosphonium salt (THPX) condensates and N-methylol dimethylphosphonopropionamide derivatives, both of which release formaldehyde upon decomposition. Phosphorus-nitrogen chemistry has shown promise as a potential alternative. In order for this chemistry to work, it must be able to be easily applied, have no formaldehyde release, have a comparable service life, be cost effective, and have low toxicity and environmental effects. [2] Work on phosphorus-nitrogen chemistry for cotton applications has been completed in Dr. El-Shafei's lab. [46,47]

2.9.2 Non-halogen Containing Back-coatings

Flame retardants for synthetic applications still prove to be difficult. PP and PET are particularly challenging because neither is inherently flame retardant, and PP has a tendency to drip with each drip being difficult to render flame retardant. An added challenge is that the synthetic backings must begin to degrade and release the FR before the textile substrate begins to burn; in the case of cotton that means the FR must degrade below 350°C. However, the FR should also be able to withstand the processing temperatures of the different fibers, and thus must degrade above the processing temperatures of the fibers creating a narrow range in which the FR should be active. Further, one test in the UK for couch backings requires the textile to be submersed in water prior to testing to evaluate the durability of the treatment. Decabromophenyl ether (decaDBE) and hexabromocyclododecane (HBCD) are two common FR additives used for synthetic materials. The hazardous nature of these chemicals was outlined above. [2,45]

Thus, there are certain requirements desired in replacements for these chemistries. First, there should be a sensitization of the decomposition and FR efficiency, the treatments should have reduced solubility, and potentially incorporate a vapor phase component to increase the FR efficacy. There is also a need to introduce char forming capabilities to synthetic fibers. Phosphorus-nitrogen chemistry has been experimented with in this capacity, but the chemicals used, APP in particular, no not meet the temperature degradation requirements. Nanofibers are another outlet being investigated, though researchers are still working to increase the dispersion and compatibility of the nanoparticles with the synthetic fibers. [2]

The final new area in this research is with surface modifications. By applying a thin coating of the nano or micro scale on the textile, the desirable properties of the textile may be less impacted. Plasma and UV irradiation treatments create exciting opportunities for the future development of durable FR coatings. [2]

2.10 Evaluation

The purpose of FR evaluation is to ensure that the time required to evacuate the enflamed compartment in the case of a fire is shorter than the time for the fire to create untenable conditions. [1] However, objective and consistent analyses of flame retardant behavior can be difficult. There are many factors that affect how a substrate burns, and many different test methods to try to accurately test the flammability for the particular application of the textile substrate. In this section, the factors affecting the tests will be addressed, and several the of the flame evaluation methods will also be discussed.

2.10.1 Challenges to FR Evaluation

There are many factors that contribute to the nature of flammability of different substrates. As such, when describing the flame resistant behavior with terms such as self-extinguishing or non-igniting, the test used to determine it should also be included to give quantitative value to the statement. [1] In type 1 testing (usually with a small heat source with a short duration), the heat source greatly affects the flammability. The size of the flame and orientation of the sample (vertical vs horizontal) can affect if the textile substrate is able to pass a given flame test. The amount of time the substrate is exposed to the flame also affects the results of the flame test. Further, the ignition source can come from a variety of areas: the edge of a textile, the center, the bottom of a vertical sample or the top of a vertical sample, and all of these affect the flammability differently. The thickness of the sample can also affect flammability, as thicker samples are more difficult to ignite and tend to burn longer as there is typically more fuel, and this thickness can change the results of flame tests. The way the specimen is mounted can also affect the tests; some textiles are able to be mounted and others are not. [23]

2.10.2 Flammability and Smoke Tests

There are many different methods to evaluate flame retardant behavior. Several will be discussed below. The types of tests range from small scale, to pilot scale, to full sized experiments. Several tests will be described below, but many other specific tests exist for different FR applications.

2.10.2.1 UL 94 Test

The UL 94 test from the Underwriters Laboratories is often used to describe flame retardant behavior in research. Its purpose is to measure "the flammability of plastic materials for parts in devices and applications," and is often run on plastics. Essentially, the test measures the duration of burning after a sample is exposed to a small flame. For the UL 94 test, a sample 125mm by 13mm is hung vertically from the top. The sample is then exposed to a 10 second flame twice, and the burn time is recorded after each exposure and the process is repeated with 5 samples. A cotton swab is placed under the sample, and if a burning drip ignites the cotton, the result is recorded. There are five different ratings in the UL 94 test, but only three are commonly referenced. A rating of V-0 is awarded if the samples all burn less than 10 seconds, with an average under 5 seconds with no burning drips that ignite cotton. Further, the afterglow should not exceed 30 seconds. A rating of V-1 is awarded if average burn time for the specimen is under 25 seconds, with no total combustion times over 50 seconds. In this case, again no burning drips ignite the cotton and the afterglow is limited to 60 seconds. A V-2 rating is awarded if the sample meets the requirements of the V-0 or V-1 but has burning drips that ignite the cotton. The test can also be performed horizontally to receive an HB rating, which is easier to achieve than the vertical flame tests. [15]

2.10.2.2 Limiting Oxygen Index (LOI)

The LOI value is another commonly reported value for flame retardants. The value reports the highest concentration of oxygen at which the tested sample self-extinguishes in under 3 minutes with less than 5 cm of material being consumed. There only exist weak correlations between the UL 94 test and the LOI. For this test, a sample about 100mm by 65mm by 3mm is placed vertically below a gas chimney and held at the bottom. Oxygen and nitrogen are fed at a specific ratio, and a burner is lit at the top of the substrate. If the surface does not ignite or extinguishes in 30 seconds, the oxygen content is increased. The iterations continue until the LOI value is determined. While this is a commonly referenced test, there are no real life scenarios that mimic the LOI test. However, the test has gained value due to its reproducibility and relative independence from sample thickness. [15]

2.10.2.3 Cone Calorimeter

The cone calorimetry test is reproducible and gives many useful measurements of combustion, and helps predict flash-over time which correlates to the escape time. A cone calorimeter measures many different parameters including: heat, smoke release rate, mass loss, ignitability, time to ignition, heat of combustions, and concentrations of CO and CO_2 in the smoke. Heat release rate is also calculated from oxygen measurements based on the oxygen consumption principle. For a cone calorimeter test, a sample is placed in a chamber and exposed to a radiant heat source at a constant temperature. However, the test can be difficult for samples that expand or intumesce because the distance to the heat source may change as the temperature increases. Regardless, cone calorimeter tests are considered a useful measure of flame retardant properties. [15]

2.10.3 Specific Application Flame Tests: Upholstered Furniture

The ASTM and NFPA have many application based tests which recreate possible situations. For instance, the children's sleepwear test mimics if a child is near a flame and the apparel catches fire, the flame should self-extinguish quickly. [15] Several tests specific to thermoplastic applications will be discussed.

2.10.3.1 Cigarette Ignition

This test is voluntary, and designed by the Upholstered Furniture Action Council (UFAC) where a cigarette is dropped on furniture and should not ignite. [15]

2.10.3.2 California Technical Bulletin 117

Mandated only in California, furniture parts are exposed to smoldering cigarettes and open flames. Each component besides the furniture covering is individually exposed to either a cigarette or open flame. For the open flame portion, no flame or flaming drips can last greater than an average of 5 seconds and 6 inches of char. Any specimen exposed to a smoldering cigarette has to retain 80% of its weight after the flame has extinguished. [15]

2.10.3.3 California Technical Bulletin 133

In California, any furniture for public occupancies must pass a rigorous open flame test. The full furniture is exposed to a 16kW open flame for 80 seconds. Specific criteria required to pass involve temperature at the 4 ft level and at the ceiling, mass loss, smoke, and CO. [15]

2.10.3.4 Federal Motor Vehicle Safety Standard 302 (ISO 3795, SAE J369)

In the US, materials in the passenger compartment must pass this test. The specimen is subjected to a horizontal flame test and should not burn more quickly than 4"/min. However, the test is easy to pass, and many manufacturers self-impose stricter limits. [15]

2.11 UV Irradiation Induced Graft Polymerization

Grafted coatings can confer different surface properties including: antibacterial, antifouling, biocompatibility, anti-fog, and improved dyeability characteristics. [48,49] Several different methods exist to induce graft polymerized coatings: chemical initiator induced graft polymerization, ion radiation induced graft polymerization, plasma induced graft polymerization, and Ultraviolet (UV) induced graft polymerization. UV irradiation has been used in conjunction with a photoinitiator to induce polymerization in many instances, and is a preferred method due to its relatively safe process. UV irradiation requires a lower radiation energy, and thus is less likely to change the bulk properties of the polymer. It can also result in energy savings as the process is conducted at room temperature and can be done in seconds. Another environmental benefit to the use of UV irradiation is that the process is solvent free, minimizing the risk of exposure. [48,49] The coating is combined with a photoinitiator which induces a free radical reaction to lead to the graft polymerization. In PP, the reaction is believed to take place at the tertiary carbon, and in PET, the reaction is believed to occur at the carbon alpha to the oxygen linkage in the ester. Both of these sites are depicted in Figure 11. [50] However, it has not been widely used to date to graft polymerize flame retardant coatings onto textiles, and examples of UV cured FR coatings are limited in the literature.

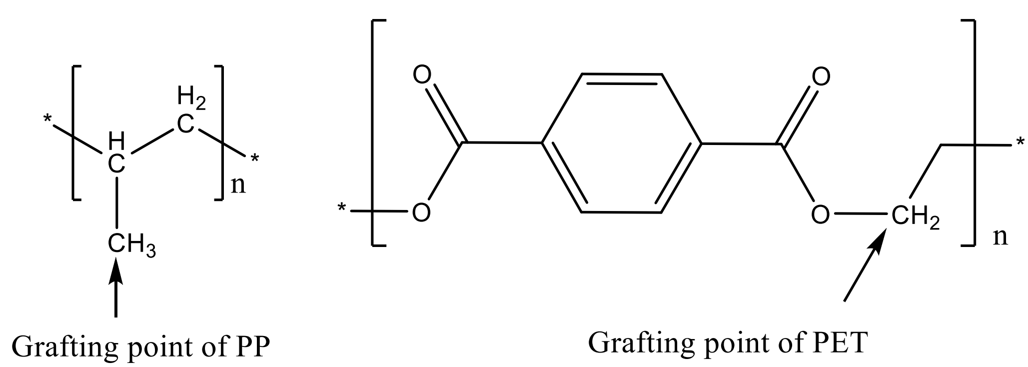

Figure 11: Grafting sites of PP and PET polymers

One group of scientists from Beijing University has been investigating the surface modification of Polyamide 6,6 (PA66) to increase its flame resistance. In their first work, the scientists modified the surface of PA66 by photografting maleic anhydride to the fiber before treating the modified sample with ethanolamine to induce an esterification reaction to enhance the flame retardancy. While this approach was able to increase the LOI value of the substrate, it was still not desirable as a two-step process. [51] The same researchers improved their process by changing the monomer used to modify the surface. Again using the photografting technique, the researchers modified the surface with acrylamide, improving the FR behavior of the compound in one step. The LOI value was increased to 26.8. The modified textile was then subjected to a water extraction and the LOI value was retested and found to be 26.2. Referencing the low drop in LOI after water extraction, the researchers deemed their coating durable. [52]

UV-cured FR coatings have also been used on cotton using phosphorous-nitrogen based FR chemistry. A compound named PDHA was synthesized from the reaction of phenyl dichlorophosphate and 2-hydroxyethyl acrylate. The compound was pad applied to cotton with a photoinitiator and UV-cured. The researchers found the coating to be a durable FR finish. [48]

In PP FR fabrics, APP is commonly used. However, it is very water soluble resulting in FR coatings that are not durable. The low compatibility between APP and PP can also hinder the FR performance of treated fabrics. Several groups have tried to use microencapsulation in conjunction with UV-curing to solve these issues. One group used EA as the resin which has properties including: good adhesion, chemical and corrosion resistant, electrical insulation, good strength and good hardness. The researchers encapsulated APP in the EA resin, and UV cured the mixture to PP. Though the mixture did not receive a UL-94 rating, the LOI increased from 20.1 with PP/APP to 24.2 with the PP/APP-EA resin with a durable coating. [49] Another group used pentaerythritol triacrylate (PETA) as the resin to encapsulate the APP. Again, the coating was durable and the FR evaluation showed that this product was a better FR material than the first. With 60% PP and 40% APP-PETA, a V-0 rating in the UL-94 test was achieved and the LOI was 30. [53] Though some work has been done to investigate UV curable FR treatments, there is much more information left to be discovered.

3 METHODS

The work presented expands upon the work previously completed in Dr. El-Shafei's lab. [46,47]Two of the FR monomers previously developed were applied to polyester and polypropylene nonwovens, and four novel monomer syntheses were attempted. This section will be divided into five sections: materials, synthesis, crosslinker determination, application methods, and evaluation techniques.

3.1 Materials

Chemicals were purchased from various sources based on availability and price, and are listed below. Triethylamine (TEA), stabilized HPLC grade methylene dichloride (DCM), and anhydrous sodium carbonate were purchased from Fisher Scientic. 99% allyl bromide (AB) stabilized in <=1000 ppm propylene oxide, 98% n,n-dimethylphosphoramic dichloride (DMPDC), 96% ethyl dichlorophosphate (EDCP), ethanolamine (EA), 98% hydrazine (HZ), 97% acryloyl chloride (AOC) stabilized in 400 ppm phenothiazine, pentaerythritol triacrylate inhibited with 300-400 ppm MEHQ, pentaerythritol tetraacrylate stabilized with 350 ppm

MEHQ, 99% ethylene diamine, 90% copper (1) chloride, 98% allyl chloride (AC), 92% 3-(trimethoxy-silyl)-propylmethacrylate (PTM) stabilized in 100 ppm BHT, and 90% lauryl acrylate (LA) inhibited with 60-100 ppm MEHQ were purchased from Sigma Aldrich. Ethyl acetate (EtOAc) which was 99.8% pure, 98% pentaerythritol and 99% anhydrous calcium sulfate were purchased from Acros Organics. Acetone was purchased from BDH and Irgacure 819 [(2,4,6-trimethylbenzoyl)phenylphosphine oxide] (photoinitiator) was provided by BASF. Finally, 80% 1-(acryloyloxy)-3-(methacryloyloxy)-2-propanol stabilized with MEHQ was purchased from TCI America and 97% n,n dimethyl phosphoramidodichloridate, which has the same chemical structure as DMDPC, was purchased from Alfa Aesar. Compressed Argon was obtained from the Machine and Welding Supply Company. Deuterated chloroform for NMR testing was purchased from Cambridge Isotope Laboratories. Spunbond nonwoven polypropylene and polyethylene terephthalate (PET) both at weights of 50 gsm were obtained from The Nonwovens Institute at North Carolina State University.

3.2 Molecular Design Motivation

The FR molecules were designed to maximize the FR behavior of polypropylene and polyester, understand the relationship between the ratio of phosphorus to nitrogen and its effect on the FR behavior of the materials, and maximize the graft polymerization yield. Thus, the molecules were designed with varying phosphorus, nitrogen and oxygen content. These percentages can be seen in Table 1. Monomer 3 was designed with an extra acryloyl group attached to double the functionality of the monomer and theoretically increase the graft polymerization yield. Greater percentages of phosphorus and nitrogen should yield the best flame retardant behavior, and monomer 3 should have the best grafting percentage because it has twice the functionality of the other monomers.

Table 1: Chemical Compositions of Monomers

Monomer	**MW**	**%C**	**%N**	**%P**	**%O**
1	320	45	8.75	9.6	30
2	319	45.14	13.17	9.72	25.01
3	411	52.55	10.22	7.54	23.36
4	289	49.83	24.22	10.73	5.54
5	317	45.43	22.08	9.78	15.14
6	233	41.2	30.04	13.3	6.87

3.3 Monomer Synthesis

All monomers were synthesized via a two-step process. Because these monomers are being created as an environmentally-friendly alternative to traditional flame retardants, the environmental impact of the synthesis of the monomers was examined, resulting in a solvent change from the previously used DCM (considered toxic by the EPA) to EtOAc this period for all monomers. A similar glassware setup was used for each reaction, and will be discussed generally before presenting each individual reaction. Monomers will be referred to as numbers (Monomer 1-6) in this text to clearly differentiate the compounds as the acronyms are very similar.

3.3.1 General Set-up for Synthesis

For all syntheses, two steps were required. The reactants were placed in a 3-neck round bottom flask (RBF). The flask had one inlet for argon flow, and a condenser was inserted in one of the necks with an oil bubbler connected to the top to monitor argon flow. Argon was continuously fed to the system throughout the reaction. In the final neck, an addition funnel was added briefly to add chemicals to the reaction slowly, and replaced with a stopper after the reactant addition. A depiction of this set-up is apparent in Figure 1. All intermediates were reacted on ice at 0°C for 1 hour, and at room temperature for 3 additional hours under constant stirring with a magnetic stirrer. For the second step of each reaction, the intermediate solution was vacuum filtered into a vacuum filtration flask, and added to a clean 3-neck round bottom flask with the same set-up as the intermediates. For monomers 1, 2, 3 and 5, the addition of acryloyl chloride resulted in a very endothermic reaction, so this reactant was added dropwise. The final reaction was again begun on ice at 0°C for 1 hour and allowed to react for 14 hours total. Again, the addition funnel was connected to one of the necks to add chemicals, and then removed once the reaction was started and replaced with a plug. For monomers 4 and 6, no addition funnel was required and the reactions took place at room temperature for 24 hours. Individual reactions will be discussed below. For all final products, the salt was removed via vacuum filtration, and the filtrate was washed with 10% sodium carbonate solution, the organic layer was recovered from the top layer of the solution, and dried with calcium sulfate. The calcium sulfate was then removed by filtration, and the final product was distilled with a Buchi V-855 Version 02.07 rotary evaporator with a Buchi vacuum pump V-710 and and Buchi heating bath B-491 at 55°C and 195 mbar.

3.3.2 Solvent Selection

When previously developing these monomers in Dr. El-Shafei's lab for cotton applications, DCM was used as a solvent. However, the triethylamine hydrochloride salt was partially soluble in the DCM, resulting in more of the salt being able to get through the filtration paper into the final product to be removed in the washing step. The reactions were first tested with tetrahydrofuran (THF), in which the triethylamine salt is completely insoluble. However, both THF and DCM are recognized as a toxic substance and has been phased out of industry. Thus, EtOAc was chosen as a replacement environmentally friendly solution. All data presented used EtOAc as the solvent for the application.

Figure 1: Apparatus Assembly for Synthesis of Monomers

3.3.3 Monomer 1 Synthesis

Monomer 1 was previously developed in Dr. El-Shafei's lab, and the synthetic process was altered to obtain a better yield. The monomer is based on phosphorous, and EA was reacted with the monomer to add nitrogen content to the monomer to synergistically enhance the flame retardant behavior. The reaction scheme for the intermediate can be seen in Figure 2. To complete the reaction, 20 mL of EtOAc was added to the RBF in an ice bath with 0.723 (0.012 mol) EA and 2.46 mL (0.018 mol) TEA. TEA was added in excess as an acid scavenger to bind the triethylamine hydrochloride salt. 0.728 mL (0.006 mol) EDCP was then dissolved in 20 mL EtOAc in the addition funnel, and added dropwise to the mixture.

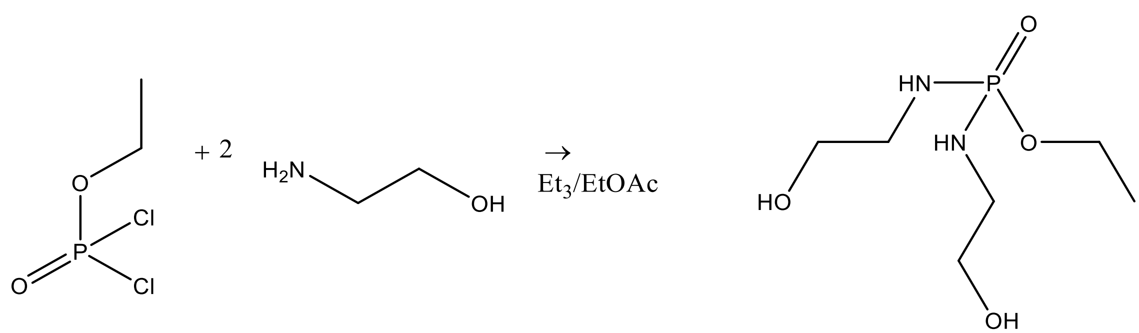

Figure 2: Reaction Scheme for Intermediate Compound 1

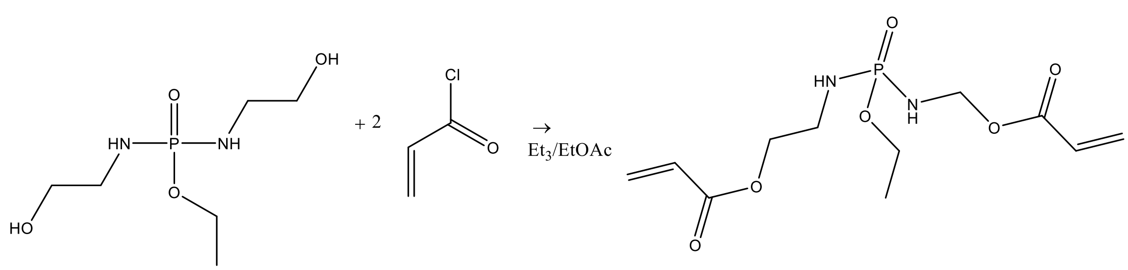

Figure 3: Reaction Scheme for Second Step of Monomer 1 Synthesis

For the second step, the filtrate and another 2.46 mL of TEA were added to a RBF on ice. An excess of AOC, 1.45 mL (0.018 mol), was dissolved in EtOAc in the addition funnel and again added dropwise to the mixture. The reaction scheme for monomer 1 can be seen in Figure 3, and a graphic representation of the monomer is shown in Figure 4.

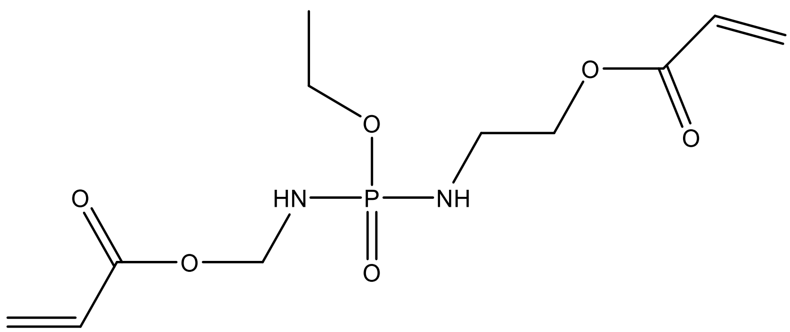

Figure 4: Monomer 1, Methyl di(acryloyloxyethyl)phosphorodiamidate (EDAEP)

3.3.4 Monomer 2 and 3 Synthesis

Monomer 2 was also previously developed in Dr. El-Shafei’s lab using DCM as a solvent for application onto cotton fabrics. The reaction began on ice, with 20 mL of EtOAc, 2.46 mL TEA, and 0.723 mL EA added to the RBF. 0.720 mL (0.006 mol) of DMPDC was dissolved in another 20 mL EtOAc and added dropwise with the addition funnel. The reaction scheme for this intermediate is shown in Figure 5. This intermediate was also used to synthesize monomer 3.

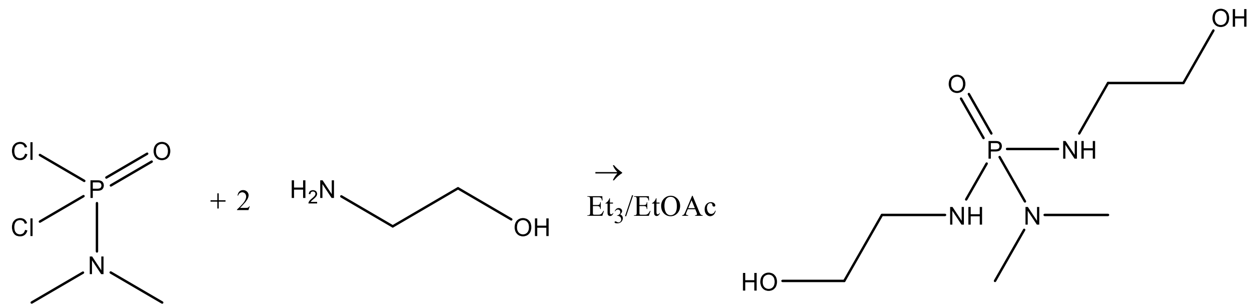

Figure 5: Reaction Scheme for Intermediate Compound for Monomers 2 and 3

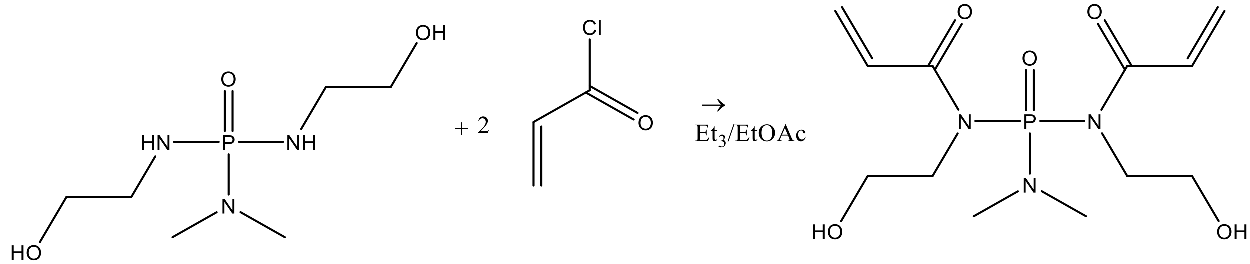

Figure 6: Reaction Scheme for Second Step of Monomer 2 Synthesis

After vacuum filtration, the filtrate was added to a clean RBF with 2.46 mL TEA and put into an ice bath. AOC was added in excess again, with 1.45 mL dissolved in 20 mL EtOAc and added dropwise via the addition funnel. The reaction scheme for the second step of monomer 2 is shown in Figure 6, and the molecule can be seen in Figure 7.

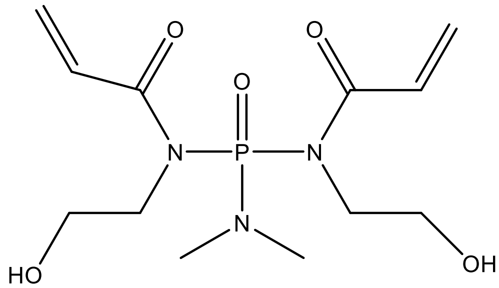

Figure 7: Monomer 2 N,N-dimethyl di(acryloyloxyethyl) phosphorodiamidate (DMDAEP)

Monomer 3 was synthesized using the same procedure as monomer 2 with different stoichiometric ratios. In step two, four equivalents of AOC, 2.44 mL (0.024 mol) were added to double the amount of functional groups available for graft polymerization. The stoichiometric ratio of TEA was also increased to capture the additional hydrochloride salt produced from the additional addition reactions that occur; 4.11 mL (0.30 mol) TEA were added. This reaction scheme is seen in Figure 8. The final monomer can be seen in Figure 9.

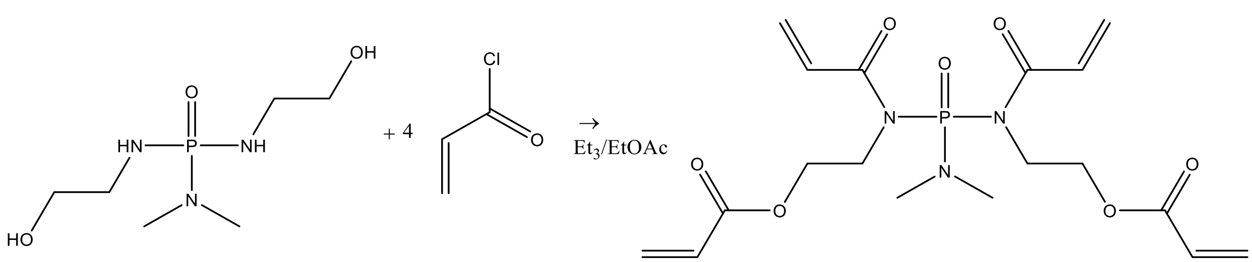

Figure 8: Reaction Scheme for Second Step in Synthesis of Monomer 3

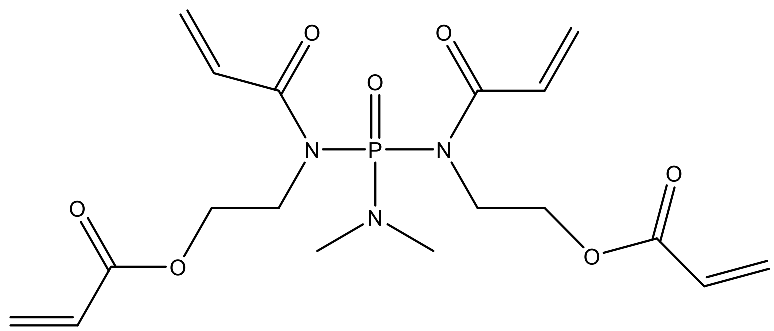

Figure 9: Monomer 3 N,N- dimethyl di(acryloyl acryloyloxyethyl)phosphorodiamidate (DMDAAEP)

3.3.5 Monomer 4 Synthesis

There is a greater percentage of nitrogen and a much lower percentage of oxygen in monomer 4. In the initial step, 0.800 mL (0.012 mol) of ED, 20 mL EtOAc, and 2.46 mL TEA were added to the round bottom flask on ice. 0.72 mL DMPDC dissolved in 20 mL EtOAc was added dropwise and the reaction was carried out similar to the first three reactions for 1 hour on ice, and 3 additional hours at room temperature. The reaction scheme can be seen in Figure 10, and the intermediate structure is shown in Figure 11. The same intermediate was used for the synthesis of monomer 5.

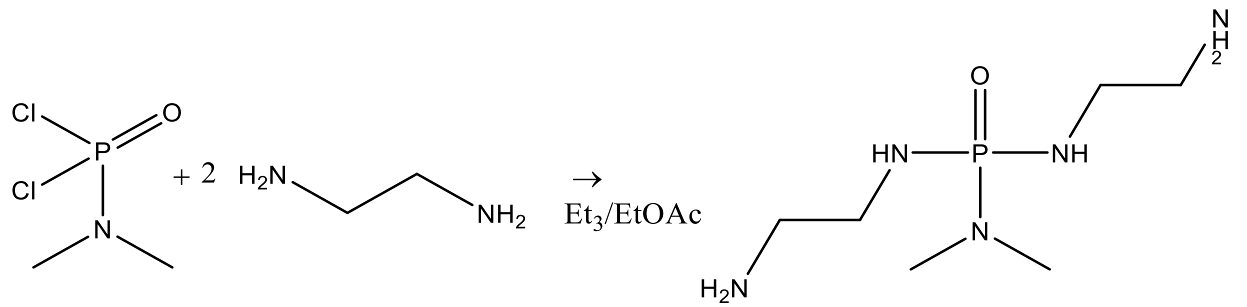

Figure 10: Reaction Scheme for Intermediate Compound for Monomers 4 and 5

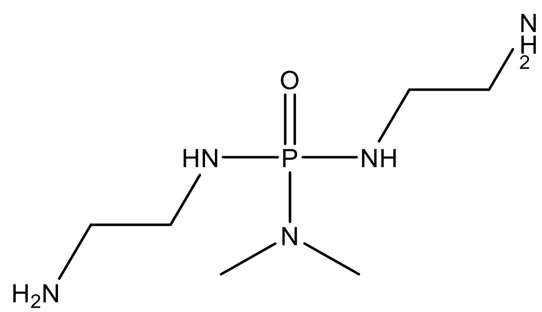

Figure 11: Intermediate Compound for Monomers 4 and 5

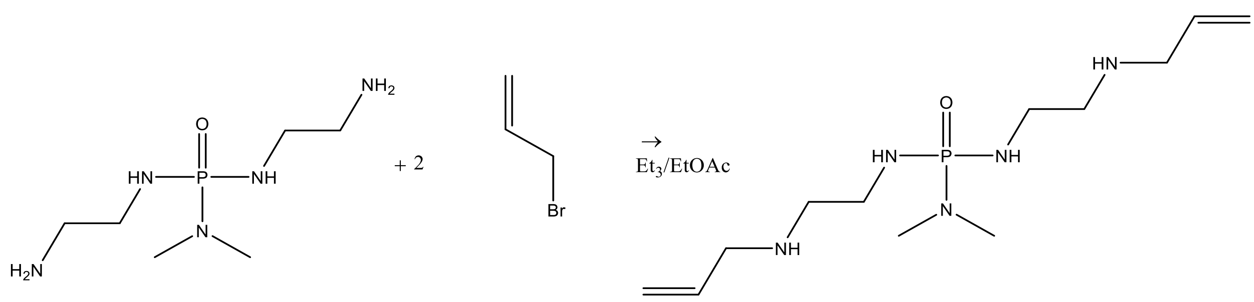

Figure 12: Reaction Scheme for Second Step in Synthesis of Monomer 4

Several different approaches were used to synthesize the desired molecule in the second step. For all attempts, the filtrate was added to a clean RBF with 2.46 mL TEA. Different approaches were used to add the allyl group. First, 0.814 mL (0.018 mol) AC was added and heated to 60°C for 48 hours. The next attempt again added 0.814 mL AC, and also 0.02 g copper (1) chloride as a catalyst. Again the mixture was heated to 60°C and allowed to react for 23 hours. For the final attempt, 0.73 mL (0.018 mol) AB was added. The bromine is less electronegative and thus more reactive than the chloride molecule. The reaction was conducted at room temperature for 30 hours. The reaction scheme is shown in Figure 12, and the monomer is depicted in Figure 13.

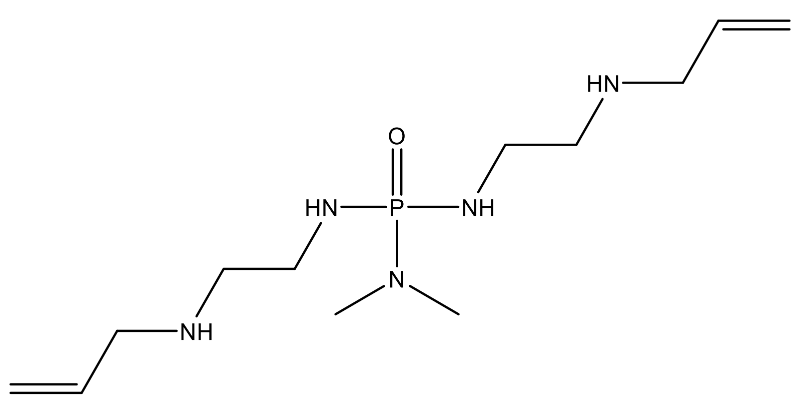

Figure 13: Monomer 4 N,N- dimethyl di(allylethylamine)phosphorodiamidate (DMDAEAP)

3.3.6 Monomer 5 Synthesis

Monomer 5 is synthesized using the same intermediate at monomer 4. However, in the second stop, three equivalents of AOC (1.45 mL) were added rather than AB, increasing the oxygen content of the monomer. The chemical equation is shown in Figure 14. AOC was much more reactive with the intermediate than AB, and thus was added dropwise dissolved in 20 mL EtOAc and reacted at 0°C for 1 hour and at room temperature overnight. The final product can be seen in Figure 15.

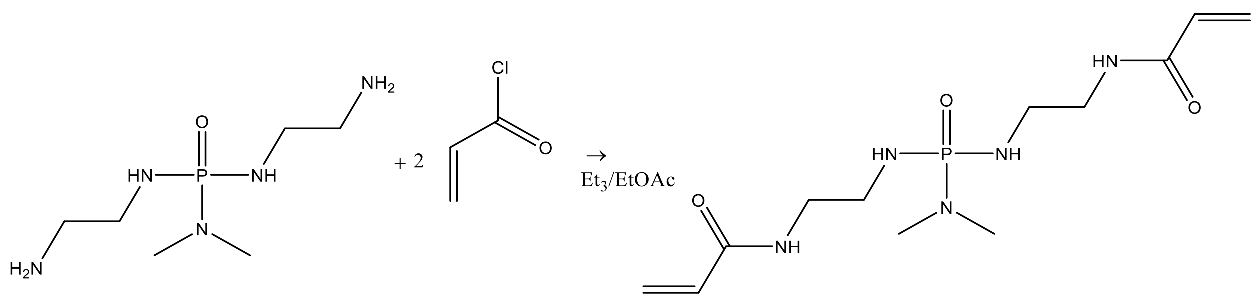

Figure 14: Reaction Scheme for Second Step in Synthesis of Monomer 5

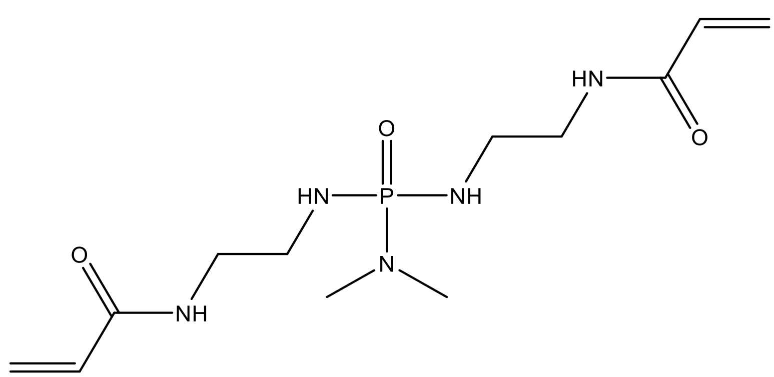

Figure 15: Monomer 5 N,N- dimethyl di(allyl allylethylamine)phosphorodiamidate (DMDAAEAP)

3.3.7 Monomer 6 Synthesis

Monomer 6 has the greatest nitrogen to phosphorus ratio. To synthesize monomer 6, 20 mL EtOAc, 0.376 mL (0.012 mol) HZ, and 2.46 mL TEA were added to the RBF on ice, and 0.720 mL DMPDC was dissolved in 20 mL EtOAc and added dropwise. The chemical equation for the intermediate is present in Figure 16, and the intermediate chemical structure is depicted in Figure 17. The reaction proceeded at 0°C for 1 hr and at room temperature for 3 hours.

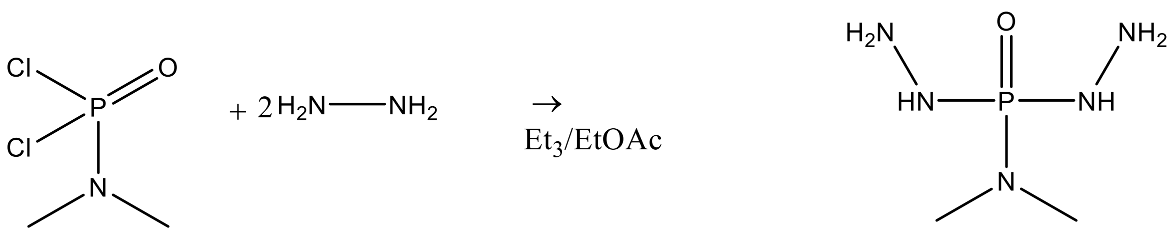

Figure 16: Reaction Scheme for Intermediate Compound for Monomer 6

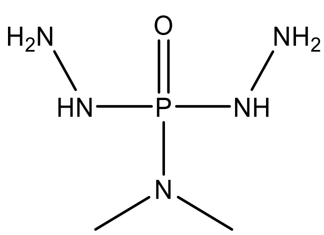

Figure 17: Intermediate Compound for Monomer 6

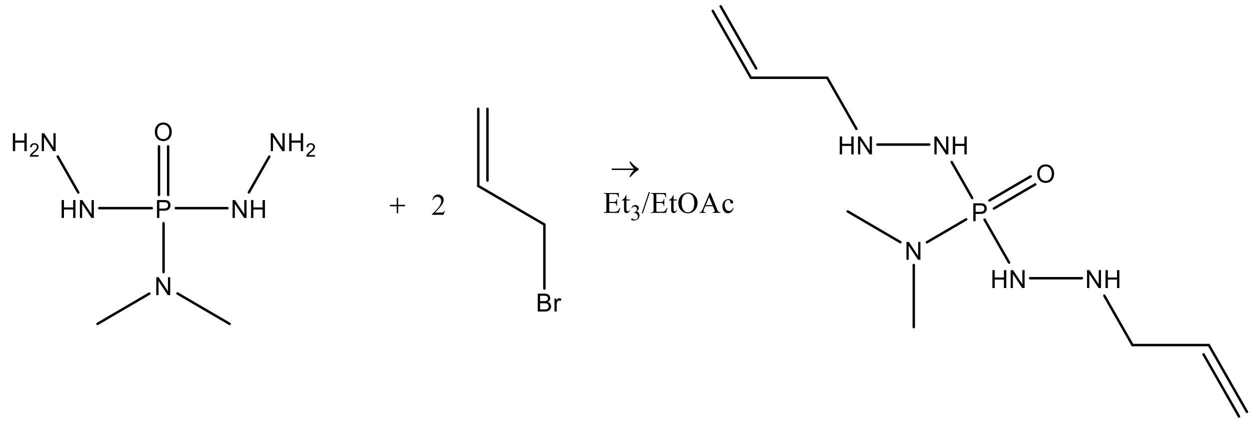

Figure 18: Reaction Scheme for Second Step in Monomer 6 Synthesis

For the second step, the filtrate from step 1, 0.730 mL AB and 2.46 mL TEA were added to a clean RBF under constant stirring and the reaction proceeded at room temperature overnight. The reaction scheme is shown in Figure 18, and the monomer can be seen in Figure 19.

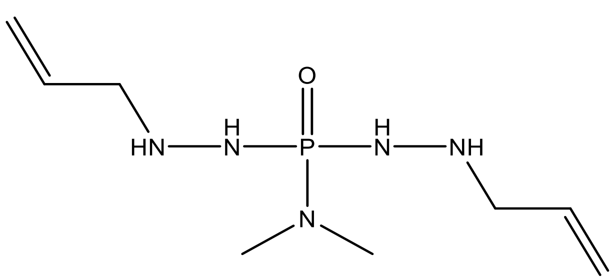

Figure 19: Monomer 6 N,N- dimethyl di(allylamine)phosphorodiamidate (DMDAAP)

3.4 Characterization

All monomers were characterized with FTIR analysis and NMR analysis. The FTIR was carried out on a Nicolet Nexus 470 spectrophotometer equipped with an Avatar OMNI-Sampler using the attenuated total reflectance (ATR) sampling technique, and ^{31}P and ^{1}H NMR was conducted at room temperature on a Bruker 500 MHz spectrometer using $CDCl_3$ (deuterated chloroform) as a solvent and TMS as a reference for the proton NMR.

3.5 Crosslinker Determination

Because polypropylene has no oxygen in its structure, a separate char-forming agent is needed for a condensed phase flame retardant mechanism in which the phosphorous containing molecule crosslinks the polymer with hydroxyl group linkages. Pentaerythritol is commonly extruded with polypropylene to provide this agent. However, pentaerythritol has no functionality, and thus cannot be graft polymerized onto the polypropylene fibers. Thus, several crosslinkers available in the lab were tested for their char forming ability: pentaerythritol (PA), laurel acrylate (LA), 3-(trimethoxy-silyl)-propyl methacrylate (TPM), pentaerythritol triacrylate (PA3), pentaerythritol tetracrylate (PA4), and 1-(acryloyloxy)-3-(methacryloyloxy)-2-propanol (AM) were tested. Each had hydroxyl groups or oxygen in its structure which could combine with the phosphorus to form phosphoric acid upon combustion, and also functional groups for free radical graft polymerization.

Each crosslinker was tested in conjunction with monomer 5. A bath was made of 40% monomer 5, 10% crosslinker, 5% photoinitiator (irgacure provided by BASF), and 45% solvent. Water was used as the solvent for PA, LA, and TPM, while acetone was used as the solvent for PA3, PA4, and AM. Each mixture was pad applied to 50 gsm spunbond polypropylene, then cured with the UV lamp for 25 seconds on each side at 100% lamp intensity. A simple vertical flame test was conducted on each of the samples to visually determine char formation. A flame was held under the sample for 3 seconds, and burn time and appearance were recorded.

PA3 and PA4 were both adequate char forming agents because they were able to form a char which maintained the original structure of the polypropylene. Thus, samples were prepared for a TGA test to determine which crosslinker was more effective. The samples were prepared with a monomer:crosslinker ratio of 1:1 using monomer 5, and 100% add-on. 0.1 g of photoinitiator was added. The samples were cured under the UV lamp for 50 seconds on each side at 100% intensity.

3.6 Application

After purification, each monomer was applied to 50 gsm spunbond nonwoven PP and PET. The first set of samples were prepared to evaluate FR behavior. Each neat PP and PET sample was weighed, and a bath was made with the correct ratio of solvent (acetone), crosslinker (PA3), monomer, and photoinitiator (BASF Irgacure 814). The photoinitiator was used to initiate the free-radical graft polymerization reaction, and was added at 20% of the total weight of the monomer and crosslinker as both had functional groups to undergo graft polymerization to the substrates. Different ratios of monomer to crosslinker were tested with 20%monomer:80%crosslinker, 50%monomer:50%crosslinker, and 80%monomer:20%crosslinker to determine the best ratio for FR. The monomer is required to slow or extinguish the flame, while the crosslinker is necessary to promote char formation. All ratios were tested on all samples. The add-on percentage was also varied at 30% add-on, 50%

add-on, and 100% add-on to determine the lowest possible add-on while still achieving the necessary FR behavior. Separate baths were made for each swatch, and each swatch of fabric was 3”X4”. Samples were placed in the baths, padded to push the solution through the fabric and allowed to dry. They were exposed to UV light to initiate the graft polymerization of the substrate using a Uvitron Intelli-ray 600 shuttered UV Flood Light. The samples were exposed to 100% intensity UV light for 50 seconds on each side. A design of experiment (DOE) was created using JMP Pro 10 Software for a full factorial experiment with two center points. A table showing the different conditions for each sample is shown in Table 2, and each condition was recreated for each monomer.

A second set of samples was prepared to evaluate the polymerization yield. Again, individual baths were made for each sample. The monomer:crosslinker ratio was held constant at 50%monomer:50%crosslinker and all coatings were applied at 75% add-on. In these experiments, photoinitiator percentage was varied from 5%, 10% and 20% of the monomer and crosslinker amount. The UV exposure time was varied with samples tested at 30 seconds for each side, 60 seconds for each side, and 100 seconds for each side. Samples were made again using 50 gsm spunbond nonwoven PP and PET, with each swatch measuring 1.5”X4”. The same pad application method was used as described above. Again, the DOE was obtained from a full factorial experiment with two center points from JMP Pro 10 software. Table 3 describes the conditions for each sample.

Table 2: Conditions for Burn Tests for Each Monomer

Sample Number	%Monomer	%Crosslinker	%Add-on
1	20	80	50
2	20	80	50
3	50	50	75
4	80	20	50
5	80	20	100
6	50	50	50
7	20	80	75
8	20	80	50
9	20	80	75
10	50	50	100
11	80	20	75

Table 3: Graft Polymerization Optimization Conditions

Sample Number	UV Exposure	% Photoinitiator
1	100	20
2	30	10
3	60	5
4	60	5
5	30	5
6	30	20
7	100	10
8	100	5
9	30	5
10	60	10
11	60	20

3.7 Flame Evaluation of Monomers

A simple vertical flame test based on the ASTM D 6413-08 test method was conducted. For each of the samples prepared with the conditions in Table 2, the fabrics were weighed, then placed in a stand which held the samples vertically and clamped them in place at the sides. A butane torch was held below the sample for 3 seconds, and then removed at which time a stopwatch was started. The time was recorded until the afterglow stopped, and the sample was reweighed to evaluate char formation. Most samples burned to the top of the substrate, but for the samples in which the flame self-extinguished, the sample was relighted for an additional 3 seconds twice. If the sample still did not burn, the length of the char was measured and recorded.

Using the results from the previous step, the monomer:crosslinker ratio that had the best flame retardant performance was used to conduct a TGA test on a Perkin Elmer Pyris 1 TGA. Each sample was obtained at the value of 100% add-on. The samples were tested in air from 30 to 600°C at a heating rate of 20°C/min.

3.8 Evaluation of Graft Polymerization Yield

The samples outlined in Table 3 were conditioned by leaving them exposed to the air overnight and then weighed. A soxhlet extraction was set up with acetone, and the set-up is shown in Figure 20. The soxhlet extraction was continued for 4 hours before the samples were removed and allowed to dry overnight before being weighed again. The coating yield was calculated by subtracting the final weight from the initial weight and dividing that number by the initial weight, and subtracting the entire value from 1. All monomers were soluble in acetone, and thus it was assumed that any ungrafted coating was removed by the acetone.

To see the coating on the substrates, scanning electron microscopy (SEM) images were obtained from a Hitachi S3200N Variable Pressure Scanning Electron Microscope with: an Everhard-Thronley secondary electron detector, a Robinson backscattered electron detector, an Oxford energy dispersive x-ray spectrometer, and a GW specimen current meter. This instrument generated surface images of the various samples and also indicated some of the elements present in different select regions of the samples. Images were obtained of sample 1 for each monomer on both substrates after the soxhlet extraction at 50X and 250X magnification.

Figure 20: Soxhlet Extraction Apparatus

4 RESULTS AND DISCUSSION

4.1 Synthesis and Characterization of Monomer 1

Both steps in the synthesis of monomer 1 were exothermic, and resulted in a white triethylamine hydrochloride salt formation. The intermediate for this compound is clear, and the final product is light yellow and slightly viscous. The reaction was first carried out with dichloromethane, and then was retried using EtOAc as a solvent to decrease the environmental impact of the synthesis.

4.1.1 Monomer 1 and Intermediate 1 FTIR Analysis

Both FTIR and NMR spectra were taken to characterize the intermediate of monomer 1. In the FTIR analysis, many of the peaks confirm the presence of the expected functional groups. The peak at 3276.3 cm^{-1} is indicative of both either the N-H in secondary amines, or the O-H stretching. Likely, the peak for both of these functional group is encompassed with this broad peak. The strong peak at 2920.2 cm^{-1} is representative of the C-H stretching in aliphatic carbons. In the fingerprint region of the FTIR, the peak at 1212.8 cm^{-1} is indicative of the C-C-N bending, while the relatively stronger peak at 1039.4 wave numbers is indicative of the P-O-C antisymmetric stretching. Table 1 highlights these values, and Figure 1 is the FTIR spectrum obtained.

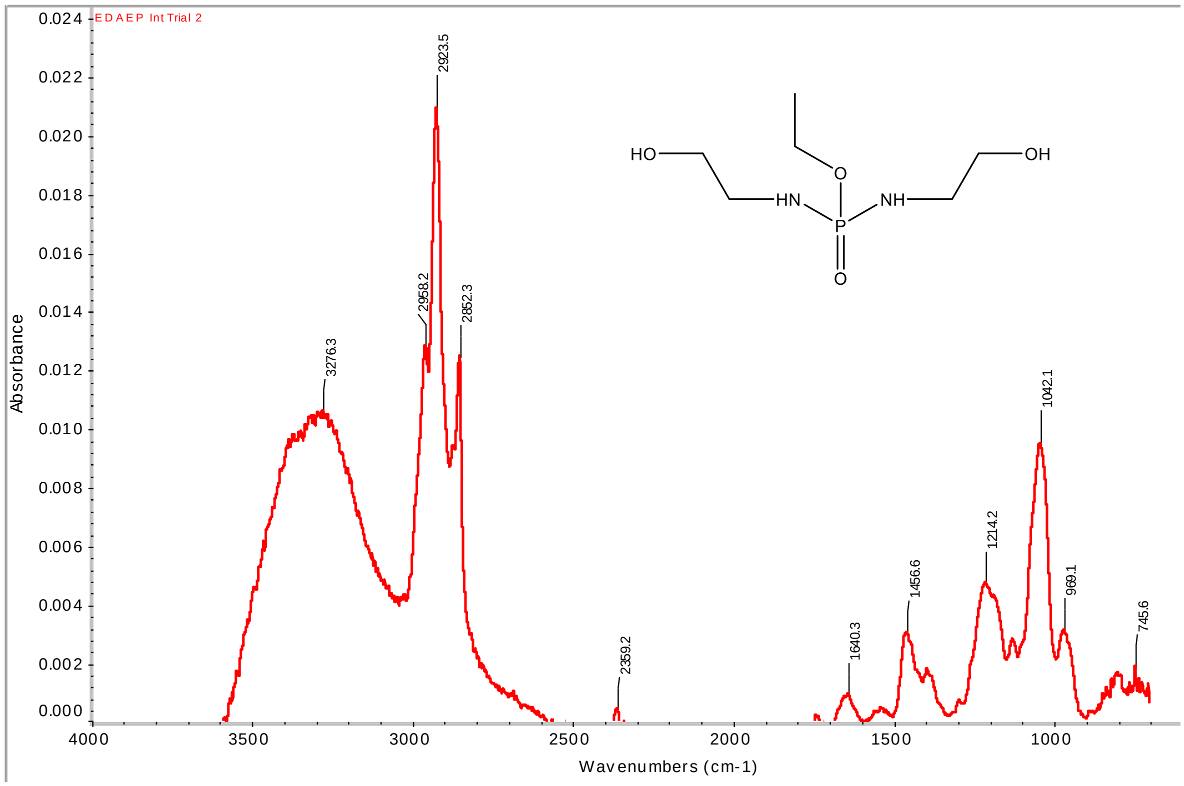

Figure 1: FTIR Spectrum of Intermediate 1

Table 1: Assignment of FTIR Peaks, Intermediate 1

Peak	Assignment
3276.3	N-H in secondary amines
2920.2	CH_3 in aliphatic compounds
1212.8	C-C-N bending
1039.4	P-O-C antisymmetric stretching

FTIR analysis also confirmed the presence of certain functional groups to support the suggested structure of monomer 1. The FTIR spectrum of monomer 1 prepared using DCM as a solvent is shown in Figure 2. These are shown below with charts assigning peaks. The peaks support the structure as shown. Particularly, the peak at 1721 cm^{-1} showing the carbonyl of the ester supports that the nitrogen of EA bonded to the phosphorus, and the AOC bonded to the end hydroxyl group as shown above. The monomers were re-analyzed after the solvent switch to ensure that there were no changes in structure with the new solvent, and this spectrum is shown in Figure 3. There are some differences in the intensity and broadness of peaks, however the peaks appear in the same places indicating that the same functional groups are present. The spectrum in ethyl acetate may have broader peaks due to residual ethyl acetate as it is less volatile than DCM. If ethyl acetate were present, we could expect some hydrogen bonding which would broaden the peak at the left of the FTIR spectrum. However, the peaks are still very similar in the fingerprint region of the FTIR.

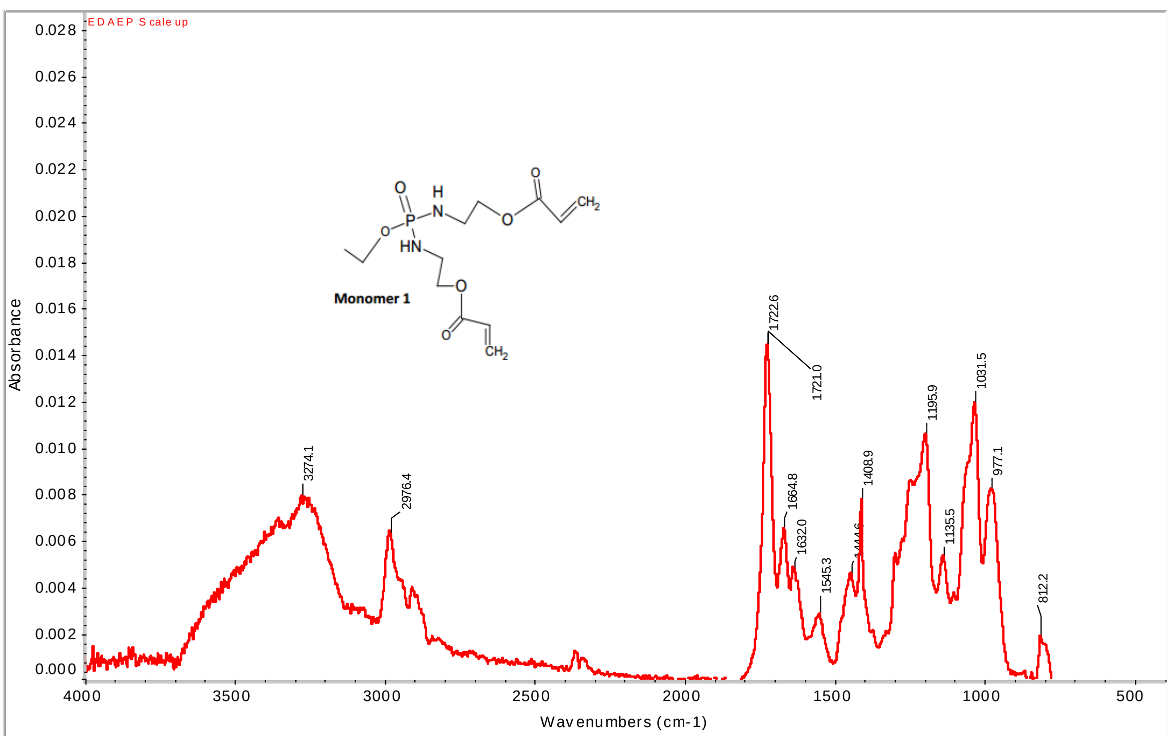

Figure 2: FTIR Spectrum of Monomer 1 Synthesized in Dichloromethane

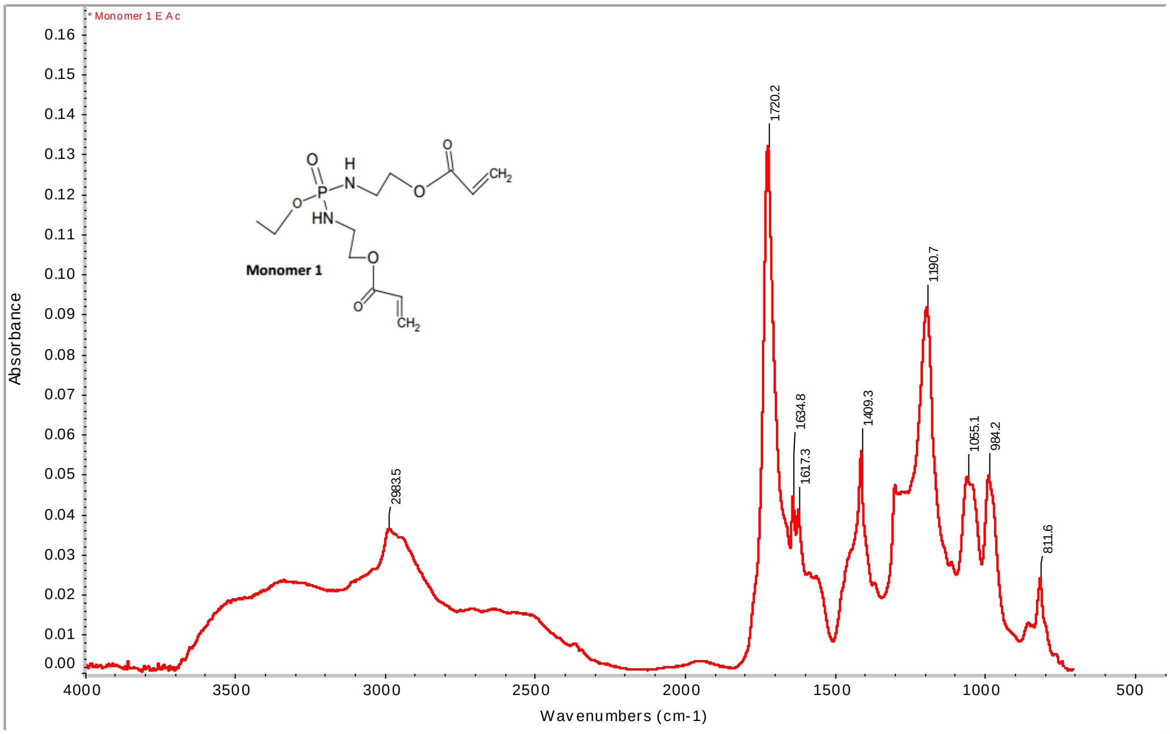

Figure 3: FTIR Spectrum of Monomer 1 Synthesized in Ethyl Acetate

Table 2: Assignment of FTIR Peaks, Monomer 1

Peak	Assignment
3274.1	N-H in secondary amines
2975.4	CH_3 in aliphatic compounds
1721.0	Carbonyl of an Ester
1195.9	Phosphorus bonded to Oxygen
1002.5	C-O-C of ester
812.4	$CH=CH_2$ in vinyl ethers

4.1.2 NMR Analysis of Monomer 1 and Intermediate 1

^{1}H and ^{31}P scans were carried out for the starting materials, intermediates, and final products of the FR compounds. The ^{31}P scan for the starting materials, EDCP and DMPDC can be seen below in Figure 4. EDCP was used to make monomer 1, and DMPDC was used to synthesize monomers 2-6. The DMPDC is very pure, with a peak at 19.28ppm. EDCP has a major peak at 6.66 and few secondary smaller peaks, indicating that there are some phosphorus impurities in the base material.

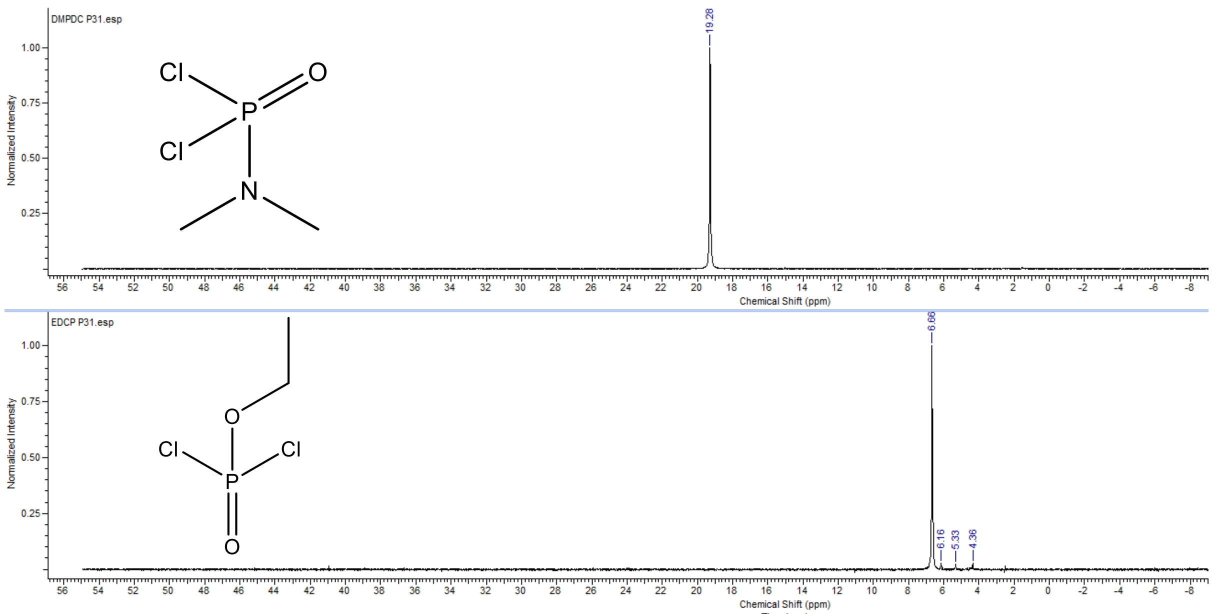

Figure 4: ^{31}P NMR Scan of Starting Materials EDCP and DMPDC

^{31}P NMR scans were also taken of the intermediate and final product for monomer 1 and shown in Figure 5. The intermediate and EDCP phosphorus peaks are in different areas indicating that a reaction took place in the first step of the monomer synthesis. There is a lot of noise around the large phosphorus peak in the final product, indicating that there are impurities containing phosphorus in the sample. This peak is also in about the same place as the intermediate peak at about 9.8 ppm with secondary peaks at 1 ppm and 15 ppm. The cause of these impurities is unknown, but may be due to premature degradation of the molecule or small side reactions with the phosphorous. The phosphorus peaks may incidentally be in about the same location; ^{1}H NMR supports that there are terminal alkenes in the structure in the final product, but not in the intermediate.

However, the ^{1}H NMR scan of the intermediate is difficult to interpret. There appear to only be two sets of protons. The peaks at 0.99 integrate to 3 and are consistent with the terminal methyl group. The peaks at 2.51 integrate to 2 and are consistent with the hydrogen molecules on the carbon alpha to the oxygen. There is only a small peak at 5.21 which is about peaks for the carbons alpha to the hydroxyl and amino group would be found. These peaks appear to be shielded heavily by the presence of the two functional groups. The NMR spectra are seen in Figure 6.

^{1}H NMR scans were also taken for the final product. For the final product, it is difficult to draw specific integration information from the spectrum. This may be a result of the impurities, or a result of the interaction of NMR active nitrogen and phosphorus with the neighboring protons. However, there are clusters of peaks where we would expect to see peaks in this structure based on the algorithm used by ChemDrawPro 13. Specifically, there are clusters of peaks centered around 6.4 ppm, 6.2 ppm and 5.58 ppm which likely correspond to the alkenic protons. The ^{1}H NMR spectra can be seen in Figure 6, with Table 3 labelling the center of the peak clusters for monomer 1.

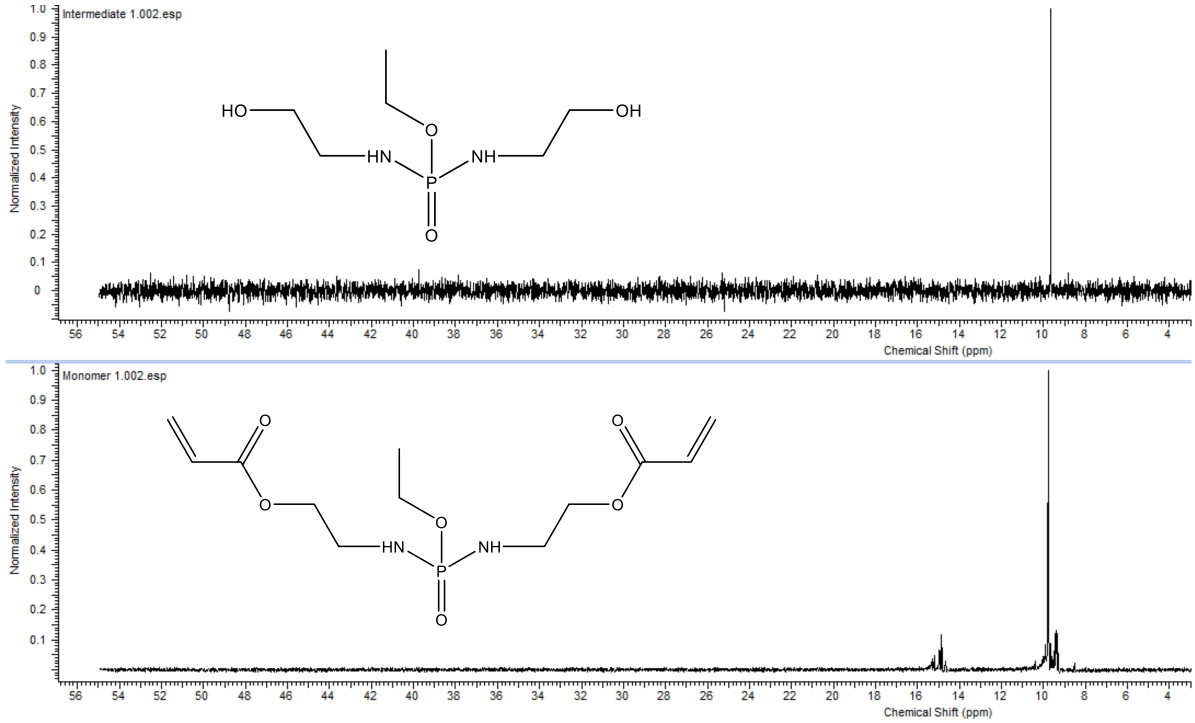

Figure 5: ^{31}P NMR Scans of Monomer 1 Intermediate and Monomer 1

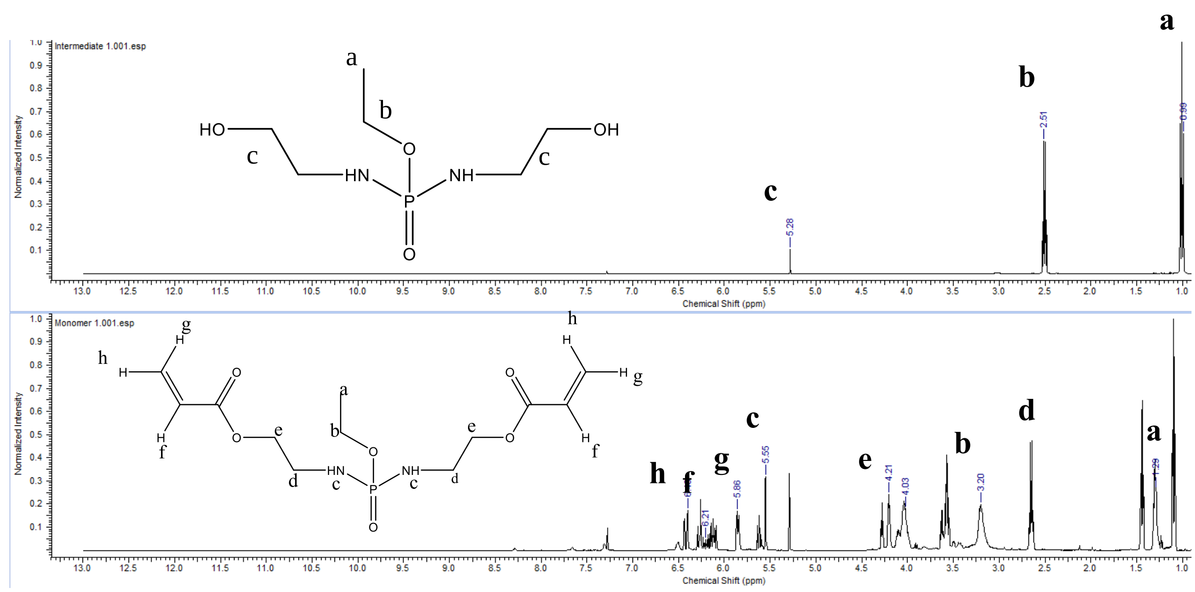

Figure 6: ^{1}H NMR Scans of Monomer 1 Intermediate and Monomer 1

Table 3: Assignment of ^{1}H Peaks: Monomer 1

Protons	Center of Peaks	Protons	Center of Peaks
A	1.29 ppm	e	4.20 ppm
B	4.01 ppm	f	6.21 ppm
C	5.89 ppm	g	5.58 ppm
D	2.93 ppm	h	6.42 ppm

4.2 Characterization Monomers 2 and 3

The synthesis and characterization of monomers 2 and 3 will be discussed simultaneously because it was determined that both resulted in creating the same final molecule. Both steps in this synthesis are exothermic and result in a white salt formation. The intermediate is a clear liquid, and the final product is an orange viscous liquid. The salt formed in the second step seems to have an affinity for the final product, and it is important to flush the salt with extra solvent to ensure that the monomer is not filtered out of the final product.

4.2.1 FTIR Analysis Intermediate 2-3

The broad doublet at 3391.0 cm^{-1} and 3271.8 cm^{-1} is indicative of the O-H and N-H stretching frequencies respectively, while the peak at 2923.8 cm^{-1} again represents the C-H stretching of aliphatic carbons. Importantly, no carbonyl peak is present, and the weak signal at 1650.7 cm^{-1} could indicate the N-H bend in primary amines. There is a very strong peak at 994.9 cm^{-1} that could be an indication of the C-O stretch in primary alcohols. The FTIR spectrum for the intermediate compound for monomers 2 and 3 is shown in Figure 7, and Table 4 assigns values for the various peaks.

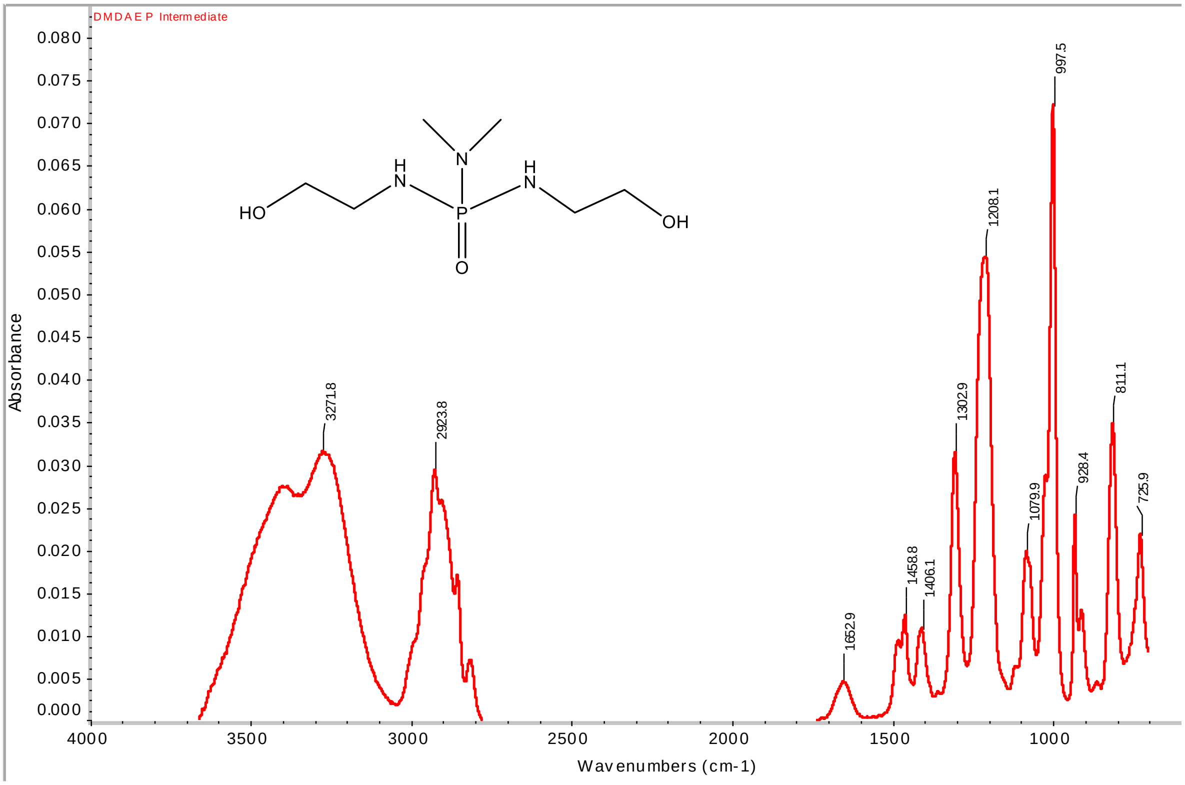

Figure 7: FTIR Spectrum for the Intermediate Compound for Monomers 2 and 3

Table 4: Assignment of Peaks for Intermediate Compound for Monomers 2 and 3

Peaks	Assignment
3391.0	O-H stretch
3271.8	N-H stretching
2923.8	C-H stretch in aliphatic carbons
1650.7	N-H in primary amines
1302.9	P=O
1208.1	C-C-N bending
994.9	C-O stretch in primary alcohols

4.2.2 FTIR Analysis Monomers 2 and 3

Again, FTIR was recompleted using ethyl acetate as a solvent to ensure that the same compound was made. These two FTIR spectra can be seen in Figures 8 (dichloromethane solvent) and 9 (ethyl acetate solvent).Though the intensities of the peaks at 3437 cm^{-1} and 2910 cm^{-1} are slightly more intense, they still represent the C-H stretch of the alkene most likely overlain with O-H stretch of the hydroxyl group. All of the peaks to the right further confirm the structure shown and are exceedingly similar in both spectra, indicating that the structure was not changed with a change of solvent. The peak at 1653 cm^{-1} indicates a carbonyl of an amide, which suggests that the structure is as shown. The peak at 1410.3 cm^{-1} further supports the presence of the hydroxyl group. Table 5 assigns these peaks. The spectrum for monomer 3 is not shown. It is extremely similar to the spectrum for monomer 2, and NMR analysis confirmed that monomer 3 and monomer 2 are the same compound, as will be explained below.

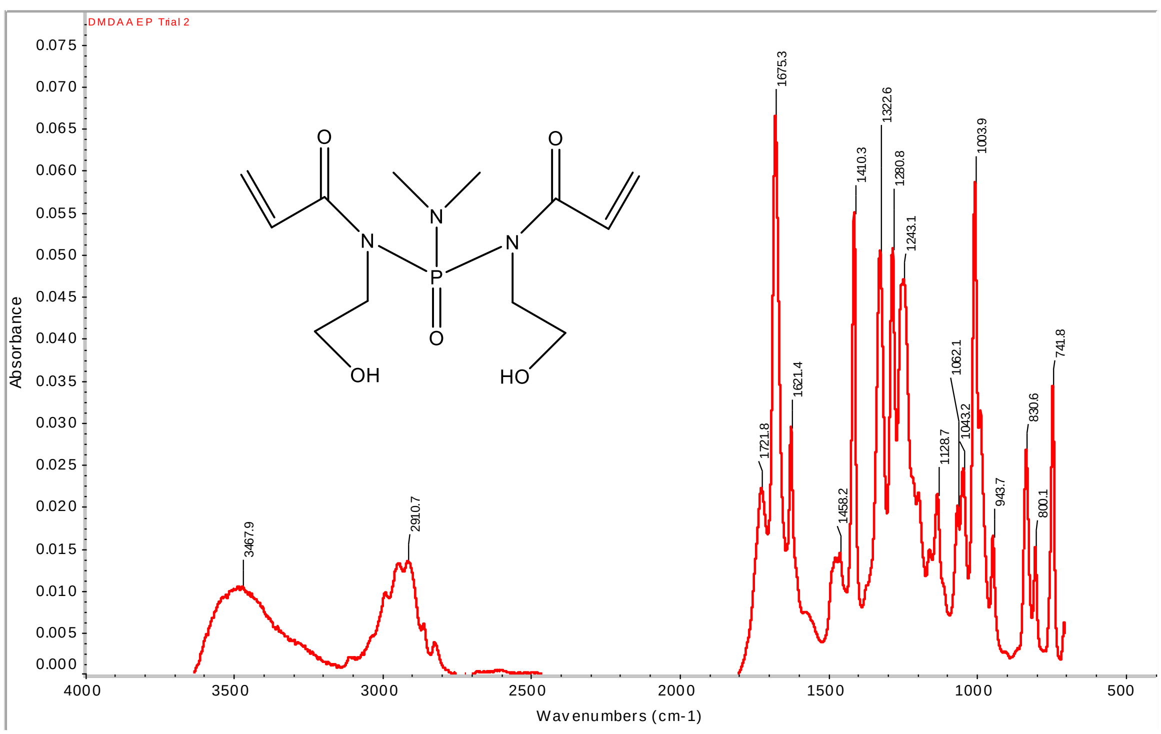

Figure 8: FTIR Spectrum of Monomer 2 Synthesized in Dichloromethane

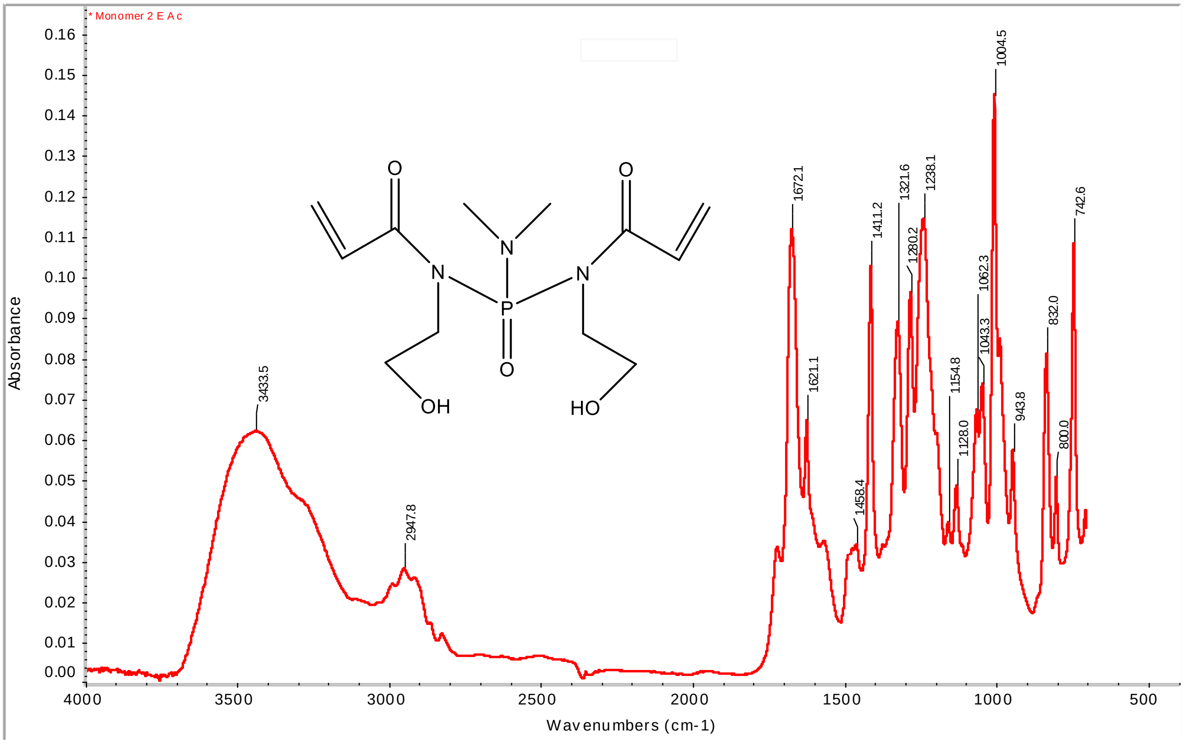

Figure 9: FTIR Spectrum of Monomer 2 Synthesized in Ethyl Acetate

Table 5: Assignment of FTIR Peaks, Monomer 2

Peaks	Assignment
3471.8	C-H stretch in $CH=CH_2$, O-H stretch in hydroxyl group
1673.8	Carbonyl of an amide
1410.7	Hydroxyl group
1280.6	P=O
1003.3	$CH=CH_2$

4.2.3 NMR Analysis of Monomer 2 Intermediate and Monomer 2

The NMR analysis of Monomers 2 and 3 was very useful. The ^{31}P scan shows a clear difference between the phosphorus peak for the starting material (19.28 ppm) and intermediate (30.90 ppm), and then intermediate and final product (17.47 ppm) as shown in Figure 30. However, the final product peaks for monomers 2 and 3 are in the same place (17.47 ppm and

17.42 ppm respectively), indicating that they are the same molecule. In the spectrum for monomer 2, there is a small peak at 30.40 ppm indicating that there is some unreacted intermediate in the sample. However, this peak is absent in the spectrum for monomer 3. Thus, it can be assumed that the third and fourth AOC molecules are not reacting with hydroxyl group, and monomer 3 was not successfully synthesized. Further, it is likely that some of the AOC is hydrolyzed by water vapor in the air as it is transferred to the dropper used for addition to the reaction before it is introduced reaction completed under argon, resulting in too few stoichiometric equivalents of this compound in the reaction mixture and thus an incomplete reaction. However, by adding an excess of AOC, the reaction can be driven to completion. Thus, the synthesis was adjusted to include an excess of this material for the synthesis of monomers 1,2, and 5. It is also likely AB is easily hydrolyzed, and thus the synthesis for monomers 4 and 6 was also adjusted to include an excess of AB.

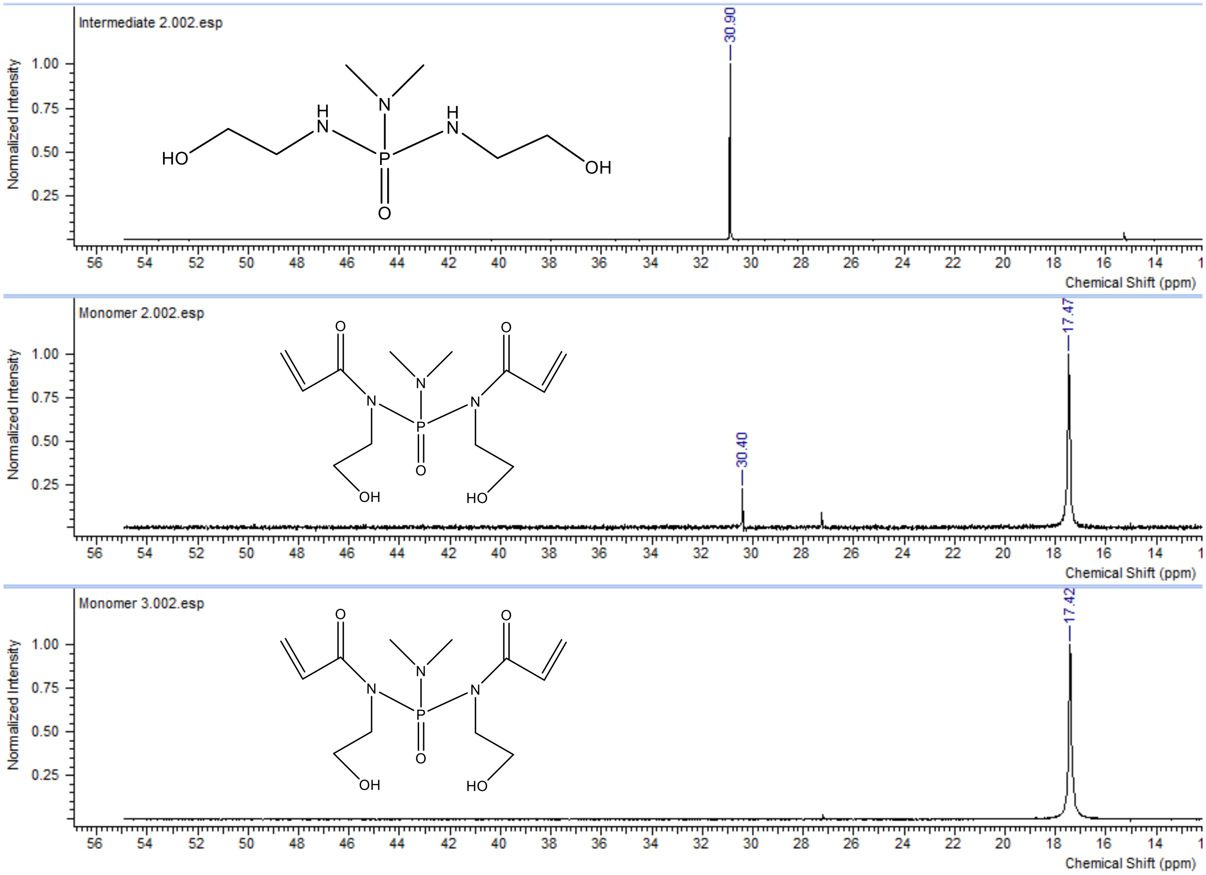

Figure 10: ^{31}P NMR Scans of Monomer 2 Intermediate, Monomer 2 and Monomer 3

An ^{1}H NMR spectrum was needed to determine the structure monomer 2 and the intermediate for monomer 2. It remained to be determined whether the amino or hydroxyl group from the EA bonded to phosphorous. From the ^{1}H NMR of the intermediate shown in Figure 31, there are two separate peaks at 4.27 and 3.56. The peaks are attributed to the N-H and O-H protons, and are likely weak due to the rapid exchange of these protons. However, this evidence supports that the terminal nitrogen of EA bonded with the phosphorous rather than the terminal hydroxyl group, as there would be no O-H indication had the oxygen bonded with the phosphorous.

From the FTIR data of monomer 2, it is clear that a carbonyl of an amide is present, indicating that the acryloyl group has bonded to the nitrogen. Had the oxygen bonded with the phosphorus, a peak would be expected around 8.4 ppm from the remaining proton on the nitrogen. However, no peaks are present in this range in the proton spectrum (see Figure 11). Thus, the structure presented is supported by the NMR and FTIR data. Figure 11 assigns the protons in the structure to the NMR data, and Table 6 outlines the assigned peaks for monomer 2. Again, the NMR scan is not exactly what was expected, but differences in multiplicity may be due to NMR active nitrogen and phosphorous in the sample or possibly a result of impurities.

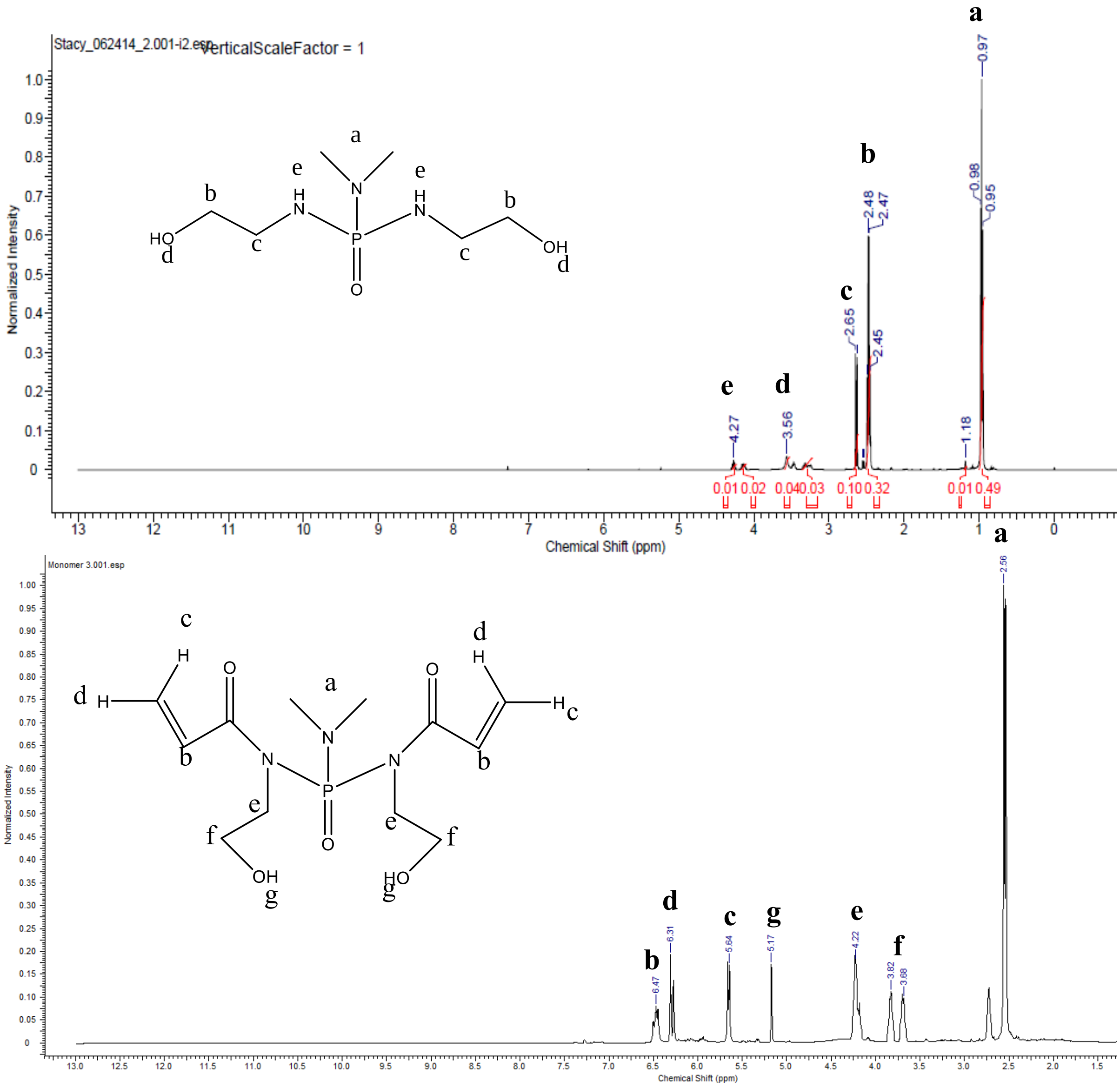

Figure 11: [1]H NMR Scans of the Intermediate Compound of Monomer 2 and Monomer 2

Table 6: Assignment of [1]H Peaks: Monomer 2

Protons	Center of Peaks	Protons	Center of Peaks
A	2.56 ppm	e	3.75 ppm
B	6.47 ppm	f	4.22 ppm
C	5.64 ppm	g	5.17 ppm
D	6.31 ppm		

4.3 Synthesis and Characterization Monomer 4

The synthesis of monomer 4 was difficult and required may iterations. The first step of the reaction is very exothermic and results in a white precipitate and clear liquid intermediate. The first attempt involved reacting AC with the intermediate. The reaction was first carried out at room temperature with no noticeable reaction (no salt formation). The reaction was raised to 60°C and allowed to react for 48 hours, still without noticeable salt formation. In the literature, copper (1) chloride was used successfully as a catalyst for an addition reaction involving AC. [54] Thus, a reaction was attempted using Cu(I)Cl as a catalyst. Again the reaction was conducted at 60°C and left for 48 hours. The resulting liquid was a light green substance, but there was still no salt formation, and thus it was determined that no reaction took place. A final attempt was made using AB in the place of AC. The reaction began at room temperature, and white salt immediately began to form. The reaction continued for 30 hours before being stopped. The final step is not noticeably exothermic in the dilute reaction environment, but if the reaction were to be performed with more concentrated reagents it is unknown if excess heat would become a concern. As AB was added in the second step, the mixture immediately formed salt and began to become yellow and cloudy. The product from this final attempt was characterized and will be described below. Though these changes indicate clearly that a reaction took place in the second step, the NMR results are inconsistent with what was expected.

4.3.1 FTIR Analysis Intermediate Compound for Monomers 4 and 5

An FTIR spectrum was obtained for the intermediate for compounds 4 and 5. Because the intermediate was so volatile, the intermediate would immediately evaporate as it was placed on the crystal for FTIR analysis resulting in a noisy spectrum. However, there are still clear peaks that support the suggested structure of the intermediate. The FTIR spectrum is presented in Figure 12. The broad peak at 3417.7 cm^{-1} is indicative of the N-H stretching of primary and secondary amines. C-H stretching in aliphatic carbons is represented by the peak at 2926.2 cm^{-1}, and the peaks in the 1460-1480 cm^{-1} range could indicate the N-H deformation in secondary amines. The FTIR spectrum supports the suggested structure. Table 7 outlines the values for the FTIR analysis of this intermediate.

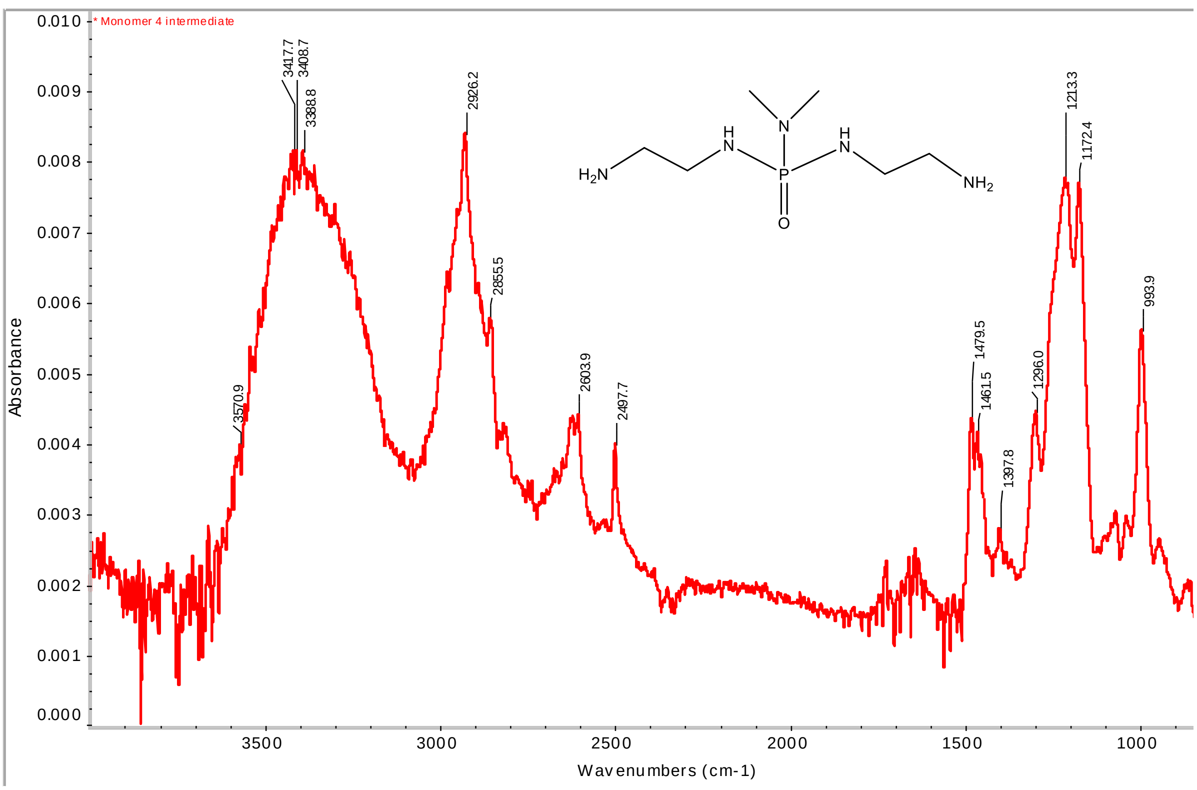

Figure 12: FTIR Spectrum of Intermediate Compound for Monomers 4 and 5

Table 7: FTIR Assigned Peaks for Intermediate Compound for Monomers 4 and 5

Peaks	Assignment
3417.7	N-H stretch in secondary amines
2926.2	CH_2, CH_3 in aliphatic compounds
1479.5	N-H deformation in secondary amines
1213.3	P=O

4.3.2 FTIR Analysis Monomer 4

The FTIR spectrum for Monomer 4 can be seen in Figure 13, and the assignment of peaks is in Table 8. The large peak at 3389.4 suggests that there are N-H stretches, as shown in the structure. This broad peak may also be covering the C-H stretches expected from the terminal alkene. Other peaks can be attributed to other carbon-nitrogen bonds, and the peak at 994.3 can be associated with C=C stretch, and supports the presence of the double bond and functionality of the monomer.

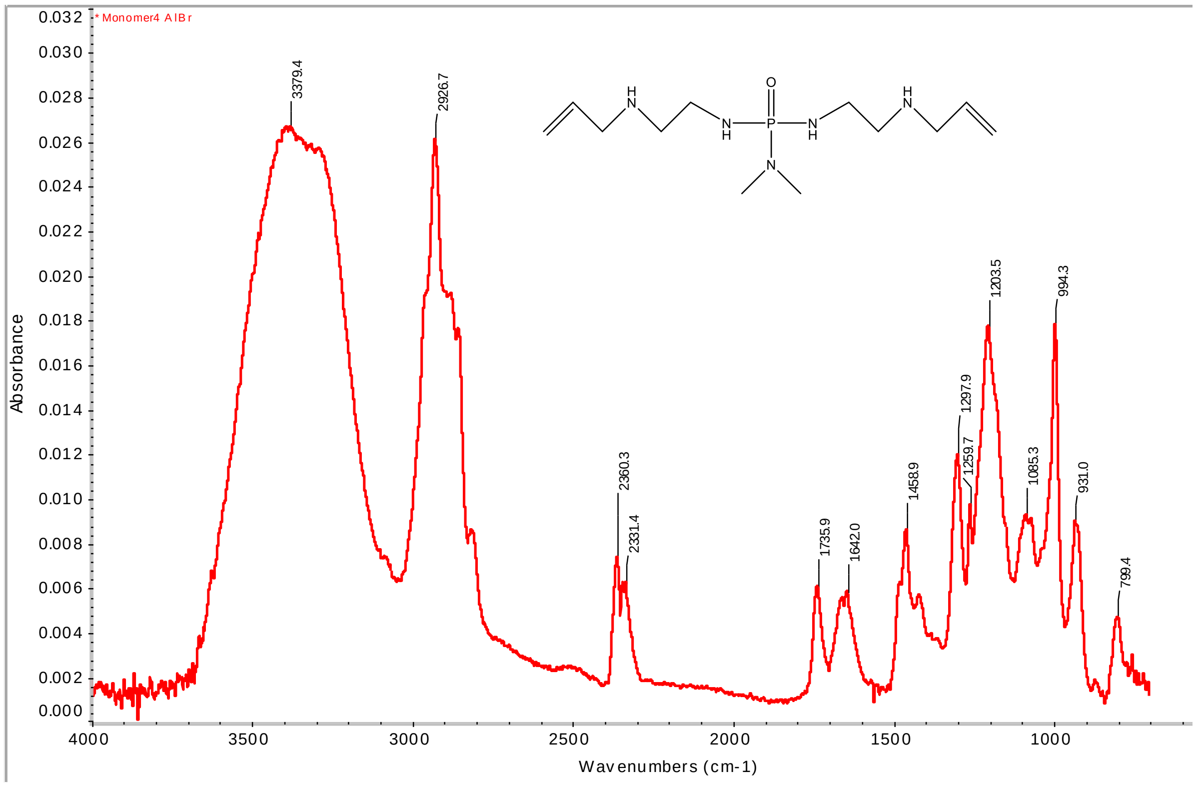

Figure 13: FTIR Spectrum of Monomer 4

Table 8: Assignment of FTIR Peaks, Monomer 4

Peaks	Assignment
3389.4.9	N-H stretch in secondary amines
2926.7	CH_2, CH_3 in aliphatic compounds
1431.3	C-N
1298.8	P=O
1203.4	C-C-N
993.8	$CH=CH_2$

4.3.3 NMR Analysis

The ^{31}P scan indicates that intermediate synthesis was successful. Though there is noise in the scans, there are several peaks that are clearly prominent. There are no phosphorus peaks at 19.3 ppm where the peak for the starting material was present. However, there are several phosphorus peaks, and others may be lost in the noise indicating that the intermediate is not pure. In the final product spectrum, there are fewer peaks, but the peaks that are present are also in the intermediate spectrum at 32.9 ppm, 31.0 ppm, 29.6 ppm, and 10.9 ppm. Both nitrogen molecules in the EDA used in this reaction have an equal affinity for phosphorous, and thus a type of polymer-like chain may be formed in which the intermediate makes up a monomer which polymerizes into a chain. Because there are fewer phosphorous peaks in the final spectrum, it seems that there are more stable chain lengths in this molecule as the reaction is allowed to continue. This suggests that the reaction may need more time or possibly heat to continue to completion. There is one new phosphorus peak at 13.67 indicating a reaction between the intermediate and AB. The ^{31}P spectrum can be seen in Figure 14.

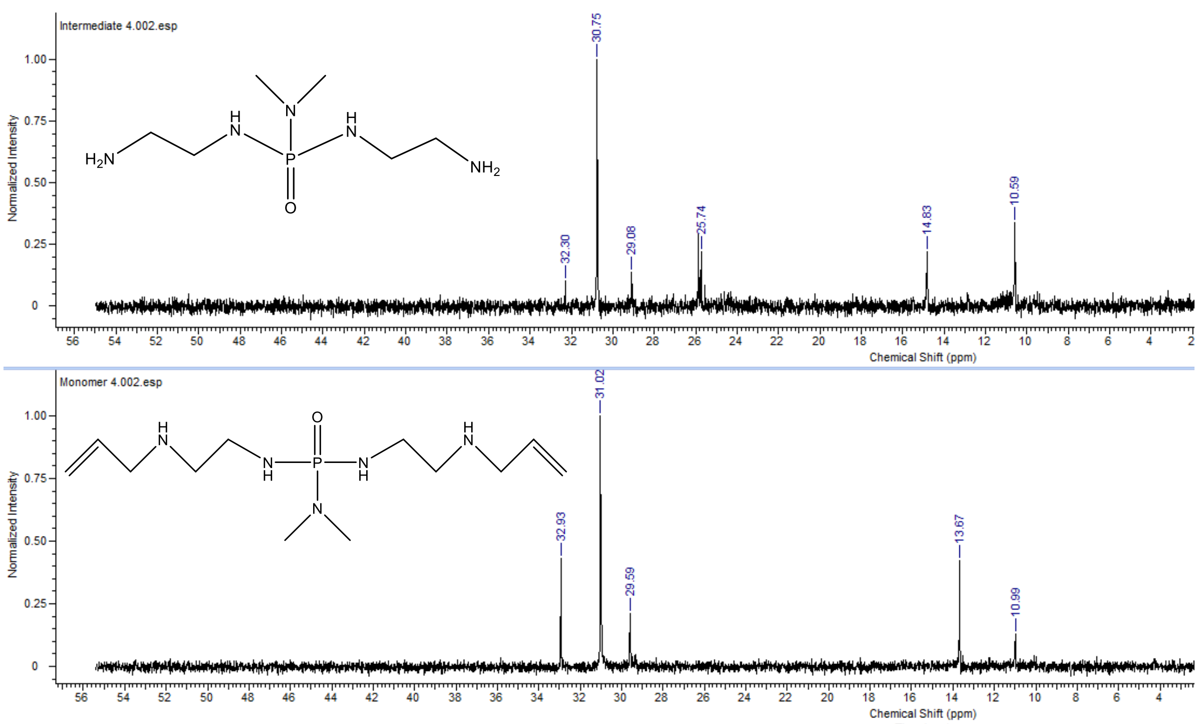

Figure 14: ^{31}P NMR Scans of Monomer 4 Intermediate and Monomer 4

The ^{1}H spectrum of the intermediate is noisy similar to the ^{31}P spectrum for the intermediate. It is difficult to estimate which signals correlate to which atoms. However, some conclusions can be drawn from the ^{1}H NMR spectrum for monomer 4. The large peak at 3.97 is likely indicative of deshielded alkenic protons. The nitrogen atoms act as a nucleophile, causing the peak for these alkenic protons to be shifted downfield. The protons on the nitrogen atoms do not appear to be present in the NMR spectrum, and are likely rapidly exchanging and thus not measured. The NMR spectrum for both monomer 4 and the intermediate compound for monomers 4 and 5 is shown in Figure 15, and Table 9 gives the values for each of the assigned peaks for monomer 4.

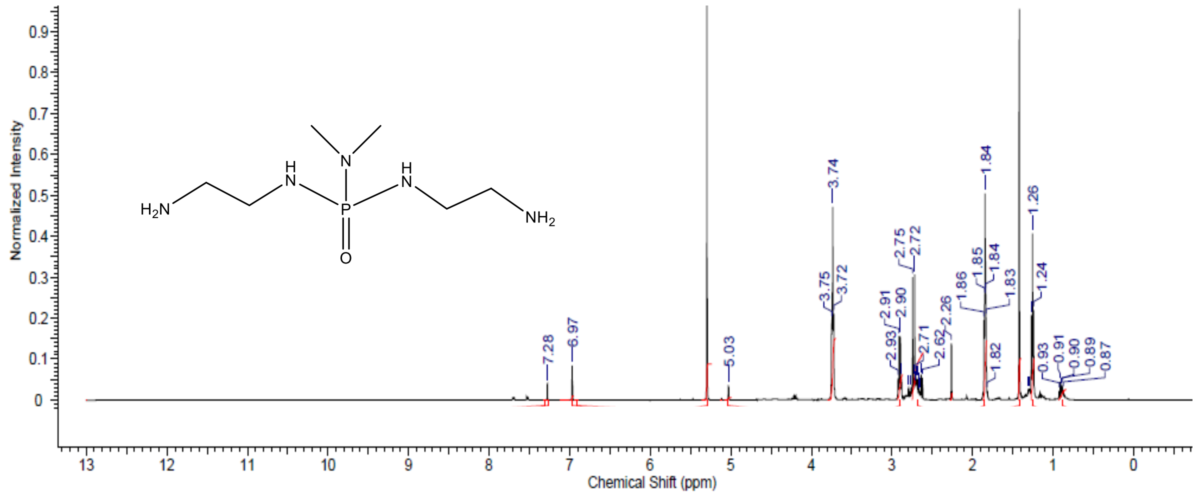

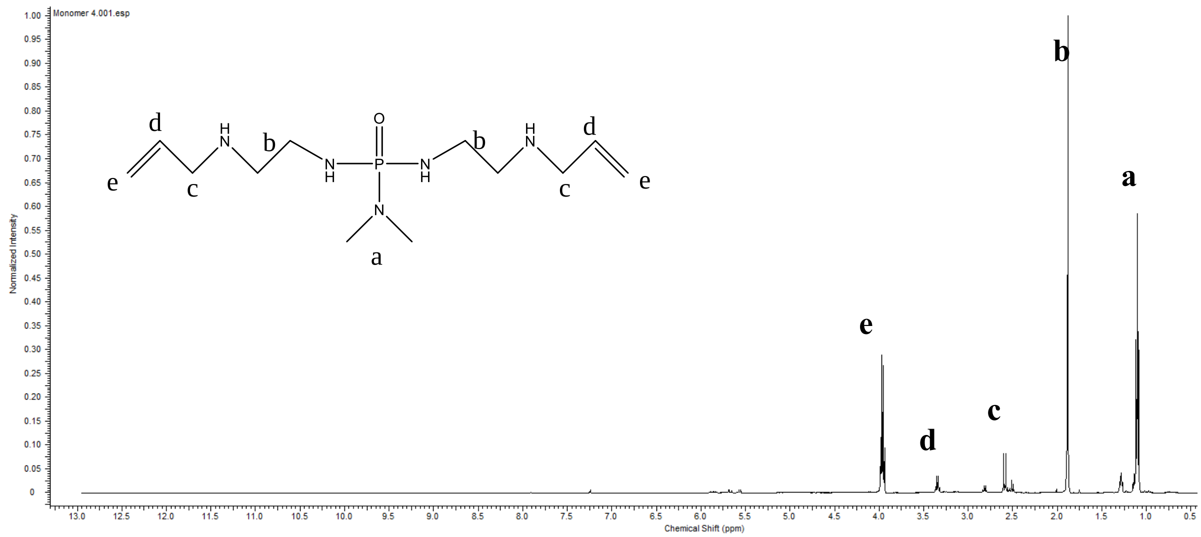

Figure 15: ^{1}H NMR Scans of Monomer 4 and its Intermediate Compound

Table 9: Assignment of ^{1}H Peaks: Monomer 4

Protons	Center of Peaks	Protons	Center of Peaks
A	1.1 ppm	d	3.35 ppm
B	1.88 ppm	e	3.97 ppm
C	2.58 ppm		

4.4 Characterization and Synthesis of Monomer 5

Monomer 5 was synthesized using the same intermediate as monomer 4. However, the final step with monomer 5 in which AOC was added was extremely exothermic with immediate salt formation. A yellow viscous product was the result of the reaction. The melting temperature of this compound is very close to room temperature. As the monomer was applied, it was beginning to crystallize at room temperature. If this monomer were used in an industrial setting, it would be important to control the temperature around where the molecule were used to prevent solidification in pipes and to ensure that the molecule is always applied in the same phase. An easy way to address this issue without the need for temperature control would also be to keep the molecule dissolved in a solvent until applied.

4.4.1 FTIR Analysis of Monomer 5

The FTIR spectrum of monomer 5 is similar to that of monomer 4. There is a very broad peak in the 3300 cm^{-1} range that is likely a combination of the N-H stretch and the C-H stretch of the alkene. The peak at 2945.4 cm^{-1} is representative of the C-H stretch in aliphatic carbons. However, as expected, there are additional peaks at 1797-1619 cm^{-1} indicating that a carbonyl of an amide is present as there should be with the acryloyl group. The carbonyl region may be messy because the molecule is not entirely pure, which will be describe in the NMR analysis. The FTIR spectrum of Monomer 5 and peak assignment can be seen in Figure 16 and Table 10 respectively.

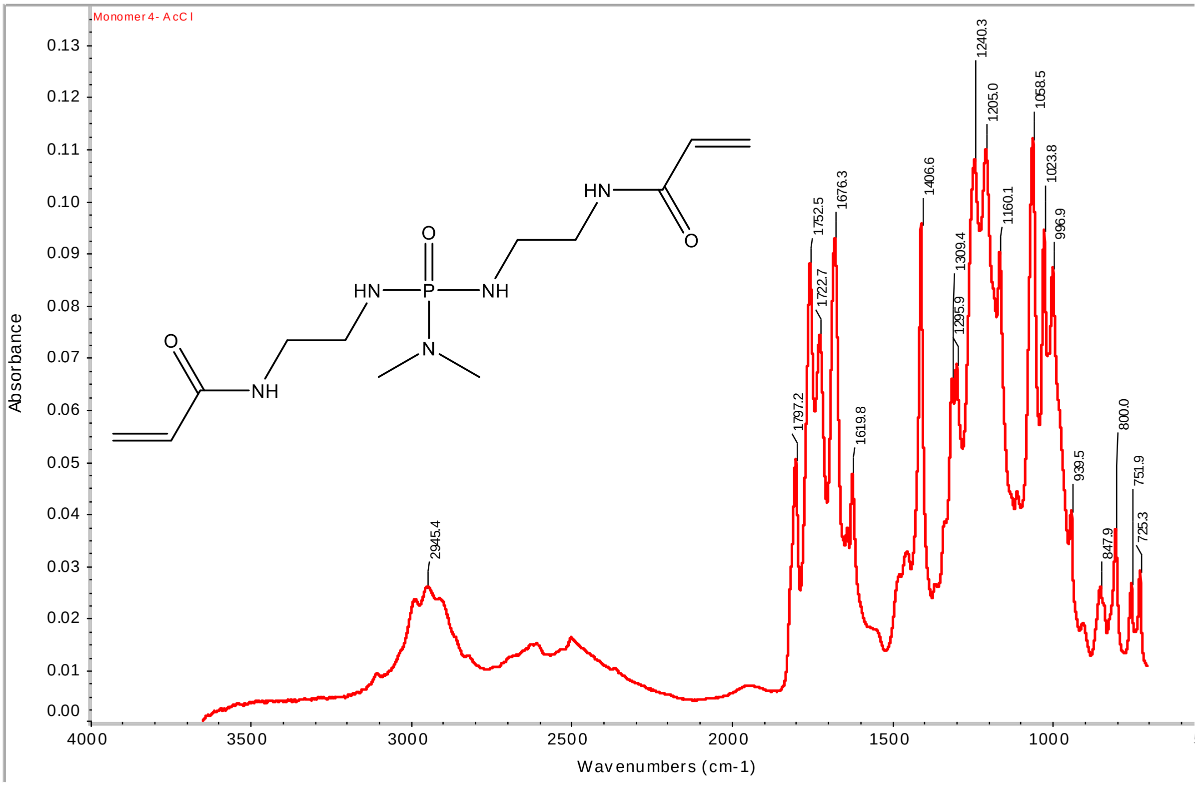

Figure 16: FTIR Spectrum of Monomer 5

Table 10: Assignment of FTIR Peaks, Monomer 5

Peaks	Assignment
3300	(broad) N-H stretch of secondary amine, C-H stretch of alkene
2945.1	C-H stretch of aliphatic carbon
1676.3	Carbonyl of an amide
1406.6	C-N
1205.0	C-C-N
1023.8	$CH=CH_2$

4.4.2 NMR Analysis of Monomer 5

The ^{31}P NMR spectrum again clearly shows that reactions took place in both the first and second step of the synthesis. The same intermediate is used to synthesize monomer 4 and monomer 5, and the intermediate spectrum was discussed in the NMR analysis of monomer 4.

In the final product, there is a very small peak at 30.64 ppm which corresponds to unreacted intermediate. There are strong peaks at 20.45 ppm and 11.85 ppm indicating that this reaction yields two products in a 13/10 ratio respectively, likely resulting from different numbers of intermediate molecules in the chain as discussed in the NMR analysis of monomer 4. Another plausible explanation of the two peaks could be that the AOC is equally reactive with both of the nitrogen molecules in the intermediate, and thus may react with either the terminal (as shown) or internal nitrogen. Both of these compounds have the phosphorous-nitrogen chemistry required to be effective in FR, so no further purification was attempted. The ^{31}P NMR spectrum is shown in Figure 17.

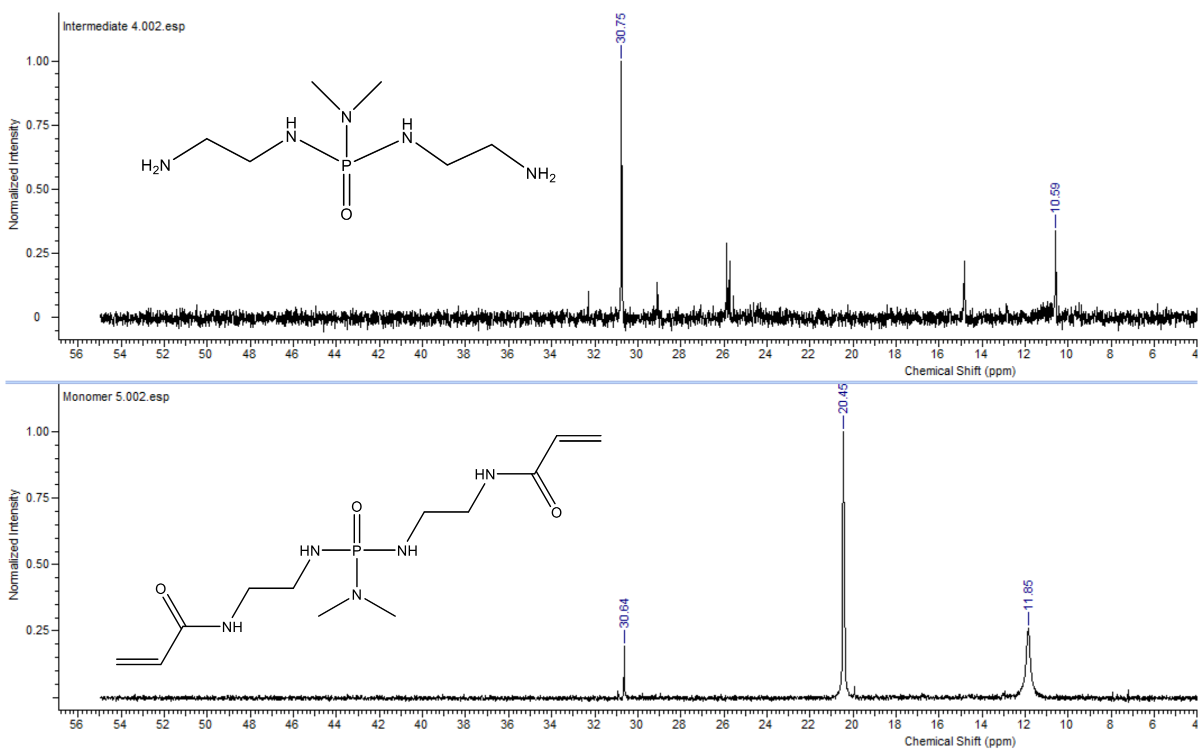

Figure 17: ^{31}P NMR Scans of Monomer 4 Intermediate and Monomer 5

Because there are two different and nearly equal peaks in the ^{31}P spectrum indicating that there are two different molecules formed, again the ^{1}H spectrum is difficult to interpret. The spectrum is further complicated by the presence of nitrogen. However, there are peaks in all the areas expected. While the NMR scan can't be used to unequivocally determine the structure, it does support the structure. The ^{1}H NMR for monomer 5 is shown in Figure 18, and plausible peak assignments are shown in Table 11.

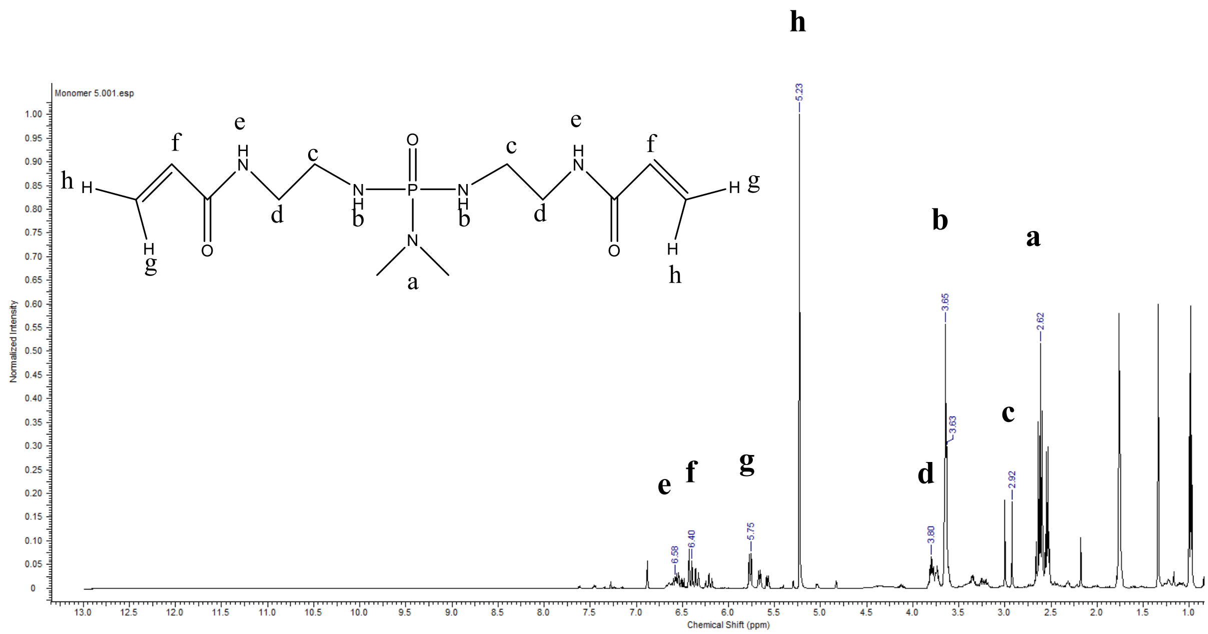

Figure 18: ^{1}H NMR Scans of Monomer 5

Table 11: Assignment of ^{1}H Peaks: Monomer 5

Protons	Center of Peaks	Protons	Center of Peaks
a	2.62 ppm	e	6.58 ppm
b	3.8 ppm	f	6.4 ppm
c	2.92 ppm	g	5.75 ppm
d	3.65 ppm	h	5.23 ppm

4.5 Characterization and Synthesis of Monomer 6

Monomer 6 was synthesized using hydrazine. In the first step, the reaction was exothermic. White salt formed immediately and became sticky. It was necessary to clean the stirrer several times at the beginning of the reaction because it would become stuck to the bottom of the reaction flask. A clear intermediate was formed after the salt was filtered. In the second step, the reaction was not noticeably exothermic, but was done heavily diluted in solvent which may have disguised some excess heat. White salt was again formed, and the resulting product was a yellow viscous substance.

4.5.1 FTIR Analysis of Monomer 6 Intermediate

The intermediate compound for monomer 6 is very noisy similar to that of the intermediate of monomer 4. Again, the intermediate was very volatile and began evaporating as soon as it was deposited onto the crystal for FTIR analysis. Regardless, the spectrum obtained supports the structure suggested for the intermediate compound. Composed primarily of N-H bonds, there is a strong peak as expected at 3402.7 cm^{-1}. A smaller peak is present at 2990.5 cm^{-1} which likely depicts the methyl groups off the nitrogen group of the starting material. There are few peaks in the fingerprint range, but there are still indications of N-H bonding. The FTIR spectrum for the intermediate compound for monomer 6 is shown in Figure 19, and Table 12 assigns the peaks.

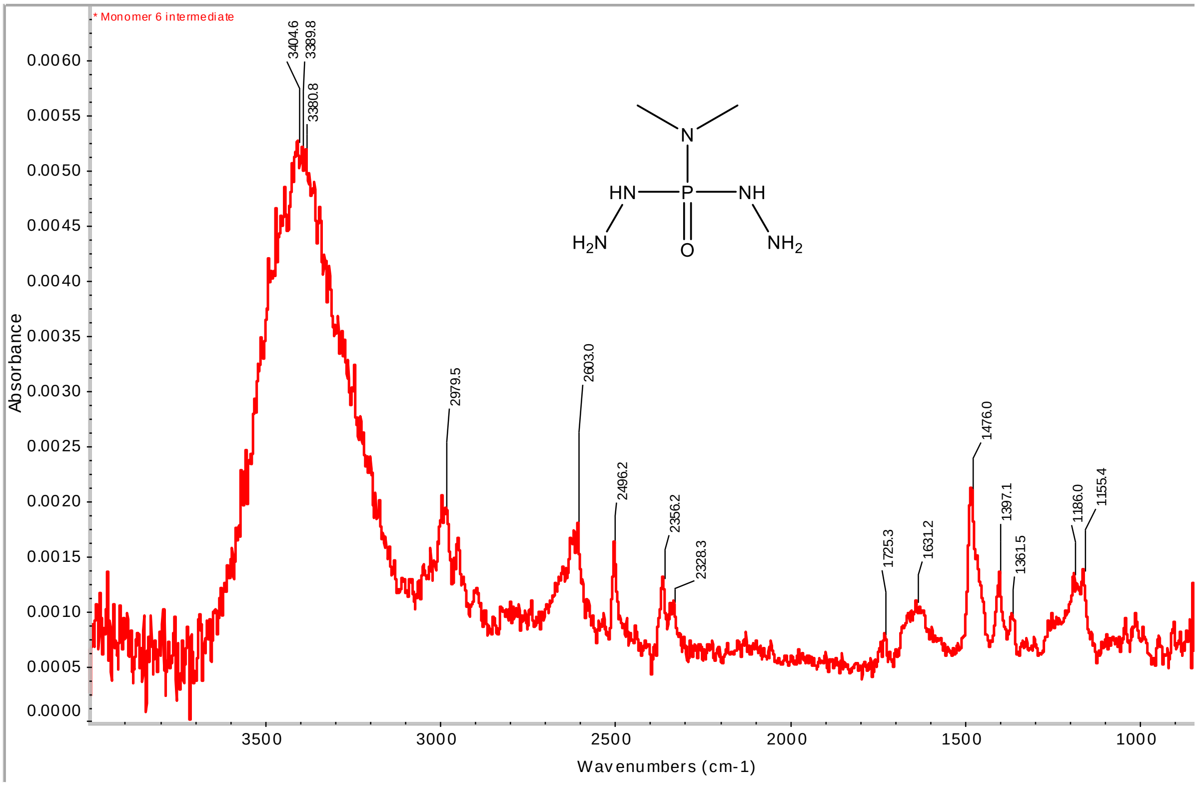

Figure 19: FTIR Spectrum for the Monomer 6 Intermediate

Table 12: Assignment of Peaks for Intermediate Compound for Monomer 6

Peaks	Assignment
3402.7	N-H stretch
2990.5	C-H_3
1634.4	N-H in primary amines
1475.1	NH in secondary amines

4.5.2 FTIR Analysis of Monomer 6

The FTIR spectrum of monomer 6 supports the structure as shown. The peak at 3634.3 cm^{-1} represents the N-H stretches, and may be covering the C-H stretch of the alkene. The peak 2938.7 cm^{-1} is indicative of the C-H stretch of an aliphatic carbon, which could be a result of the allyl addition to the intermediate. The FTIR spectrum for monomer 6 is shown in Figure 20, and Table 13 assigns the peaks in the spectrum to the molecule.

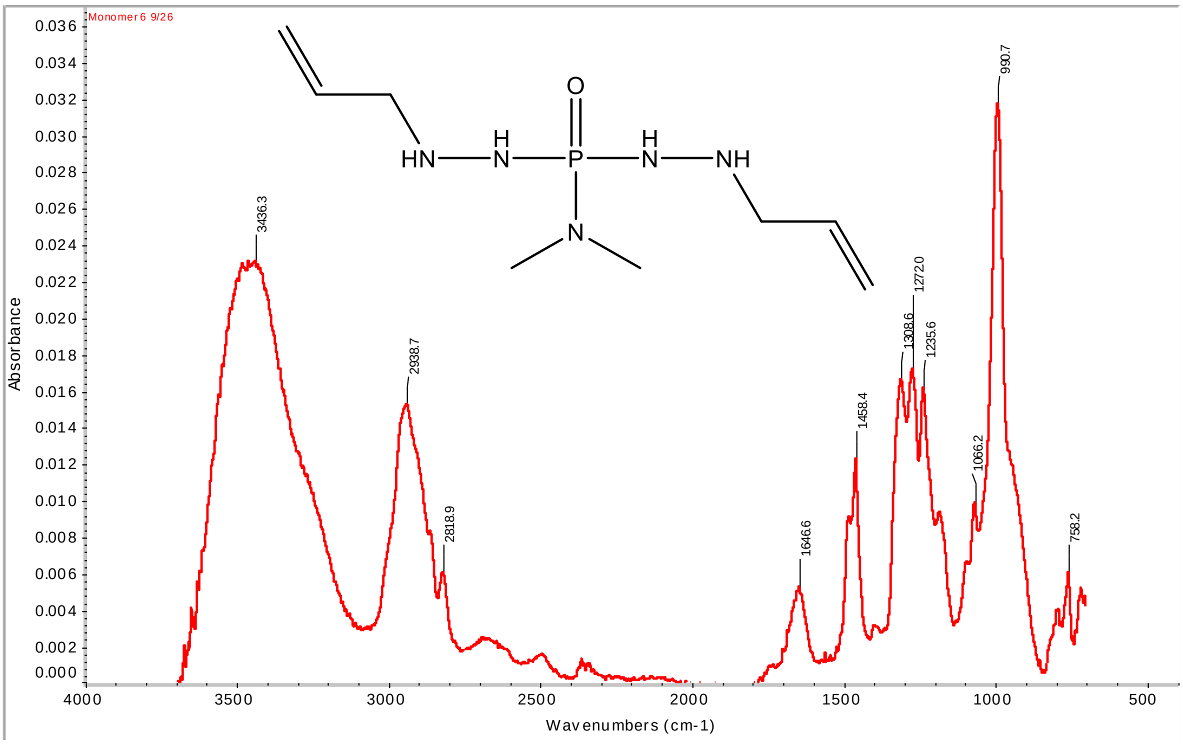

Figure 20: FTIR Spectrum of Monomer 6

Table 13: Assignment of Peaks, Monomer 6

Peaks	Assignment
3386.4	N-H stretch, C-H stretch in alkene
2924.5	-CH_2-
2622.5	N-CH_3
1478.6	NH in secondary amines
990.7	CH_2 in terminal alkene

4.5.3 NMR Analysis Of Monomer 6 Intermediate and Monomer 6

In the ^{31}P NMR scans, the intermediate spectrum was very noisy. There is a clear peak at 15.62 ppm, and possibly a smaller peak at 30.76 ppm. Neither of these correspond with the peak for the starting material, indicating that the reaction took place. For the final product, there is only one clear peak at 31.05 ppm. The ^{31}P NMR scans for monomer 6 and its intermediate are presented in Figure 21.

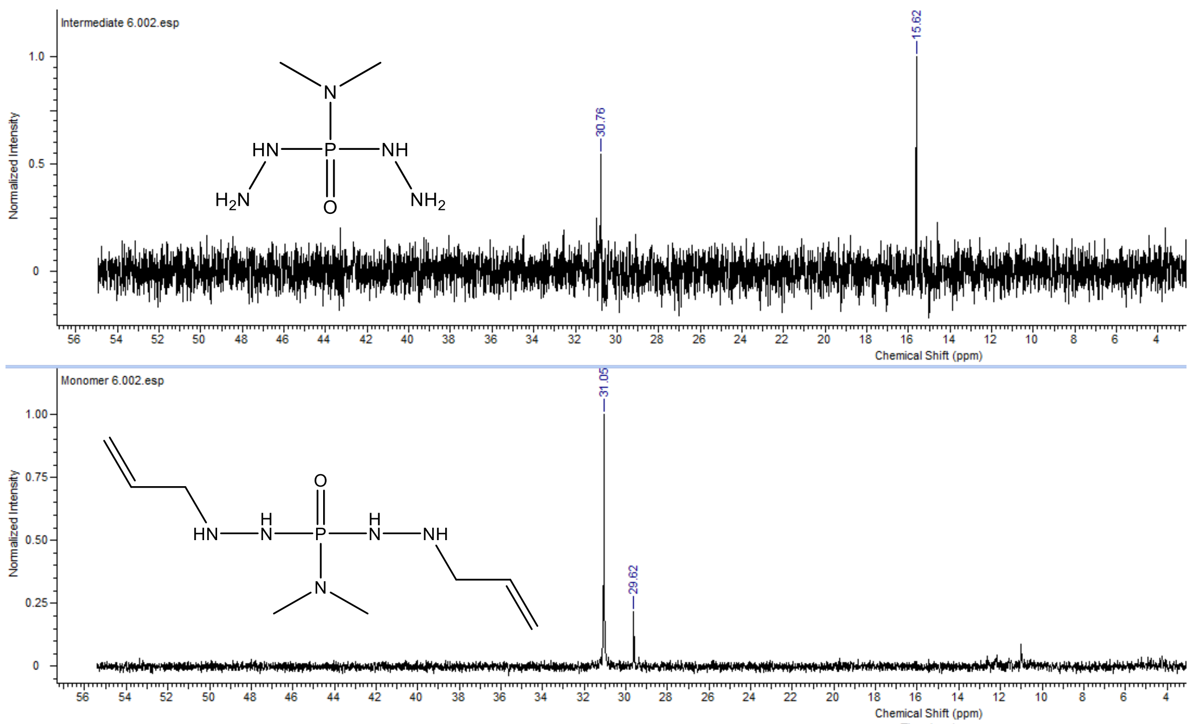

Figure 21: ^{31}P NMR Scans of Monomer 6 Intermediate and Monomer 6

In the ^{1}H NMR spectra for the intermediate and monomer 6, the values are much lower than expected. The high percentage of nitrogen content may make the scans difficult to analyze due to nitrogen interfering the signals. However, there are clear differences between the two spectra, indicating that a chemical change has taken place in the reaction. In the intermediate, two separate peak clusters are present. The peak cluster centered at 2.53 ppm is a quartet, and the cluster at 1.01 ppm is a triplet. This suggests that there are only two sets of protons present. It is possible that the protons attached to nitrogen are rapidly exchanging with the solvent, and thus do not appear in the scan. This also explains why there are no peaks in the higher regions of the scan as would be expected with protons attached to a nitrogen atom.

In the ^{1}H NMR spectra for the final product of monomer 6, it is expected that all protons except the methyl protons would appear as peaks between 4 and 8. However, there is only 1 set of peaks centered at 4.0 ppm, similar to that of monomer 4. Again, the NMR active nitrogen may be affecting the signal and pushing the signal downfield. Protons from the amino groups are also likely rapidly exchanging and may not appear in the NMR spectrum. The ^{1}H NMR scans for monomer 6 and its intermediate can be seen in Figure 22, and Table 14 assigns the peaks.

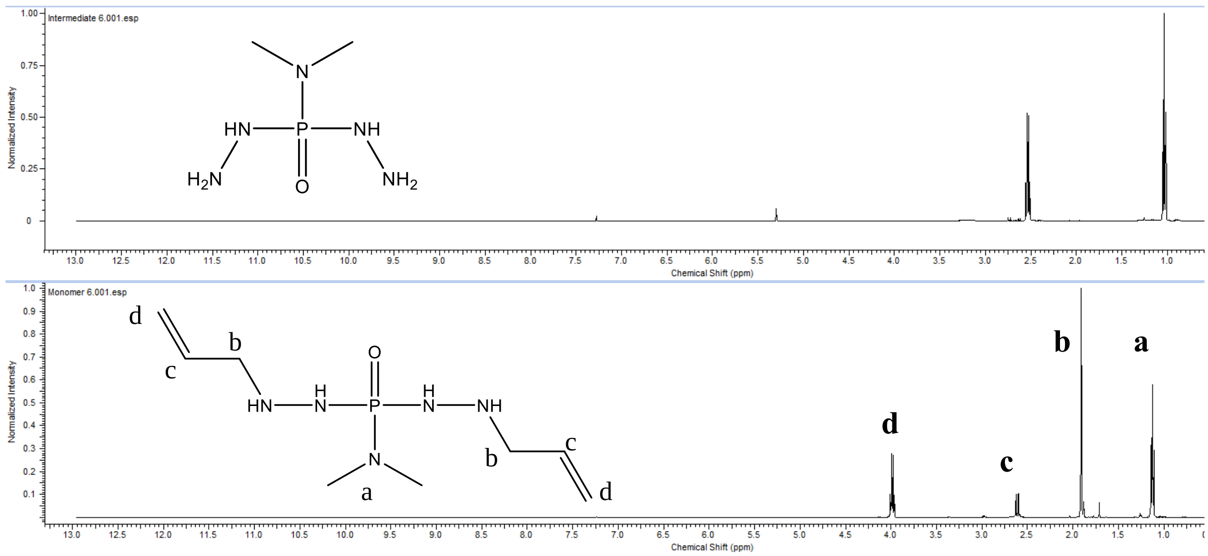

Figure 22: ^{1}H NMR Scans of Monomer 6 Intermediate and Monomer 6

Table 14: Assignment of ^{1}H Peaks: Monomer 6

Protons	Center of Peaks	Protons	Center of Peaks
a	1.12 ppm	c	2.63 ppm
b	1.19 ppm	d	3.99 ppm

4.6 Char-forming Crosslinkers

Though all the crosslinkers tested had oxygen available for phosphorous crosslinking, they did not all perform well. The results of the vertical flame tests can be seen in Table 15. Figure 23 shows pictures of the results of the burn tests. The PP control did not ignite at the temperature at which the test was conducted, and the area exposed to the flame only melted. However, as is explained further in this section, the FR needs to decompose a temperature much lower than the ignition temperature of PP. PA did not dissolve well in the water to get a truly even application. Because there were no functional groups in the PA, it was unable to be graft polymerized to the PP. Though it only burned for 4 seconds, the sample treated with PA did not form any char, and is not a useful char-forming agent in this application. LA and AM resulted in the substrate dripping while burning, which is unacceptable for a flame retardant. PTM did not form a uniform char over the substrate as well as PA3 and PA4 were able to do. PP is a plastic, and begins to melt at about 350^{o}C, as seen in the TGA curve in Figure 24. LA, AM, and PTM all begin to decompose at temperatures greater than 350^{o}C. Thus, as these crosslinkers decompose and crosslink to form the char, the polypropylene is already melting. The result is a line of charred plastic along the edge of the burn area as seen in Figure 23, and a greater likelihood for dripping. However, PA3 and PA4 begin to decompose at just over 300^{o}C, as seen in the TGA curve in Figure 24. This allows these two crosslinkers to form a uniform char over the surface as desired. Thus, PA3 and PA4 were further tested with TGA to determine which performed best.

Table 15: Crosslinker Determination

Crosslinker	Burn Time	Drip yes/no	General Appearance
PA	4 sec	No	No char formation
LA	25.35 sec	Yes	Completely melt substrate
PTM	20.25 sec	No	Some char, but much of the substrate burned
PA3	21.37 sec	No	Char formed over substrate, shape retained
PA4	32.13 sec	No	Char formed over substrate, shape retained
AM	17.67 sec	Yes	No substrate left at end of flame test

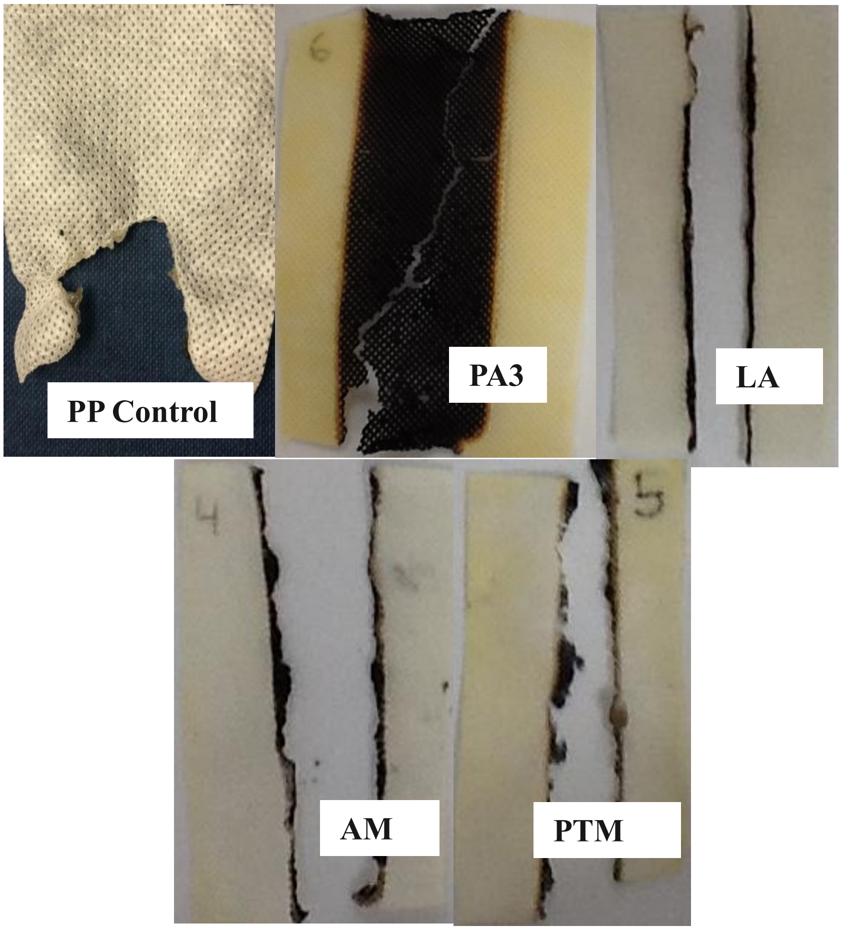

Figure 23: Char Formation of Different Crosslinkers

The TGA curve shown in Figure 42 highlights that PA3 is the best crosslinker for this application. The X axis shows temperature from 30°C to 600°C, while the Y axis shows the percent weight loss to show weight loss percentage with respect to time. The PP control curve is solid blue, PA3 is dotted green and PA4 is dashed red. PP decomposes at about 350°C, and there is 0% of the original substance left after 400°C. Both PA3 and PA4 show an initial linear weight loss curve. This is likely because the samples were not soxhlet extracted prior to this test, so the ungrafted coating was free to evaporate off without reacting. The onset temperatures of PA3 and PA4 were 308.65°C and 306.58°C respectively, close enough that no real distinction can be made between these temperatures. However, it is important to note that both are well above 220°C, the typical processing temperatures of PP and 350°C, the onset of the weight loss of PP control. At 600°C PA3 has about 17% of the original weight left, while PA4 has only about 11% of the original weight remaining. Thus it was determined that PA3 will be used as the crosslinker for this application.

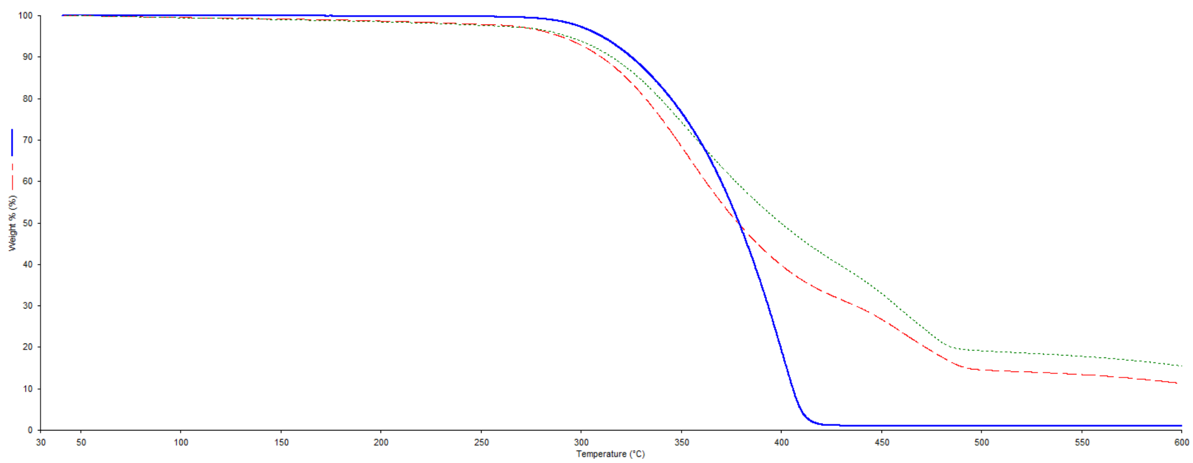

Figure 24: TGA Curve for PP (solid blue) Treated with Monomer 5 and Crosslinkers PA3 (dotted green) or PA4 (dashed red)

4.7 Ideal Stoichiometry for FR Behavior

To find the ideal stoichiometry, the best burn properties are desired. Ideally, the sample will self-extinguish. If not, a longer burn time is desired as it indicates slower flame propagation. These compounds are designed to perform in the condensed phase and should form a char. Thus, the weight loss should be minimal. Weight loss is reported as the percent of the original treated sample lost. Thus, smaller values are desired. To optimize percent add-on, the lowest possible add-on that still achieves the desired properties should be found. In the literature, typical values of FR addition are 30% of the total product to 50% of the total product. In terms of total mass of the FR, this correlates to 50% add-on to 100% add-on in the pad application terminology. It should be noted that these values are relative. Each side of the sample was placed in a metal holder, so only about a third of each sample was exposed to the flame. However, each sample had the same surface area exposed to the flame, so the numbers are relative to one another, but not representative of the actual weight loss had the entire sample had been burned. As expected, PET samples performed better than PP samples. PET has some carbonyl groups which contribute oxygen to the substrate and does not degrade as easily as the simple PP chain. Thus, in general, a greater weight percentage remained after burning in the PET sample, and the flame propagation was less rapid than with the PP samples. For all PP samples besides those which self-extinguished, the flame consumed the entire exposed area, while for some PET samples, the flame propagation continued only vertically, with some unburned PET remaining to the sides of the sample. These results will be discussed individually in more detail below.

4.7.1 Monomer 1: PP

While monomer 1 was not able to self-extinguish when applied to polypropylene, it was able to slow the propagation of the flame, and the monomer 1:PA3 combination formed a char over the substrate. A picture of a sample with 100% add-on and a monomer:crosslinker ratio of 80:20 is shown in Figure 25. The sample also had the optimal burn time with 32.43 seconds. As shown below, increasing monomer percentage led to longer burn times and also higher final weight percentages. It was expected that higher crosslinker content would result in a higher final weight percentage as the crosslinker is high portion of the char. Because the higher monomer content had a higher final weight percentage, it can be assumed that much of the monomer crosslinked and remained in the final structure as well. For monomer 1, 80% monomer concentration had the ideal burn properties. As expected, increasing coating percentage increased the burn time. However, added coating percentage decreased the final weight. This may be because as the flame burned more slowly, it had more time to fully decompose the substrate. A graphical representation of these results is shown in Figure 26. Figure 25 also shows the PP control. It can be noted that the control sample did not burn because the temperature was not hot enough with the butane flame. However, to get an effective char on plastic substrates, the FR must decompose before the plastic. As such, the vertical flame test is still applicable to compare the FRs. It can also be noted that no char formed on the burned portion of the control.

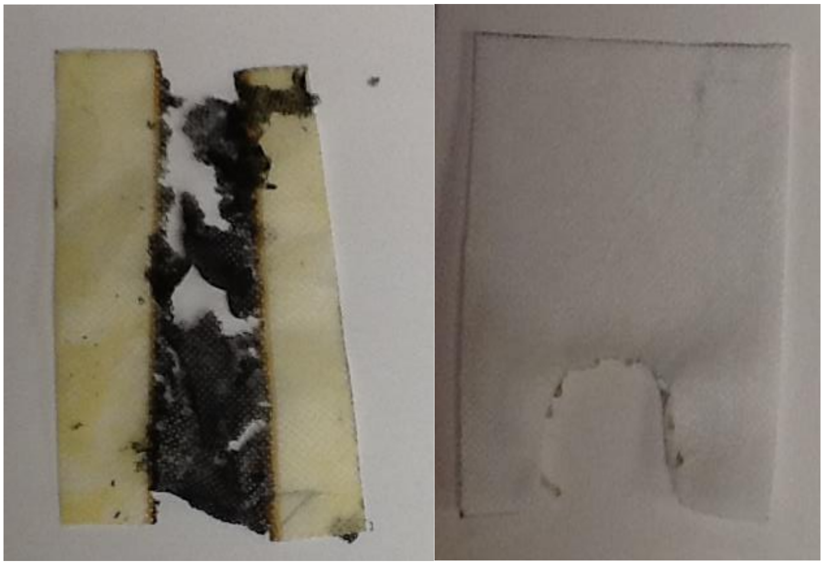

Figure 25: Char Formation on Sample of Monomer 1:PP and PP Control, Respectively

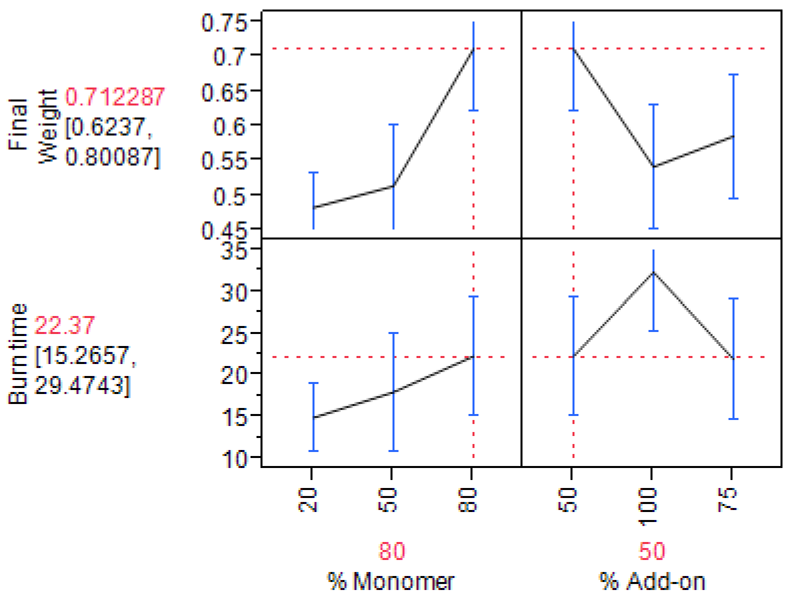

Figure 26: Burn Test Analysis for Monomer 1:PP

4.7.2 Monomer 1: PET

Similar to the test on PP, the longest burn time was achieved on a sample with a monomer:crosslinker ratio of 80:20. However, in this case the longest burn time was on a sample with only 75% add-on. A photo of the burned sample is shown in Figure 27. A uniform char was formed over the surface of the PET. It can also be seen that the edges of the char are not straight. As the flame propagated up the substrate, it travelled primarily in the vertical direction, and did not consume all of the fiber in available as it did not travel horizontally. The results regarding the monomer percentage were as expected and shown in Figure 28. With increasing monomer percentage, the final weight and burn time both increased indicating that the 80:20 monomer:crosslinker ratio was the best tested. Further, both final weight and burn time increased with increasing add-on, as expected. Figure 27 also shows the PET control. Similar to the PP control, the temperature was not high enough to ignite the sample. There is very little char formed on the burned portion of the PET, though more than the PET.

Figure 27: Char Formation on Sample of Monomer 1:PET and PET Control, Respectively

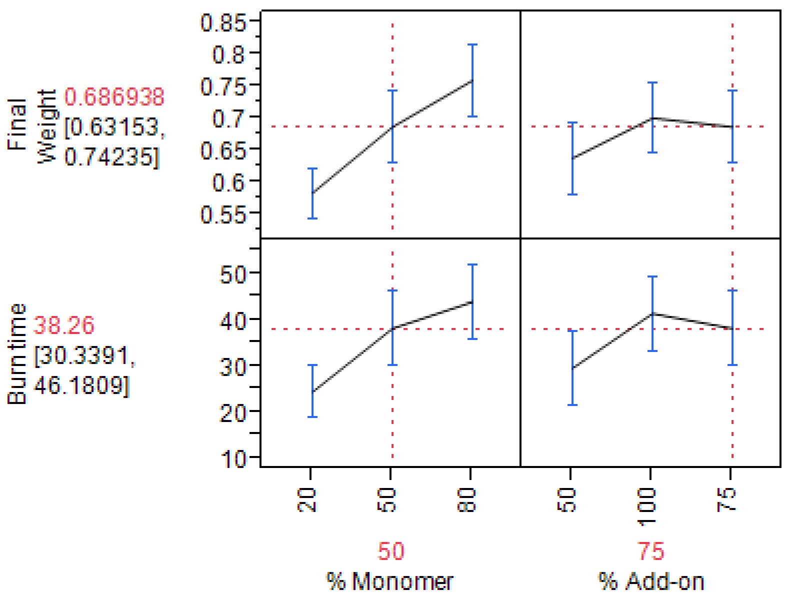

Figure 28: Burn Test Analysis for Monomer 1:PET

4.7.3 Monomer 2: PP

For the samples tested with monomer 2, the results were slightly more difficult to interpret. With 80% monomer, the greatest final weight was achieved. However, the burning rate was increased drastically with a quicker final burn time. Consistently, the slowest burning rate was achieved at a 50:50 monomer:crosslinker ratio as shown below in Figure 48. As expected, 100% add-on yielded the largest final weight and longest burn time. The sample that performed the best had a 50:50 ratio and 100% add-on, and formed an even char over the surface of the polypropylene. This sample is shown in Figure 29, and the analysis of the greatest final weight is shown in Figure 30.

Figure 29: Char Formation on a sample of Monomer 2:PP

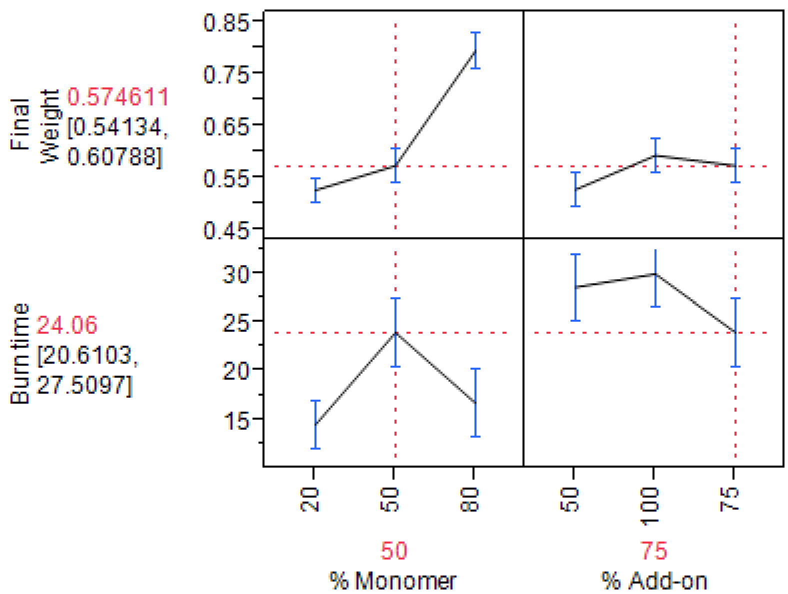

Figure 30: Burn Test Analysis for Monomer 2:PP

4.7.4 Monomer 2: PET

It was expected that the monomer would behave similarly on both PET and PP. The error in the measurements for the PET tests was high, but the 50:50 ratio yielded the best results as expected, with the longest burn time at 30.74 seconds for 75% add-on as shown in Figure 32. The final weight measurements were similar for all conditions tested, and though the final weight was highest for a 20:80 monomer:crosslinker ratio, this result is well within the error for the other measurements. As expected, a higher add-on percentage yielded a longer burn time. Again, the final weight percentages are not what was expected, with 50% add-on having the highest weight percentage. However, there is again a lot of error in the measurements, and each reading was within the error for other readings. A picture of the sample with 100% add-on and a 50:50 ratio is shown in Figure 31, and a uniform char can be seen over the surface of the PET sample. Again, the flame and subsequent char is in the vertical direction and did not fully propagate horizontally as evidenced by the diagonal char line on the left side of the substrate.

Figure 31: Char Formation on Sample of Monomer 2:PET

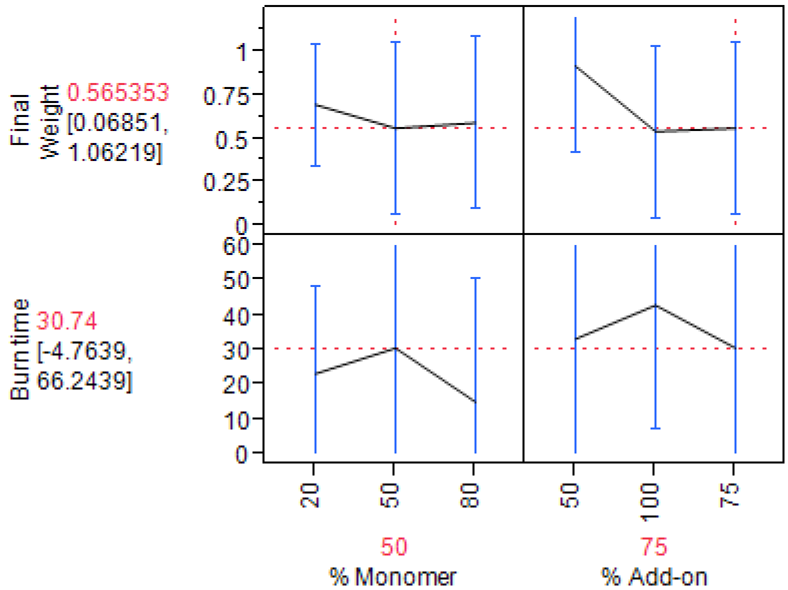

Figure 32: Burn Test Analysis for Monomer 2:PET

4.7.5 Monomer 4:PP

Monomer 4 yielded exciting results with the burn tests. It was expected that this monomer would perform well as it had a higher ratio of nitrogen to phosphorus. At a monomer:crosslinker ratio of 80:20, the samples self-extinguished. This is depicted in the graph as a burn time of 50 sec if the sample self-extinguished, and 100 sec if the sample did not ignite so that trends could be seen in the graph shown in Figure 34. At 75% add-on with a ratio of 80:20, the sample did not ignite, and at 100% add-on with the same ratio the sample self-extinguished. However, with this high rate of add-on, the samples did not form a uniform char over the surface. A sample of this is shown in Figure 33 A. In this case, the final weight percentages reflect the unburned substrate rather than the remaining char, and thus the final weight percentages are highest for the monomers at the 80:20 ratio. At a ratio of 50:50 or 20:80, a uniform char was formed over the surface of the substrate, likely because there was enough of the PA3 to form the crosslinked network. This sample is also seen in Figure 33 B.

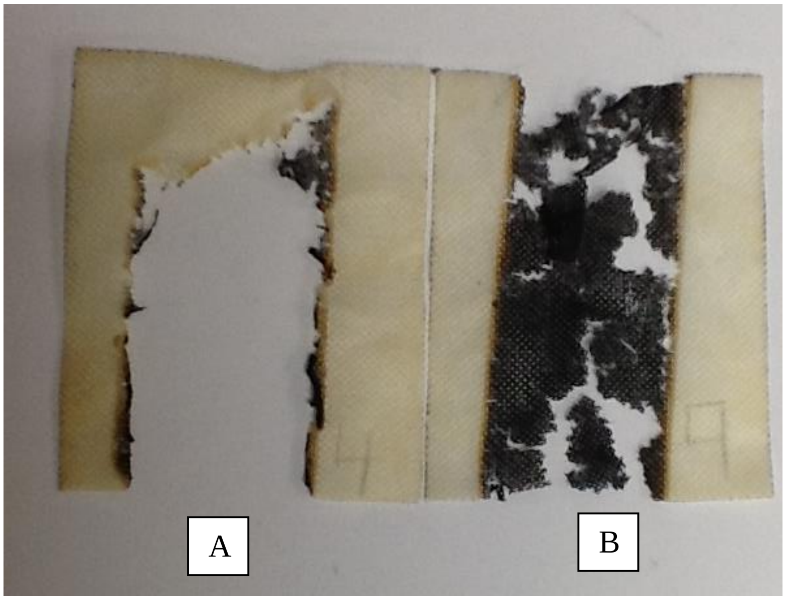

Figure 33: Char Formation on Samples of Monomer 4:PP

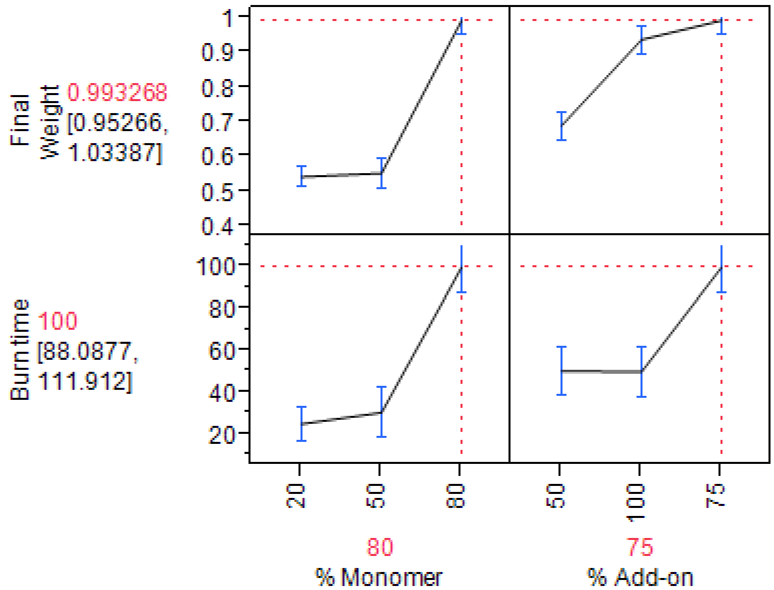

Figure 34: Burn Test Analysis for Monomer 4:PP

4.7.6 Monomer 4: PET

More exciting results were achieved when applying monomer 4 to PET. At a monomer:crosslinker ratio of 80:20, all samples self-extinguished. At the ratio of 50:50, at 75 and 100% add-on the samples self-extinguished. However, the char formed at the 50:50 ratio was more uniform than the char formed at the 80:20 ratio as evidenced in Figure 35. Sample A shows the result of a burned sample with a ratio of 80:20: the sample self-extinguished as is evidenced by the lack of char up the substrate, but the area that is burned did not form a uniform char. Sample B depicts the 50:50 ratio in which the entire substrate burned, but a more uniform char was formed. Thus, for low add-ons, a ratio of 80:20 monomer:crosslinker will be most beneficial for FR properties, but at higher add-on percentages, a ratio of 50:50 will yield the most consistent charring layer. The percent-add on did not greatly affect the final weight percent or burn time because many of the samples self-extinguished, and thus were input as 50 seconds and a very large portion of the substrate remained contributing to the final weight. Figure 36 depicts these results.

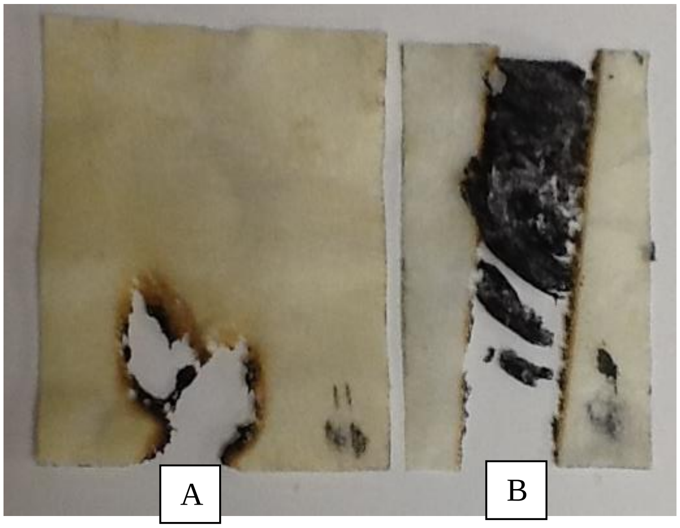

Figure 35: Char Formation of Sample of Monomer 4:PET

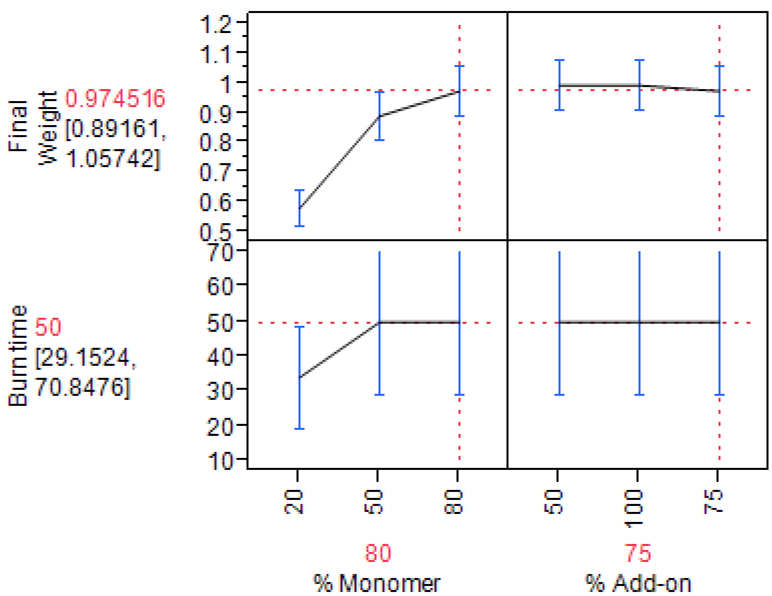

Figure 36: Burn Test Analysis for Monomer 4:PET

4.7.7 Monomer 5: PP

Monomer 5 was similar to monomer 4 with two additional carbonyl groups per monomer unit. The FR performance of monomer 5 did not match the performance of monomer 4; none of the samples self-extinguished. However, a uniform char was formed over the surface of the PP as shown in Figure 37. Again, a monomer:crosslinker ratio of 80:20 yielded the best FR results with the highest final weight percentage and longest burn time as seen in Figure 38. The highest final weight percentage is apparent at only 50% add-on. The trend correlates increasing add-on percentages to decreasing final weight percentages, but increasing burn time. Likely, as the percent add-on increases, the FR works to slow the flame propagation, allowing the flame to burn each section of the substrate for a longer period of time, allowing for more complete decomposition. However, for all conditions tested, a char layer was formed.

Figure 37: Char Formation on Sample of Monomer 5:PP

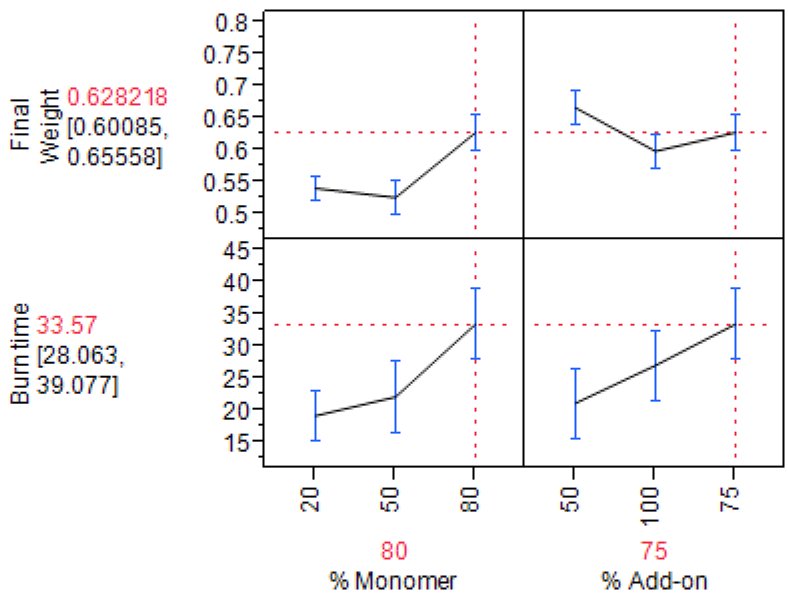

Figure 38: Burn Test Analysis for Monomer 5:PP

4.7.8 Monomer 5: PET

Similar to other monomers, similar results were results were obtained with monomer 5 applied to both PP and PET. Again, a monomer:crosslinker ratio of 80:20 yielded the best FR performance with the highest burn time and final weight percentage as shown in Figure 40. Though the burn times for both 50:50 and 80:20 ratios are similar, the greater final weight percentage for the 80:20 ratio is the greatest evidence for the superior performance of this ratio. The greatest final weight percentage was again obtained at only 75% add-on. The longest burn time was recorded at 50% add-on, but this time was very close to the burn times at 75% and 100% add-on, and within the standard error. Thus it could be assumed that the burn time is not as dependent on the % add-on in this case. Again, a uniform char was formed over the surface of the PET, and can be seen in Figure 39.

Figure 39: Char Formation on Sample of Monomer 5:PET

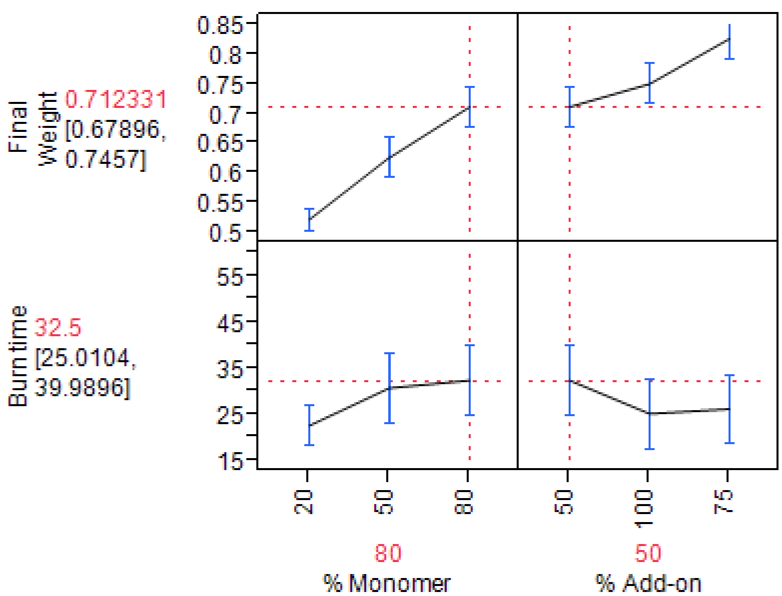

Figure 40: Burn Test Analysis for Monomer 5:PET

4.7.9 Monomer 6: PP

Monomer 6 had the highest percentage of nitrogen and phosphorus in its make-up. Unlike for monomer 4, there were no samples that self-extinguished, but at a monomer:crosslinker ratio of 80:20 and 50% and 100% add-on, the samples did initially self extinguish and then burn after being lit a second time. It was determined that the 80:20 ratio was superior in FR performance because it had a significantly longer burn time correlating to much slower flame propagation. This ratio also had the greatest final weight percentage as shown in Figure 42. Similar to previous graphs, it appears that a longer burn time correlates to lower final weight percentages as add-on percentage is varied, with 75% add-on having the longest burn time, but lowest final weight percentage. Char was formed for all conditions, but the char structure was more intact for the 50:50 monomer:crosslinker ratio. Figure 41 depicts a sample with a 50:50 ratio (A) and a sample with an 80:20 ratio (B), and the more defined char structure is evident in the sample with the 50:50 ratio.

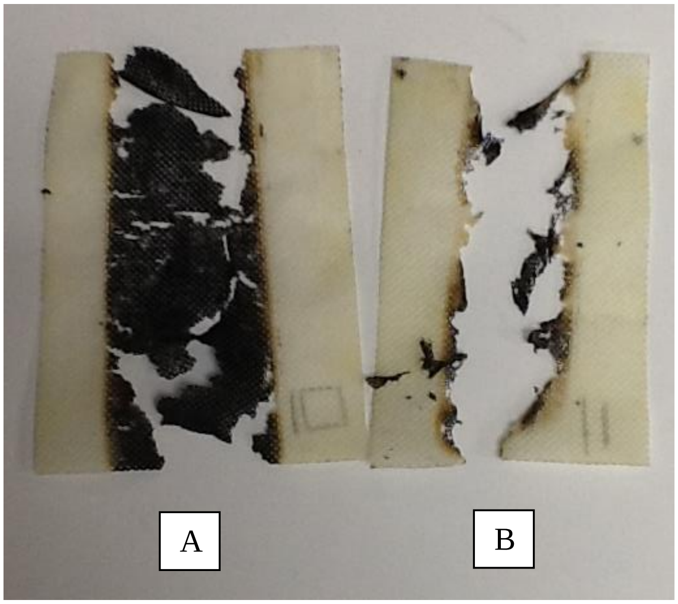

Figure 41: Char Formation on Samples of Monomer 6:PP

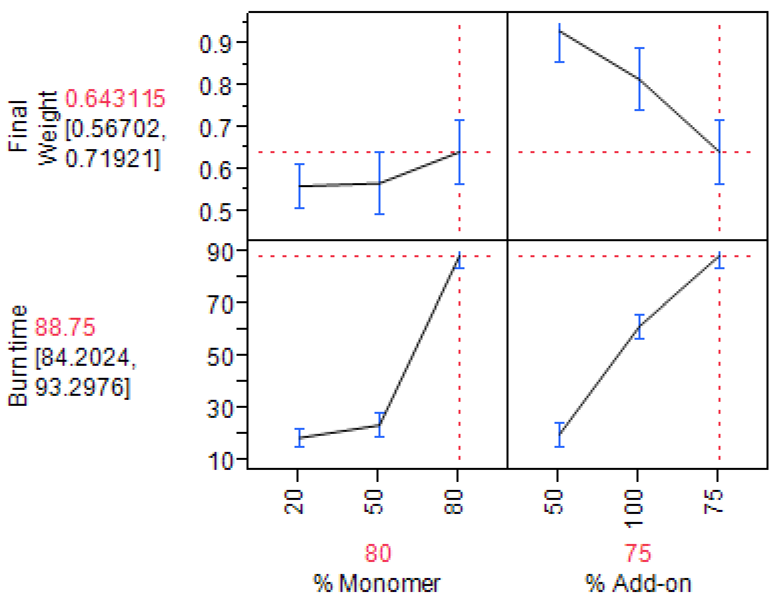

Figure 42: Burn Test Analysis for Monomer 6:PP

4.7.10 Monomer 6:PET

On PET, monomer 6 had a better performance, self-extinguishing on several samples. The self-extinguishing effect took place between 12 and 14 seconds, but was input in the graph as 100 seconds to show the trend consistent with the previous charts. The final weight was much greater for the samples with a monomer:crosslinker ratio of 80:20 as shown in Figure 44. Burn time could not be accurately depicted for this ratio as each sample self extinguished, and the final weight percentages were very close for all samples tested at the 80:20 ratio. In Figure 43, a uniform char can be seen in the sample. For the 80:20 ratio (A) there is not as robust a char as there was in the sample with a 50:50 ratio (B). It is also seen that the flame did not propagate up the entire substrate in sample A as a result of the sample self-extinguishing.

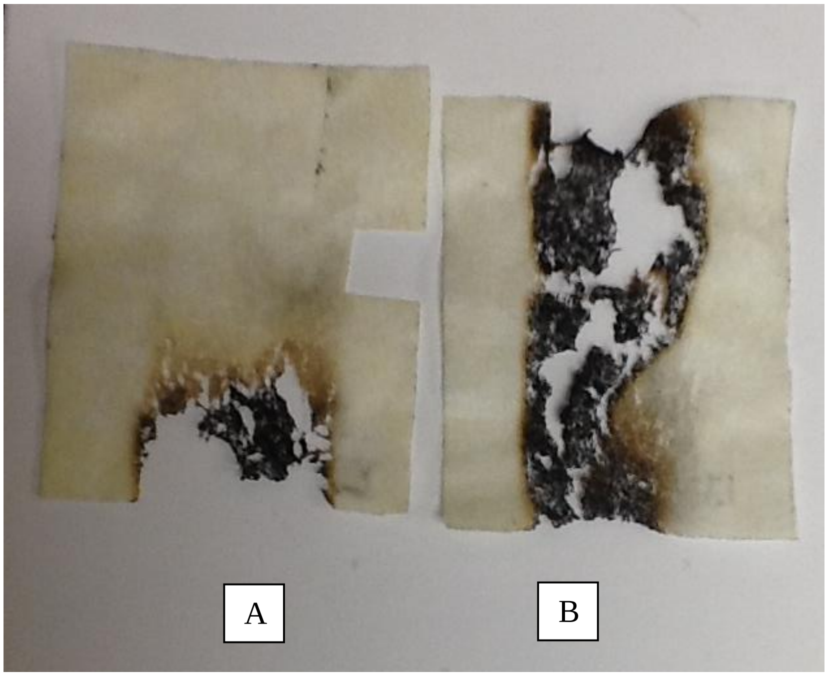

Figure 43: Char Formation on Samples of Monomer 6:PET

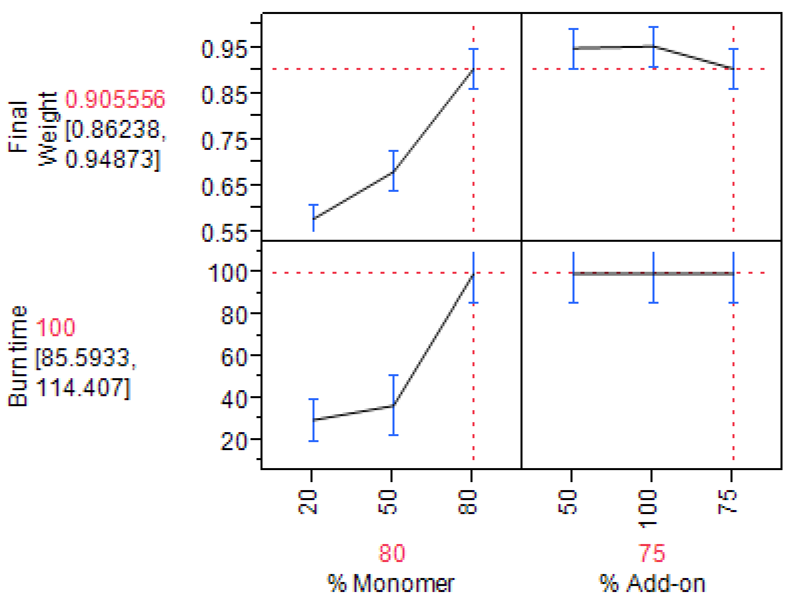

Figure 44: Burn Test Analysis for Monomer 6:PET

4.8 Thermogravimetric Analysis

TGA testing was used to objectively determine the weight lost over time. The ideal ratio of each monomer was used at 100% add-on to perform the test. Thus, for monomers 1,4,5 and 6, a sample with a ratio of 80:20 was used, while for monomer 2 the sample with a 50:50 ratio was used. Using the TGA test, the different FR monomers could be easily compared for each substrate on a basis of the percent of weight lost (y axis) at a particular temperature (x axis).

4.8.1 FR Tested on PP

Table 16 shows the values obtained for each monomer with regards to initial weight loss, onset of degradation, and peak degradation temperatures for the PP samples. From this table, it is apparent that all monomers have an effect on the degradation. The start of the decomposition all occur at temperatures lower than that of neat PP. This is essential so that the FR can begin to form a char before the polymer begins to degrade. Monomers 2 and 5 begin to degrade at temperatures much closer to that of neat PP, both less than 10°C away from the decomposition temperature of PP, with monomers 1, 4 and 6 all begin to degrade at much lower temperatures. The onset temperature is indicative of the rate of degradation, and represents the intersection of lines tangent to the start of decomposition and peak degradation temperature. All values are relatively similar, with only monomer 6 having a significantly lower onset temperature of 312.87°C. The peak degradation temperature indicates the temperature at which the majority of the decomposition occurs. Monomers 1, 2, 4 and 5 have peak degradation temperatures slightly above that of PP, which monomer 6 has a peak degradation temperature slightly below that of PP. The final weight percentage reveals what amount of the initial substrate remains at 600°C. Neat PP is nearly completely gone, with only 1.037wt% remaining at 600°C. Monomer 2 had the greatest final weight percentage at 20.291%. However, this may be because this was the only monomer to have a ratio of 50:50, so more of the char forming agent, PA3, was present. However, because this was the condition that gave the best FR behavior in the burn test, it can be assumed that monomer 2 performed best for this TGA test. A graphical representation of these results is shown in Figure 45. Numbers at the right hand side of the graph depict which curve represents each monomer. From the curves, it is apparent that all monomers begin to degrade before neat PP, have a slower decomposition rate, and greater final weight percentage than PP.

Table 16: Values from TGA Testing for PP Samples

Monomer	**Start of Decomposition (°C)**	**Onset (°C)**	**Peak Degradation (°C)**	**Final Weight %**
1	151.16	340.82	415.89	12.265
2	274.65	364.38	426.71	20.291
4	198.83	378.35	425.94	14.48
5	272.92	338.73	423.66	8.773
6	114.02	312.87	393.78	7.148
Neat PP	277.75	349.84	407.05	1.037

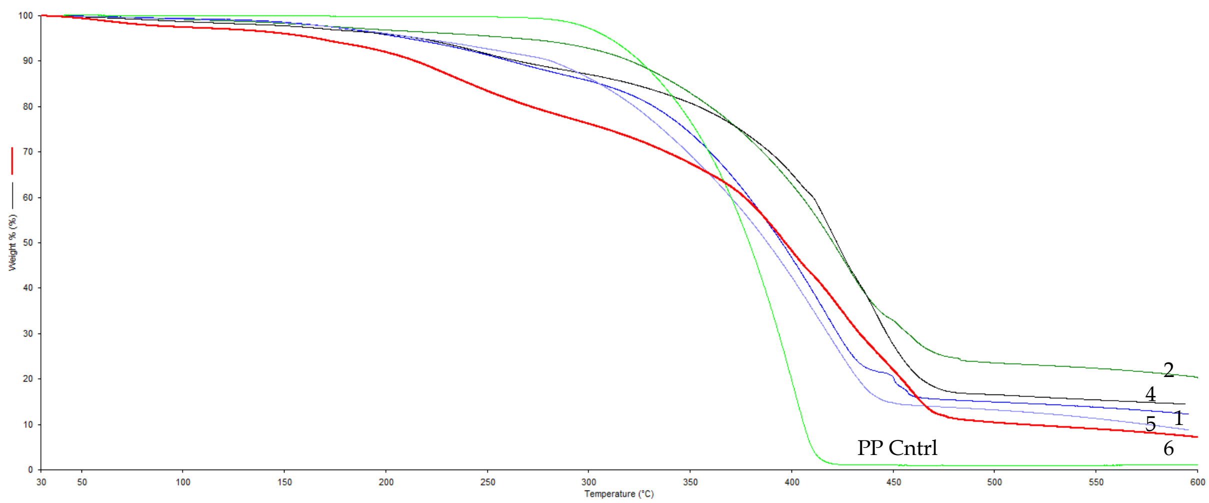

Figure 45: TGA for all Monomers Applied to PP

4.8.2 FR Tested on PET

Table 17 shows the values obtained for each monomer with regards to initial weight loss, onset of degradation, and peak degradation temperatures for the PET samples. The start of decomposition for each monomer is significantly lower than that of neat PET, as are the onset temperatures. The peak degradation also occurs at a lower temperature for all monomers than for PET. Figure 46 shows a graphical representation of the TGA data. All of the monomers follow a similar curve with the exception of monomer 5, which has a steeper weight loss curve. Both Table 17 and Figure 46 demonstrate the final weight % at 600°C. Both monomer 1 and monomer 2 have over 20% of the initial weight left, with monomer 4 performing worst in this category with only 16.4% left at the final temperature. Thus, according to the TGA test, monomer 1 performed best closely followed by the performance of monomer 2. All monomers were an improvement over the performance of neat PET.

Table 17: Values from TGA Testing for PET Samples

Monomer	Start of Decomposition (°C)	Onset (°C)	Peak Degradation (°C)	Final Weight %
1	150.35	331.65	415.53	24.713
2	265.91	363.77	415.46	23.891
4	170.54	362.94	419.05	16.423
5	153.66	374.78	428.23	19.963
6	143.52	354.5	396.57	17.591
Neat PET	380.27	418.92	454.11	1.993

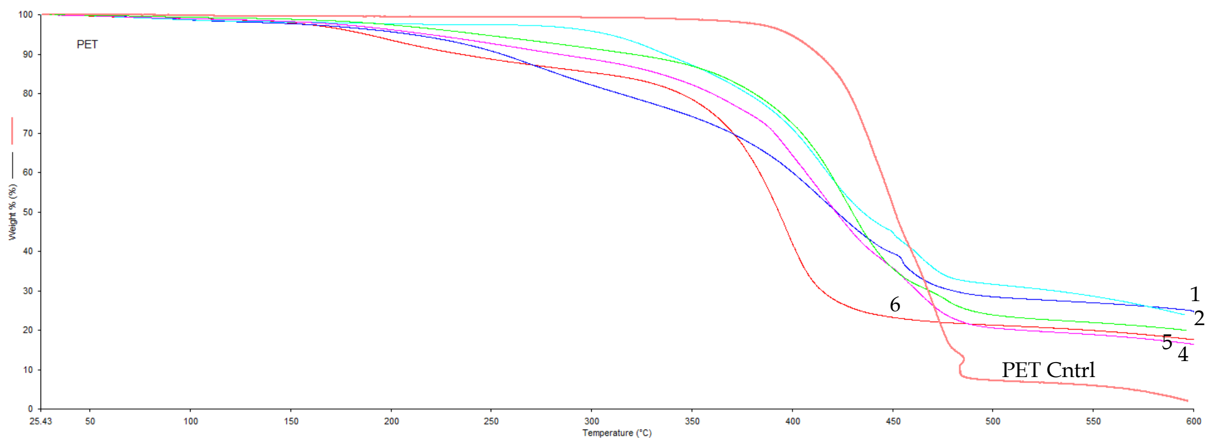

Figure 46: TGA for all Monomers Applied to PET

4.9 Optimization of Coating Yield

The percent photoinitiator and UV exposure time were varied to determine maximum coating yield and durability. The final weight is reported as a function of UV exposure time for each photoinitiator concentration. The final weight is given as a percentage of the weight of the treated sample before undergoing soxhlet extraction. The photoinitiator is used to initiate the radical reactions which graft polymerize the coating to the PP. As such, graft polymerization and coating yield are analogous. The UV lamp provides energy to begin and sustain the reaction. If too little photoinitiator is used and the sample is not exposed to the UV irradiation for a long enough period, the reaction may not reach completion quickly. If too much photoinitiator is used or the sample is exposed for too long, it may result in chain scission and small polymer chains that do not react with PP and thus are not graft polymerized to the PP. Some weight loss is expected as the photoinitiator will wash out of the sample during the extraction. Keeping both photoinitiator and UV exposure time to a minimum will also help reduce the cost and energy footprint of this process. Further, samples become stiffer as they spend more time under the UV lamp. Potentially after treatments could reduce this effect if stiffness was an important fiber parameter.

4.9.1 Graft Polymerization Yield on PP Samples

Exceptional results were found in monomers 1, 2, and 5. These monomers contained a carbonyl group next to the double bond, which increased the reactivity of the double bond. As such, for all conditions tested, the graft polymerization yield was at least 95%. Future tests with lower photoinitiator concentrations and UV exposure times would need to be conducted to truly optimize these monomers. However, at 5% of the monomer concentration of photoinitiator and 30 seconds per side of UV exposure, all samples had ample graft polymerization as shown in Figure 47 for monomer 1, Figure 48 for monomer 2, and Figure 49 for monomer 5. For all samples, there was a smaller polymerization yield at 20% photoinitiator. This is partially because the photoinitiator was removed in the soxhlet extraction, but a contributing factor could be that the polymerization continued beyond the ideal amount. In this case, small the polymer may be been broken into smaller chains and removed with the soxhlet extraction.

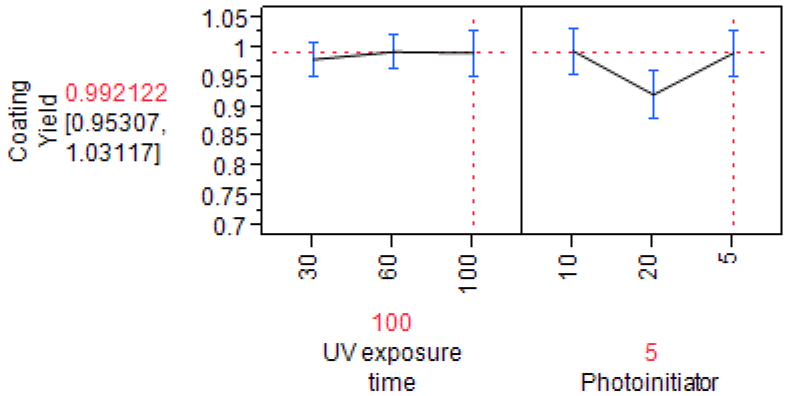

Figure 47: Graft Polymerization Yield for Monomer 1:PP

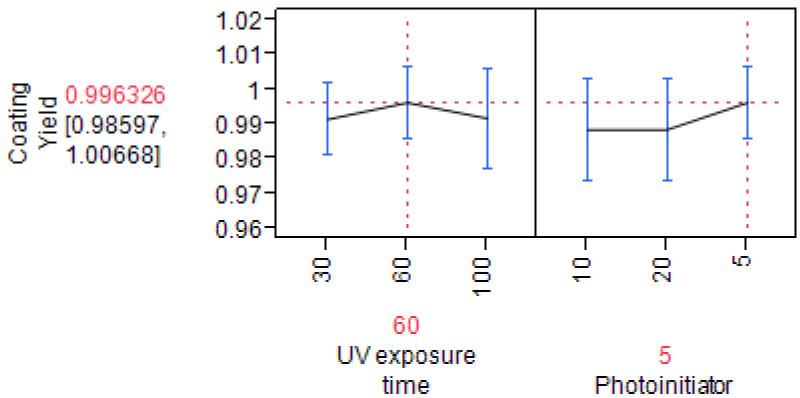

Figure 48: Graft Polymerization Yield for Monomer 2:PP

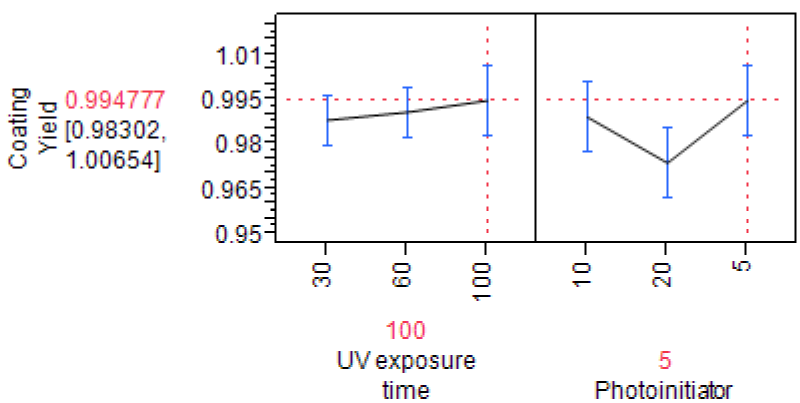

Figure 49: Graft Polymerization Yield for Monomer 5:PP

Monomers 4 and 6 did have optimal values in this graft polymerization test. For monomer 4, above the conditions of 5% photoinitiator and 30 seconds of UV exposure time, the coating yield decreased significantly. With added photointiator, too many free radial polymerization sites were initiated, leading to lower molecular weight polymers and low coating yield as shown in Figure 50. A similar trend is seen in Figure 51 showing the graft polymerization yield of monomer 6. However, at 5% photoinitiator, the monomer had greater success at higher UV exposure times, with nearly 98% coating yield at 60 and 100 seconds of UV exposure.

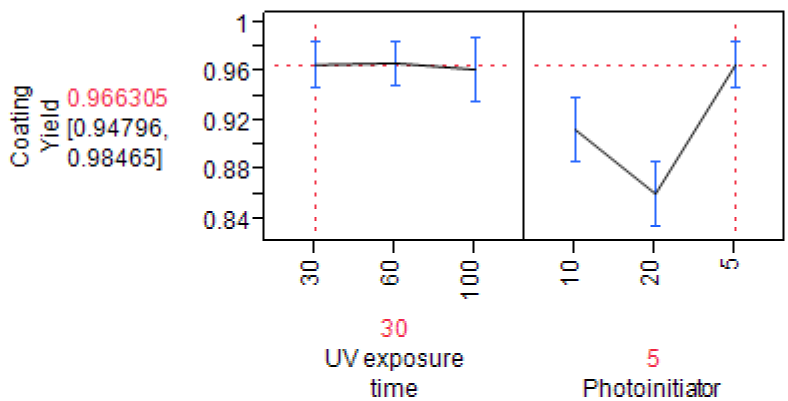

Figure 50: Graft Polymerization Yield for Monomer 4:PP

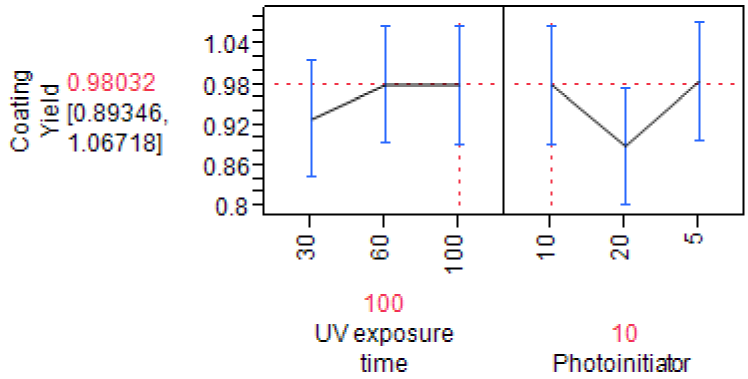

Figure 51: Graft Polymerization Yield for Monomer 6:PP

4.9.1.1 SEM Analysis for PP Samples

SEM images for washed samples of PP are shown in Figure 52 below with 50x magnification on the left and 250x magnification on the right. It can be seen that the control PP sample does not have any film or coating between the fibers, while each of the treated samples do have a coating between the fibers. From these images, it appears that monomers 2 and 5 have formed the most robust coating, while monomers 4 and 6 have a somewhat more sparse covering. This could be because the sample tested was at 20% photoinitiator and 100 seconds UV exposure to each side, which yielded lower than 90% coating polymerization for both monomers 4 and 6.

Figure 52: SEM Images at 50x (left) and 250x(right) for PP samples

Control

1

2

4

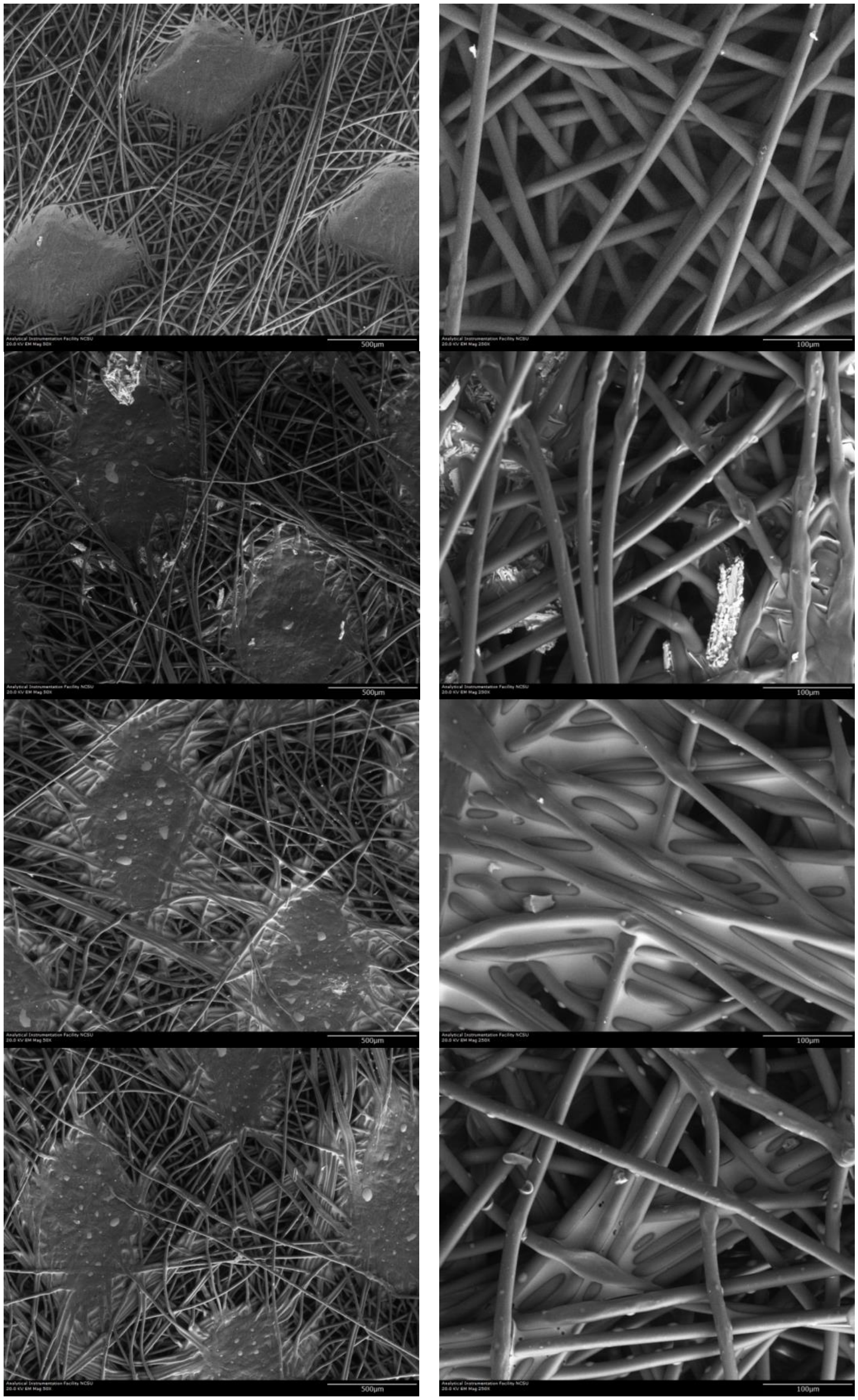

5

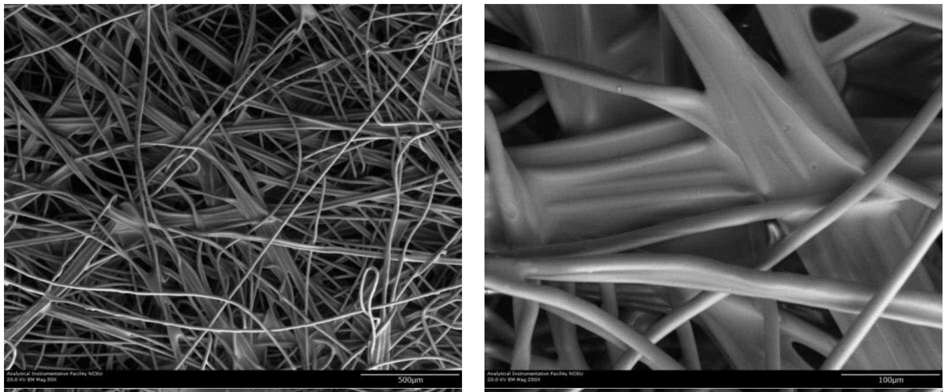

6

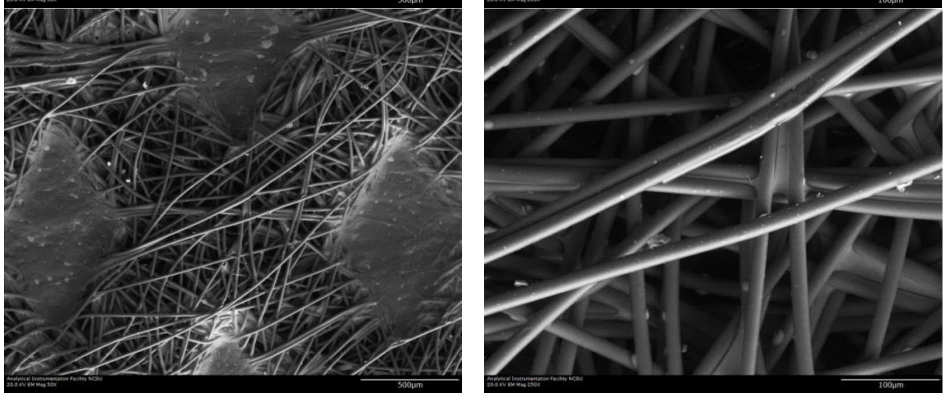

An elemental analysis was also conducted with the SEM by bombarding the sample with electrons and measuring the count of elements at different x-ray energies measured in KeV. While this measurement was a good indicator of the elements present, it did not accurately represent the respective quantities of the elements present. Table 18 depicts which elements were present in each sample. Carbon and oxygen were present in all samples. It should be noted, however, that far less oxygen was detected in the neat PP sample. Likely, some of the surface PP molecules were oxidized or have some amount of hydroxyl groups at the surface from processing. Phosphorus was present in all treated samples as expected further indicating that the coating is present. Aluminum was also present in many of the samples in trace amounts likely because small aluminum particles were transferred to the sample from the scissors used to cut the samples. Monomer 4 also had chlorine present which may indicate that the reaction for Monomer 4 did not go to completion with some residual chlorine.

Table 18: Elements Present in SEM Analysis on PP Samples

Sample	Carbon	Oxygen	Phosphorus	Chlorine
Control	X	X		
Monomer 1	X	X	X	
Monomer 2	X	X	X	
Monomer 4	X	X	X	X
Monomer 5	X	X	X	
Monomer 6	X	X	X	

4.9.2 Graft Polymerization Yield on PET Samples

Similar to the results on polypropylene, monomers 1, 2, and 5 had exceptional graft polymerization yields for all conditions tested on PET. Again, outstanding graft polymerization was achieved at the lowest conditions tested: 5% photoinitiator and 30 seconds per side exposure to UV light. Both photoinitiator and UV exposure time are expensive, and thus finding the acceptable minimum for both is desired. As such, future tests are required to truly determine the minimum for each of these parameters. Figure 53 shows the coating yield for monomer 1, Figure 54 depicts the coating yield for monomer 2, and Figure 55 depicts the coating yield for monomer 5.

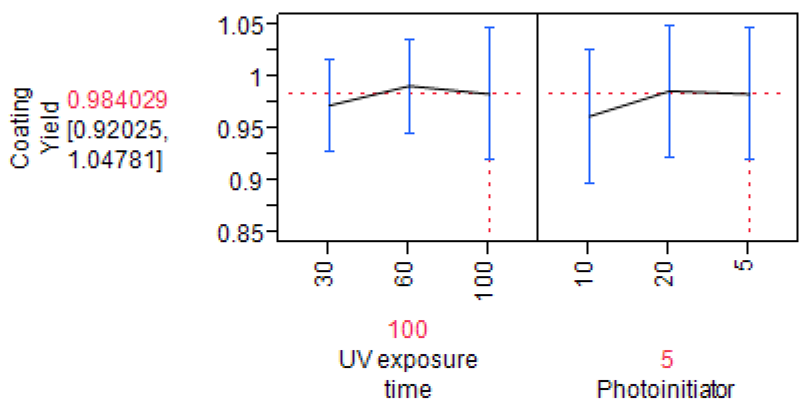

Figure 53: Graft Polymerization Yield for Monomer 1:PET

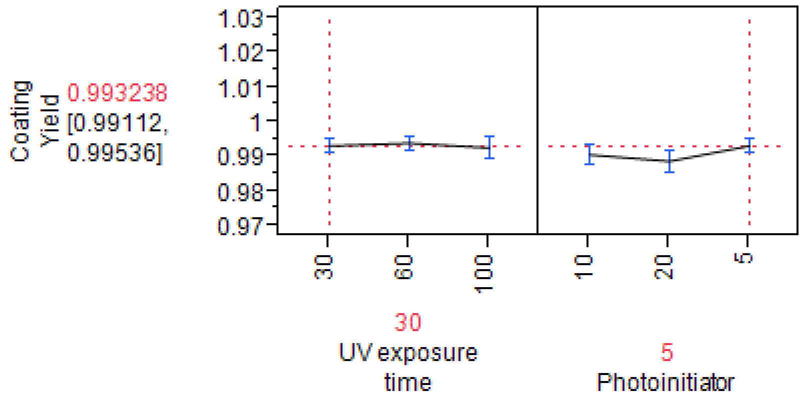

Figure 54: Graft Polymerization Yield for Monomer 2:PET

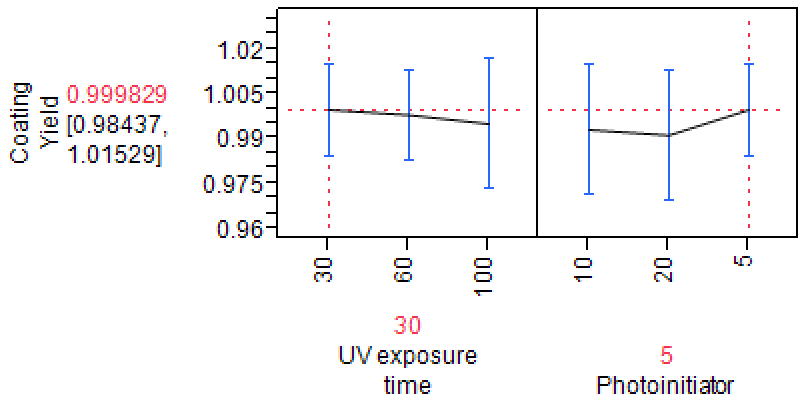

Figure 55: Graft Polymerization Yield for Monomer 5: PET

For Monomer 4, there were certain conditions that did not have ample graft polymerization. However, the coating yield was well above 95% at 5% photoinitiator and 30 seconds of UV exposure. Thus, more tests should be completed at lower test parameters to truly optimize this test. The graft polymerization is graphically represented in Figure 56.

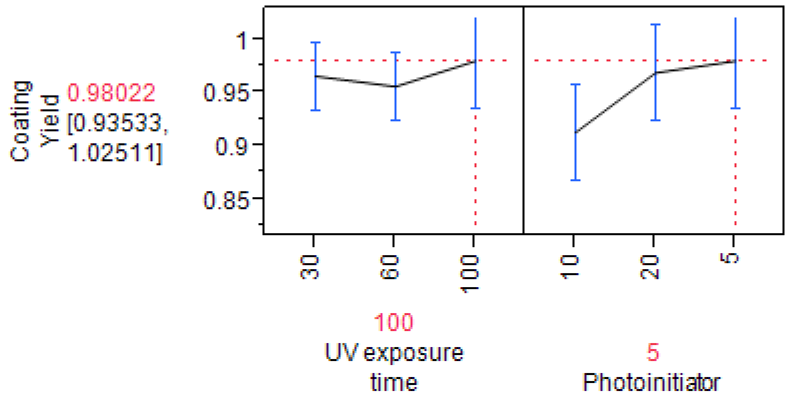

Figure 56: Graft Polymerization Yield for Monomer 4:PET

On PET, Monomer 6 only had 88% and 91% graft polymerization yields at the test conditions of 30 seconds UV exposure time and 5% photoinitiator. The best yield found was 99% at the conditions of 5% photoinitiator and 60 seconds of UV exposure. Thus, in this case, the optimal value was obtained. Depending on the actual energy cost of the UV lamp and price of the photoinitiator, these ratios could be adjusted to better optimize this monomer as well. Figure 57 shows a graphical representation of the optimal conditions.

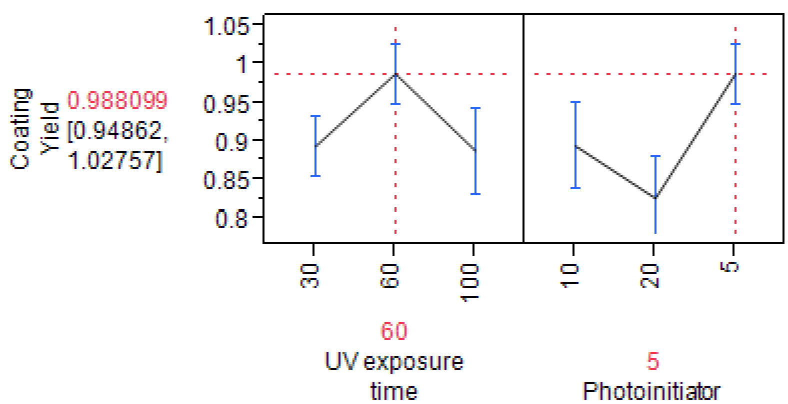

Figure 57: Graft Polymerization Yield for Monomer 6:PET

4.9.2.1 SEM Analysis for PET Samples

The SEM images obtained for all PET samples are shown in Figure 58, with images at 50x magnification on the left, and 250x magnification on the right. It is clear that the control sample has no film between the fibers, though there are some impurities present in the sample likely from the sample having been in the lab and exposed to dirt. In all of the samples which were coated, there is a film present between the fibers indicating that the FR coating was effectively grafted onto the surface. Because these samples were examined post soxhlet extraction, the remaining coating is durable.

Figure 58: SEM Images at 50x (left) and 250x(right) for PET samples

Control

1

2

4

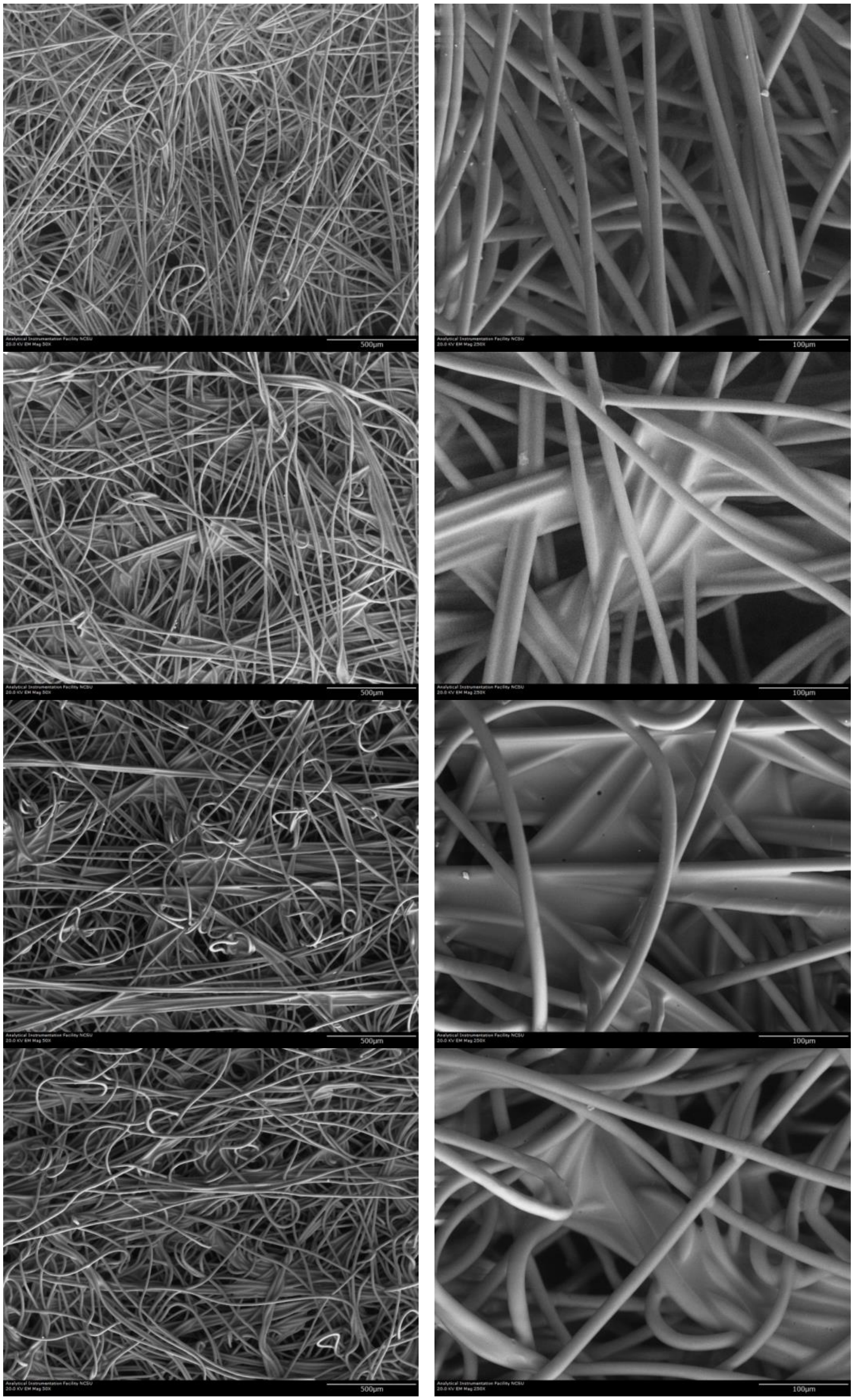

5

6

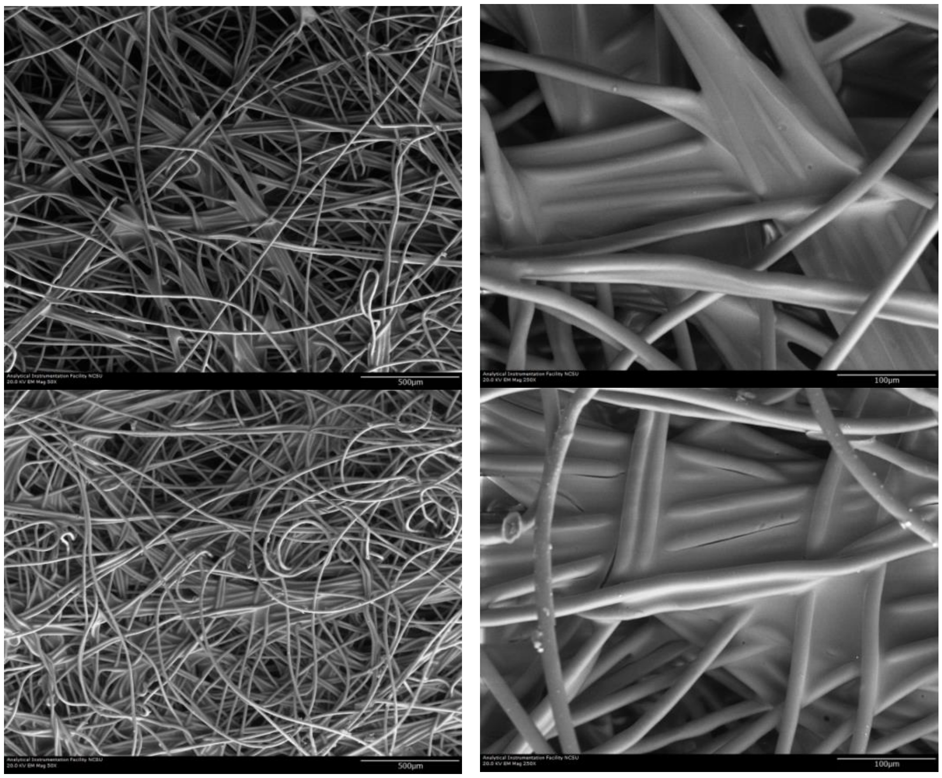

Again, an elemental analysis was conducted with the SEM. Table 19 shows which elements were present in each sample. Nitrogen is not shown because it is not compatible with this test. Most samples showed trace amounts of aluminum, most likely transferred to the sample during the cutting process as the samples were cut with aluminum scissors. On the control, there is only carbon and oxygen present. However, in each of the treated samples, phosphorus is also present indicating again that the coating was effectively grafted onto the surface. In the sample treated with monomer 4, chlorine is present as it was in the sample with PP. This indicates that the reaction did not occur to completion and some chlorine remained in the monomer.

Table 19: Elements Present in SEM Analysis on PET Samples

Sample	Carbon	Oxygen	Phosphorus	Chlorine
Control	X	X		
Monomer 1	X	X	X	
Monomer 2	X	X	X	
Monomer 4	X	X	X	X
Monomer 5	X	X	X	
Monomer 6	X	X	X	

5 CONCLUSIONS

Phosphorus based compounds are effective flame retardants in the condensed phase mechanism. Nitrogen has been shown to have a synergistic effect of the flame retardancy of phosphorus. Through this work, five FR monomers were synthesized based on phosphorus/nitrogen chemistry, and each of the synthesis was analyzed and adjusted based on the anticipated environmental impact. Two of these monomers had been previously developed in El-Shafei's lab, and three are novel compounds. All were characterized with FTIR and NMR analysis. The monomers have varying composition percentages of phosphorus, nitrogen, and oxygen so that the structure property relationships of these elements with regards to flame retardancy can be assessed. In order for phosphorus based FR to be effective on PP and PET, a char forming agent must also be present. In this work, different char forming crosslinkers were tested. All were bifunctional or multifunctional so that they could be graft polymerized as a coating onto polypropylene. Pentaerythritol triacrylate was found to be the best char forming crosslinker.

From flame test results, monomer 4 performed best on both PP and PET with several samples self-extinguishing with a monomer:crosslinker ratio of 80:20. Monomer 6 also had some samples self-extinguish on PET. As such, it can be inferred that a higher ratio of nitrogen to phosphorus is more effective in preventing flame spread, with a nitrogen to phosphorus ratio of 2.25. However, in the TGA test, monomer 2 had the greatest weight percentage remaining at 600°C, suggesting that this monomer was most effective for char formation on PP. On PET, both monomer 1 and monomer 2 were very close, with about 23-24% of the weight remaining at 600°C, and either of these monomers form an effective char on PET. If char formation is the desired trait, a higher percentage of carbon and oxygen is more valuable than increased nitrogen and phosphorus ratios. Thus, different monomers can be selected depending on the needs of the FR material. Further, all monomers are bifunctional or multifunctional so that they can be graft polymerized onto nonwoven PP and PET via UV irradiation. On PP, all monomers were effective at the lowest process conditions, and thus can be evaluated further to minimize both photoinitiator concentration and UV exposure time. On PET, monomers 1,2,4,and 5 were effective at the lowest process conditions and can also be evaluated further. Monomer 6 had the best graft polymerization yield at 5% photoinitiator and 60 seconds per side of UV exposure.

5.1 Future Work

The implications of the research presented leave much room for future work. First, each experiment can be better optimized, as the highest conditions tested for monomer:crosslinker ratio in monomers 1,4,5, and 6 were the most effective. Further, the photoinitiator content and UV exposure time can continue to be reduced. Based on the price of UV light and photoinitiator, the process can be optimized to minimize costs. UL 94 testing and cone calorimetry can also be performed on these samples to get industry standard results to be able to better compare to other FR on the market. The monomers were only tested on PP and PET, which do not inherently operate as FR with phosphorus based coatings. Based on the exceptional performance of the monomers on these substrates, they hold much promise if applied to cotton which crosslinks without the added need for a char forming agent.

REFERENCES

1. *Plastics flammability handbook : Principles, regulations, testing, and approval* (2004). In edited by Jürgen Troitzsch., Troitzsch J. (Eds.). Munich; Cincinnati: Hanser; Hanser Gardener.
2. Horrocks, A. R. (2011). Flame retardant challenges for textiles and fibres: New chemistry versus innovatory solutions. *Polymer Degradation and Stability, 96*(3), 377-392.
3. Karter, MJ. *Fire Loss in the United States during 2013*. January 2015, National Fire Protection Association, Retrieved from: http://www.nfpa.org/~/media/Files/Research/Fact%20sheets/FireLossFacts.pdf
4. Fire Analysis and Research Division. *Home Structure Fires that Began with Upholstered Furniture*. January 2015, National Fire Protection Association, Retrieved from: http://www.nfpa.org/research/reports-and-statistics/printable-fact-sheets
5. *Flame-retardant polymeric materials* (1975). In edited by Menachem Lewin, S. M. Atlas, and Eli M. Pearce, contributors S. M. A. e. a., Atlas S. M. and Pearce E. M. (Eds.). New York: Plenum Press.
6. Hogue, Cheryl. (2012). EPA Targets Flame Retardants. *Chemical & Engineering News, October 29, 2012, 90*(44), 34-37. Retrieved from: http://cen.acs.org/content/cen/articles/90/i44/EPA-Targets-Flame-Retardants.html
7. The Stockholm Convention. *Listing of POPs in the Stockholm Convention*. January 2015, Retrieved from: http://chm.pops.int/default.aspx

8. The Essential Chemical Industry Online. *Polymers*. January 2015, The University of York, Retrieved from: http://www.essentialchemicalindustry.org/polymers.html
9. Zhang, S., & Horrocks, A. R. (2003). A review of flame retardant polypropylene fibres. *Progress in Polymer Science (Oxford), 28*(11), 1517-1538. doi:10.1016/j.progpolymsci.2003.09.001
10. Wang, J., Wang, L., & Xiao, A. (2009). Recent research progress on the flame-retardant mechanism of halogen-free flame retardant polypropylene. *Polymer-Plastics Technology and Engineering, 48*(3), 297-302. doi:10.1080/03602550802675645
11. Schindler, W. D., Hauser, P. J., & Textile Institute (Manchester, E. (2004). *Chemical finishing of textiles*. Boca Raton: CRC.
12. Levchik, S., Hirschler, M., & Weil, E. (2011). *Practical guide to smoke and combustion products from burning polymers*. Shrewsbury, Shropshire, GBR: Smithers Rapra.
13. Hornsby, P. R., & Watson, C. L. (1989). Mechanism of smoke suppression and fire retardancy in polymers containing magnesium hydroxide filler. *Plastics and Rubber Processing and Applications, 11*(1), 45-51.
14. van der Veen, I., & de Boer, J. (2012). Phosphorus flame retardants: Properties, production, environmental occurrence, toxicity and analysis. *Chemosphere, 88*(10), 1119-1153. doi:http://dx.doi.org.prox.lib.ncsu.edu/10.1016/j.chemosphere.2012.03.067
15. Weil, E. D. (2009). In Levchik S. V. (Ed.), *Flame retardants for plastics and textiles electronic resource]: Practical applications*. Cincinnati: Hanser Publications.

16. Horrocks, A. R. (1996). Developments in flame retardants for heat and fire resistant textiles - the role of char formation and intumescence. *Polymer Degradation and Stability, 54*(2-3), 143-154. doi:10.1016/S0141-3910(96)00038-9

17. Feng Zhang , Jun Zhang & Chuanmei Jiao (2008) Study on Char Structure of Intumescent Flame-Retardant Polypropylene, Polymer-Plastics Technology and Engineering, 47:11, 1179-1186, DOI: 10.1080/03602550802392001

18. Wen, P., Wang, X., Xing, W., Peng, X., Yu, B., Shi, Y., Yuen, R. K. K. (2013). Synthesis of a novel triazine-based hyperbranched char foaming agent and the study of its enhancement on flame retardancy and thermal stability of polypropylene. *Industrial & Engineering Chemistry Research, 52*(48), 17015-17022. doi:10.1021/ie401955n

19. Cai, T., Jin, V., & Kong, X. (2006). Advance in studies on charring of flame retardant polypropylene. *Hecheng Shuzhi Ji Suliao/China Synthetic Resin and Plastics, 23*(4), 69-71.

20. Chen, S., Li, J., Zhu, Y., Guo, Z., & Su, S. (2013). Increasing the efficiency of intumescent flame retardant polypropylene catalyzed by polyoxometalate based ionic liquid. *Journal of Materials Chemistry a, 1*(48), 15242-15246. doi:10.1039/c3ta13538a

21. Nie, S., Peng, C., Yuan, S., & Zhang, M. (2013). Thermal and flame retardant properties of novel intumescent flame retardant polypropylene composites. *Journal of Thermal Analysis and Calorimetry, 113*(2), 865-871. doi:10.1007/s10973-012-2815-3

22. Li, N., Xia, Y., Mao, Z., Wang, L., Guan, Y., & Zheng, A. (2013). Synergistic effect of SiO2 on intumescent flame-retardant polypropylene. *Polymers & Polymer Composites, 21*(7), 439-447.

23. *Advances in fire retardant materials* (2008). In edited by A.R. Horrocks and D. Price., Horrocks A. R., Institute of Materials, Minerals,and Mining and Price D.,Professor (Eds.), . Cambridge, England; England?]; Boca Raton, FL: Woodhead Publishing; Maney Publishing; CRC Press.

24. Camino, G., Costa, L., & Trossarelli, L. (1984). Study of the mechanism of intumescence in fire retardant polymers: Part II—Mechanism of action in polypropylene-ammonium polyphosphate-pentaerythritol mixtures. *Polymer Degradation and Stability, 7*(1), 25-31. doi:http://dx.doi.org/10.1016/0141-3910(84)90027-2

25. Liu, Y., Wang, J., Deng, C., Wang, D., Song, Y., & Wang, Y. (2010). The synergistic flame-retardant effect of O-MMT on the intumescent flame-retardant PP/CA/APP systems. *Polymers for Advanced Technologies, 21*(11), 789-796. doi:10.1002/pat.1502

26. Wang, C., Wei, P., Qian, Y., & Liu, J. (2011). The synthesis of a novel flame retardant and its synergistic efficiency in polypropylene/ammonium polyphosphate system. *Polymers for Advanced Technologies, 22*(7), 1108-1114. doi:10.1002/pat.1958

27. Cichy, B., Luczkowska, D., Nowak, M., & Wadyka-Przybylak, M. (2003). Polyphosphate flame retardants with increased heat resistance. *Industrial and Engineering Chemistry Research, 42*(13), 2897-2905. doi:10.1021/ie0208570

28. Peng, H., Zhou, Q., Wang, D., Chen, L., & Wang, Y. (2008). A novel charring agent containing caged bicyclic phosphate and its application in intumescent flame retardant polypropylene systems. *Journal of Industrial and Engineering Chemistry, 14*(5), 589-595. doi:http://dx.doi.org/10.1016/j.jiec.2008.05.011

29. Li, G., Wang, W., Cao, S., Cao, Y., & Wang, J. (2014). Reactive, intumescent, halogen-free flame retardant for polypropylene. *Journal of Applied Polymer Science, 131*(7). doi:10.1002/app.40054

30. Dufton, P. W. (2003). In Rapra Technology Limited. (Ed.), *Flame retardants for plastics market report*. Shrewsbury: Rapra Technology Ltd.

31. Sheng, Y., Chen, Y., & Bai, Y. (2014). Catalytically synergistic effects of novel LaMnO3 composite metal oxide in intumescent flame-retardant polypropylene system. *Polymer Composites*. doi:10.1002/pc.22908

32. Wu, N., & Yang, R. (2011). Effects of metal oxides on intumescent flame-retardant polypropylene. *Polymers for Advanced Technologies, 22*(5), 495-501. doi:10.1002/pat.1539

33. Song, P., Fang, Z., Tong, L., Jin, Y., & Lu, F. (2008). Effects of metal chelates on a novel oligomeric intumescent flame retardant system for polypropylene. *Journal of Analytical and Applied Pyrolysis, 82*(2), 286-291. doi:http://dx.doi.org.prox.lib.ncsu.edu/10.1016/j.jaap.2008.04.008

34. Laoutid, F., Persenaire, O., Bonnaud, L., & Dubois, P. (2013). Flame retardant polypropylene through the joint action of sepiolite and polyamide 6. *Polymer Degradation and Stability, 98*(10), 1972-1980. doi:http://dx.doi.org/10.1016/j.polymdegradstab.2013.07.018

35. Hofmann, D., Wartig, K., Thomann, R., Dittrich, B., Schartel, B., & Muelhaupt, R. (2013). Functionalized graphene and carbon materials as additives for melt-extruded flame retardant polypropylene. *Macromolecular Materials and Engineering, 298*(12), 1322-1334. doi:10.1002/mame.201200433

36. Huang, G., Wang, S., Song, P., Wu, C., Chen, S., & Wang, X. (2014). Combination effect of carbon nanotubes with graphene on intumescent flame-retardant polypropylene nanocomposites. *Composites Part A: Applied Science and Manufacturing, 59*(0), 18-25. doi:http://dx.doi.org/10.1016/j.compositesa.2013.12.010

37. Yi, J., Liu, Y., Pan, D., & Cai, X. (2013). Synthesis, thermal degradation, and flame retardancy of a novel charring agent aliphatic-aromatic polyamide for intumescent flame retardant polypropylene. *Journal of Applied Polymer Science, 127*(2), 1061-1068. doi:10.1002/app.37910

38. Cao, K., Wu, S., Qiu, S., Li, Y., & Yao, Z. (2013). Synthesis of N-alkoxy hindered amine containing silane as a multifunctional flame retardant synergist and its application in intumescent flame retardant polypropylene. *Industrial & Engineering Chemistry Research, 52*(1), 309-317. doi:10.1021/ie3017048

39. Gray, R. L., & Lee, R. E. (1995). UV stabilization of flame retarded polypropylene. Paper presented at the *Part 1 (of 3), May 7, 1995 - October 11, 1995, 3* 3527-3535.

40. Hochberg, A., & Glogovsky, J. (1995). Key properties of FR engineering thermoplastics for demanding applications. Paper presented at the *Part 1 (of 3), May 7, 1995 - October 11, 3* 3518-3526.

41. Ou, Y., Fang, X., Liu, J., Xu, D., & Xia, Z. (2007). Light stabilization of flame-retarded polypropylene. *Gaofenzi Cailiao Kexue Yu Gongcheng/Polymeric Materials Science and Engineering, 23*(2), 41-44+49.

42. Jha, N. K., Misra, A. C., & Bajaj, P. (1984). Flame-retardant additives for polypropylene. *Journal of Macromolecular Science - Reviews in Macromolecular Chemistry and Physics, C24*(1), 69-116.

43. Kim, Y. R., Harden, F. A., Toms, L. L., & Norman, R. E. (2014). Health consequences of exposure to brominated flame retardants: A systematic review. *Chemosphere, 106*, 1-19. doi:10.1016/j.chemosphere.2013.12.064

44. Lim, D., & Lastoskie, C. M. (2011). A dynamic multimedia environmental and bioaccumulation model for brominated flame retardants in Lake Huron and Lake Erie, USA. *Environmental Toxicology and Chemistry, 30*(5), 1018-1025. doi:10.1002/etc.482

45. Textile Flammability: Current and Future,Issues Conference. (1999). In Textile Institute (Manchester E. (Ed.), *Textile flammability: Current and future issues*. Manchester, England: Textile Institute.

46. Cheema, H. A., El-Shafei, A., & Hauser, P. J. (2013). Conferring flame retardancy on cotton using novel halogen-free flame retardant bifunctional monomers: Synthesis, characterizations and applications. *Carbohydrate Polymers, 92*(1), 885-893. doi:10.1016/j.carbpol.2012.09.081

47. Edwards, B., El-Shafei, A., Hauser, P., & Malshe, P. (2012). Towards flame retardant cotton fabrics by atmospheric pressure plasma-induced graft polymerization: Synthesis and application of novel phosphoramidate monomers. *Surface & Coatings Technology, 209*, 73-79. doi:10.1016/j.surfcoat.2012.08.031

48. Deng, C., Deng, C., Zhao, J., Fang, W., Lin, L., & Wang, Y. (2014). Water resistance, thermal stability, and flame retardation of polypropylene composites containing a novel ammonium polyphosphate microencapsulated by UV-curable epoxy acrylate resin. *Polymers for Advanced Technologies, 25*(8), 861-871. doi:10.1002/pat.3319

49. Yuan, H., Xing, W., Zhang, P., Song, L., & Hu, Y. (2012). Functionalization of cotton with UV-cured flame retardant coatings. *Industrial & Engineering Chemistry Research, 51*(15), 5394-5401. doi:10.1021/ie202468u

50. Yu, L., Zhang, S., Liu, W., Zhu, X., Chen, X., & Chen, X. (2010). Improving the flame retardancy of PET fabric by photo-induced grafting. *Polymer Degradation and Stability, 95*(9), 1934-1942. doi:http://dx.doi.org.prox.lib.ncsu.edu/10.1016/j.polymdegradstab.2010.04.005

51. Liu, W., Zhang, S., Yu, L., Chen, X., Li, L., Feng, Q., & Zhu, X. (2011). Surface photografting: New application for flame retardant finishing of polyamide6.6 (PA6.6) fabric. *Journal of Applied Polymer Science, 119*(1), 66-72. doi:10.1002/app.32319

52. Liu, W., Zhang, S., Chen, X., Yu, L., Zhu, X., & Feng, Q. (2010). Thermal behavior and fire performance of nylon-6,6 fabric modified with acrylamide by photografting. *Polymer Degradation and Stability, 95*(9), 1842-1848. doi:http://dx.doi.org/10.1016/j.polymdegradstab.2010.04.023

53. Deng, C., Deng, C., Zhao, J., Li, R., Fang, W., & Wang, Y. (2015). Simultaneous improvement in the flame retardancy and water resistance of PP/APP through coating UV-curable pentaerythritol triacrylate onto APP. *Chinese Journal of Polymer Science*, *33*(2), 203-214. doi:10.1007/s10118-015-1575-5

54. Manufacture of triallyl isocyanurate

Jpn. Kokai Tokkyo Koho (1992), 4 pp. CODEN:JKXXAF; JP04049284